The histone acetyl transferase Tip60 as a regulator of tumor suppression

Dissertation

zur Erlangung des Doktorgrades
der Naturwissenschaften
(Dr.rer.nat.)

dem Fachbereich Biologie
der Philipps-Universität Marburg

vorgelegt von

Christoph Dohmesen

aus Mönchengladbach

Marburg/Lahn Oktober 2006

Für Gaby, Klaus und Anne,
Hildegard und Hans,
Irmgard und Heinrich,
und Dominique

TABLE OF CONTENTS

4 METHODS   27

1. SUMMARY

Tip60 is a histone acetyl transferase (HAT) and a cofactor of transcription, but also an interaction partner of the Mdm2 oncoprotein. The functional consequences of this interaction are only partially understood and were further explored in this study. We found that Tip60 expression leads to an increase of Mdm2 and p53 protein levels, which is due to elevated protein half-lifes of these proteins. To explore the underlying mechanisms, the impact of Tip60 on the Mdm2-mediated ubiquitination of p53 was studied. However, we found that Tip60 expression does not affect p53-ubiquitination by Mdm2. Strikingly, Tip60 is capable of selectively inhibiting the Mdm2-mediated conjugation of the neural precursor cell expressed developmentally downregulated 8 (Nedd8) to p53, which had been shown to reduce its transcriptional activity. In contrast, the known Mdm2 antagonist p14arf preferentially blocked Ubiquitin conjugation by Mdm2. To identify underlying mechanisms, we studied the intracellular localization of Tip60 and Mdm2. Both proteins relocalized each other to the PML nuclear bodies, but a similar localization pattern was observed even in the absence of PML. Analysis of Tip60 deletion mutants revealed a stringent correlation between relocalization with Mdm2 and reduced neddylation of p53 and Mdm2. For both activities, the MYST domain but not the HAT domain of Tip60 was required. We propose that Tip60 can act as a selective antagonist to Mdm2-mediated neddylation. Hence, the two different E3-Ligase activities of Mdm2 can be regulated individually.

Furthermore, the effect of Tip60 on the transcriptional activity of p53 was investigated. Surprisingly, Tip60 overexpression did not result in a stimulation of p53 transcriptional activity, whereas the overexpression of the known Mdm2 antagonist p14arf did so. Studies of Tip60 knockdown showed that reduced Tip60 expression only mildly affects the p53-dependent transactivation of its target gene promoters under non-stress conditions.

Therefore, we investigated the role of Tip60 after ultraviolet (UV) irradiation. Immunoblot analysis after siRNA-mediated knockdown of the *HTATIP* gene (which encodes Tip60) expression showed that the cleavage of the poly(ADP-ribose) polymerase (PARP) upon UV irradiation was reduced, suggesting an impaired apoptotic response. However, the removal of p53 did not affect PARP cleavage, arguing that Tip60 enables UV induced apoptosis independently of p53. Instead, Tip60 knockdown led to reduced phosphorylation of histone 2AX (H2AX) and jun-N-terminal kinase (JNK), suggesting a role of Tip60 in the immediate early response to UV light exposure through JNK.

In this work, two additional roles of Tip60 have been unveiled that potentially contribute to tumor suppression. First, Tip60 can inhibit the Mdm2-mediated conjugation of the Nedd8 protein to p53, thereby possibly releaving it from transcriptional inhibition by Mdm2. Moreover, Tip60 apparently is required for the proper activation of the UV-induced JNK-signaling pathway, thereby ensuring an efficient response to DNA damage and apoptosis induction.

1.1 ZUSAMMENFASSUNG

Das Tip60 Protein ist eine Histonazetyltransferase (HAT) und ein Transkriptionskofaktor, der zugleich auch mit dem Mdm2 Onkoprotein interagiert. Die funktionellen Konsequenzen dieser Interaktion sind allerdings nur teilweise bekannt und wurden deshalb in dieser Arbeit näher erforscht. Die Untersuchungen ergaben, dass die Überexpression von Tip60 zu einem Anstieg der Proteinmengen von p53 und Mdm2 führt, was auf eine erhöhte Stabilität dieser Proteine zurückzuführen ist. Allerdings resultierte die Expression von Tip60 nicht in einer Inhibition der Mdm2-vermittelten p53-Ubiquitinierung. Vielmehr reduzierte Tip60 die Mdm2-vermittelte Konjugation des Nedd8 (neural precursor cell expressed developmentally downregulated 8)-Proteins an p53, dem eine Transkriptions-reprimierende Wirkung zugeschrieben wird. Im Gegensatz hierzu führte die Expression des bekannten Mdm2-Regulators p14arf hauptsächlich zu einer Inhibition der p53-Ubiquitinierung. Um die zugrundeliegenden Mechanismen aufzuklären, wurde die intrazelluläre Lokalisation von Tip60 und Mdm2 untersucht. Beide Proteine relokalisierten sich gegenseitig und assoziierten mit den Promyelozytischen nukleären Domänen; jedoch wurde ein ähnliches Kolokalisationsmuster auch in Abwesenheit von PML beobachtet. Die Analyse von Tip60 Deletionsmutanten zeigte eine stringente Korrelation zwischen der Relokalisation von Mdm2 und der Inhibition der p53- und Mdm2-Neddylierung. Für beide Aktivitäten war die MYST-Domäne von Tip60, nicht aber dessen HAT-Domäne notwendig. Wir folgern, dass Tip60 als ein selektiver Antagonist der Mdm2-vermittelten Neddylierung fungieren kann. Die zwei E3-Ligase Aktivitäten von Mdm2 können also individuell reguliert werden.

Weiterhin wurde der Einfluss von Tip60 auf die transkriptionelle Aktivität von p53 untersucht. Erstaunlicherweise konnte Tip60, im Gegensatz zu p14arf, den reprimierenden Einfluss von Mdm2 nicht abschwächen. Die Suppression der Tip60-Genexpression durch RNA-Interferenz zeigte nur einen schwachen inhibitorischen Effekt auf die transaktivierende Funktion von p53.

Aus diesem Grund wurde die Rolle von Tip60 nach ultravioletter Strahlung (UV) untersucht. Die Analyse der Proteinexpression nach UV Bestrahlung zeigte, dass die Spaltung der Poly(ADP-Ribose) Polymerase (PARP) nach Suppression des *HTATIP* Gens (welches Tip60 kodiert) reduziert ist, was auf eine Inhibition der apoptotischen Antwort hinweist. Die Suppression der p53-Expression hingegen, beeinflußte die

PARP-Spaltung nicht, was darauf hindeutet, dass Tip60 unabhängig von p53 die UV-induzierte Apoptose fördert. Weiterhin wurde eine verringerte Phosphorylierung des Histon 2AX und der jun-N-terminalen Kinase (JNK) beobachtet, was auf eine frühe Inhibition der zellulären Antwort auf DNA-Schäden hindeutet.

In dieser Arbeit wurden zwei neue Funktionen von Tip60 identifiziert, die potentiell zur Tumorsuppression beitragen. Einerseits inhibiert Tip60 die Mdm2-vermittelte p53-Neddylierung und trägt damit evtl. zur Aktivierung von p53 bei. Weiterhin wird Tip60 anscheinend für die Aktivierung des UV-induzierten JNK-Signalwegs benötigt und trägt somit zu einer effizienten Antwort auf DNA-Schäden durch Aktivierung von Apoptose bei.

2   INTRODUCTION

2.1   The tumor suppressor p53

The tumor suppressor p53 is encoded by a gene that is frequently mutated in human cancer. About 50% of all human tumors have no p53 or carry mutations in the *TP53* gene that lead to the inactivation of the p53 protein (Hollstein et al., 1994). The rest of the tumors exhibit mutations in other genes that finally result in a functional inactivation of p53. The p53 protein is a nuclear protein and acts mainly as a transcription factor. Upon activation, p53 forms first dimers that then further associate to tetramers. The p53 tetramer then binds to conserved p53 elements, inverted sequences, in the promoters of its target genes (Lu and Levine, 1995). After the recruitment of further cofators such as histone acetyl transferases, the transcription of its target genes begins. Under certain circumstances, p53 can act independently of transcriptional activation by stimulating the induction of apoptsis directly at the mitochondria (Mihara et al., 2003).

p53 is activated upon exposure of the cell to various stress stimuli including DNA damage, activation of oncogenes like Ras or hypoxia (reviewed in Vousden and Lu, 2002). It is also called the "guardian of the genome", because it is required for maintaining the genomic integrity of a cell. p53 integrates various stress and survival signals to decide whether the damage of a cell can be repaired or whether the survival of the cell would be detrimental for the whole organism. In the latter case, p53 activates the transcription of apoptosis-related genes whose effects finally lead to the death of the cell, thereby preventing the development of a potential tumor cell. The outcome of p53 activation can be cell cycle arrest, senecence or apoptosis.

The p53 protein exerts its function as a tumor suppressor by activating basically two groups of target genes: genes involved in cell cycle regulation like the inhibitor of cyclin-dependent kinases (CDK) p21wafcip or the 14-3-3sigma protein which is involved in regulating the G2/M transition (el-Deiry et al., 1994; el-Deiry et al., 1993; Hermeking et al., 1997). The p21 protein binds to the CDK-cyclin complexes like CDK2-cyclin E and inhibits their kinase activity towards their targets, the proteins of the retinoblastoma family (Obaya and Sedivy, 2002). The second group of p53 target genes, like *Noxa*, *Puma* or *Bax,* is involved in the induction of programmed cell death or apoptosis*.* Bax for example stimulates the cytochrome c-release from the mitochondria, resulting in the activation of a group of specific proteases, called

caspases, which among others, leads to cleavage of the Poly(ADP-Ribose) polymerase (PARP), DNA fragmentation and finally cell death (reviewed in Green and Evan, 2002).

p53 exhibits a highly conserved domain structure, its C-terminus contains the oligomerisation domain. The DNA binding of p53 is mediated by the central DNA binding domain and the N-terminal domain, the so-called transactivation domain, is required for transcriptional activation, by the recruitment of transcription cofactors.

The p53 protein must be regulated very tightly to avoid its activation under non-stress conditions, which would be harmful for the cell. This regulation is mainly accomplished on the posttranslational level. Under non-stress conditions, p53 is present only at very low levels. However, upon the induction of DNA damage, p53 becomes phosphorylated by several DNA-damage induced kinases like ATM or ATR, leading to its stabilisation and subsequent activation (reviewed in Niida and Nakanishi, 2006). The protein levels of p53 are regulated by ubiquitination, which is mainly mediated by the oncoprotein Mdm2. Ubiquitinated p53 is exported from the nucleus to the cytoplasm and subsequently degraded by the 26S proteasome (Figure 2.1 A). Apart from Mdm2, the E3-Ligases hPirh2 and COP1 have been described recently to antagonise p53 by ubiquitination (reviewed in Brooks and Gu, 2006).

2.2 The Ubiquitin ligase Mdm2

Originally, the *MDM2*-gene was isolated from the transformed mouse cell line 3T3DM (Cahilly-Snyder et al., 1987). The Mdm2 protein is a nuclear phospho protein of about 90 kDa that is encoded by the human homolog of the mouse double minute gene. In several sarcomas, the *MDM2*-gene was found to be amplified, hinting at a potential contribution of Mdm2 to tumorigenesis (Oliner et al., 1992).

Mdm2 is a RING-finger protein that catalyses the addition of ubiquitin moieties to its substrate p53 by virtue of its E3 Ubiquitin ligase activity (Figure 2.1 A). The ubiquitination of p53 by Mdm2 predominantly occurs on six lysines, located at the extreme C-terminus of p53, but recently also lysine residues in the central domain of p53 have ben described as ubiquitination targets (Chan et al., 2006).

Some reports demonstrated that Mdm2 mainly functions to monoubiquitinate p53, thereby stimulating its nuclear export (Figure 2.1 B) where it is polyubiquitinated and subsequently degraded. The histone acetyl transferase p300 has recently been

implicated in the polyubiquitination of monoubiquitinated p53, thereby acting as an E4-Ligase (Grossman et al., 2003; Michael and Oren, 2003).

Moreover, Mdm2 binds to p53 in the vicinity of its transactivation domain, thereby inhibiting its interaction with transcription cofactors (Momand et al., 1992; Oliner, 1993). The Mdm2 protein binds to p53 via its N-terminal domain (Chen et al., 1993), while the central domain contains binding sites for proteins like TBP, p14arf, p300 and pRb as well as signal sequences that play a role in the shuttling of Mdm2 between the nucleus and the cytoplasm. The C-terminal RING-finger domain mediates the ubiquitination of p53 (for a review, see Meek and Knippschild, 2003). Apart from ubiquitinating p53, Mdm2 is also capable of ubiquitinating itself, a process
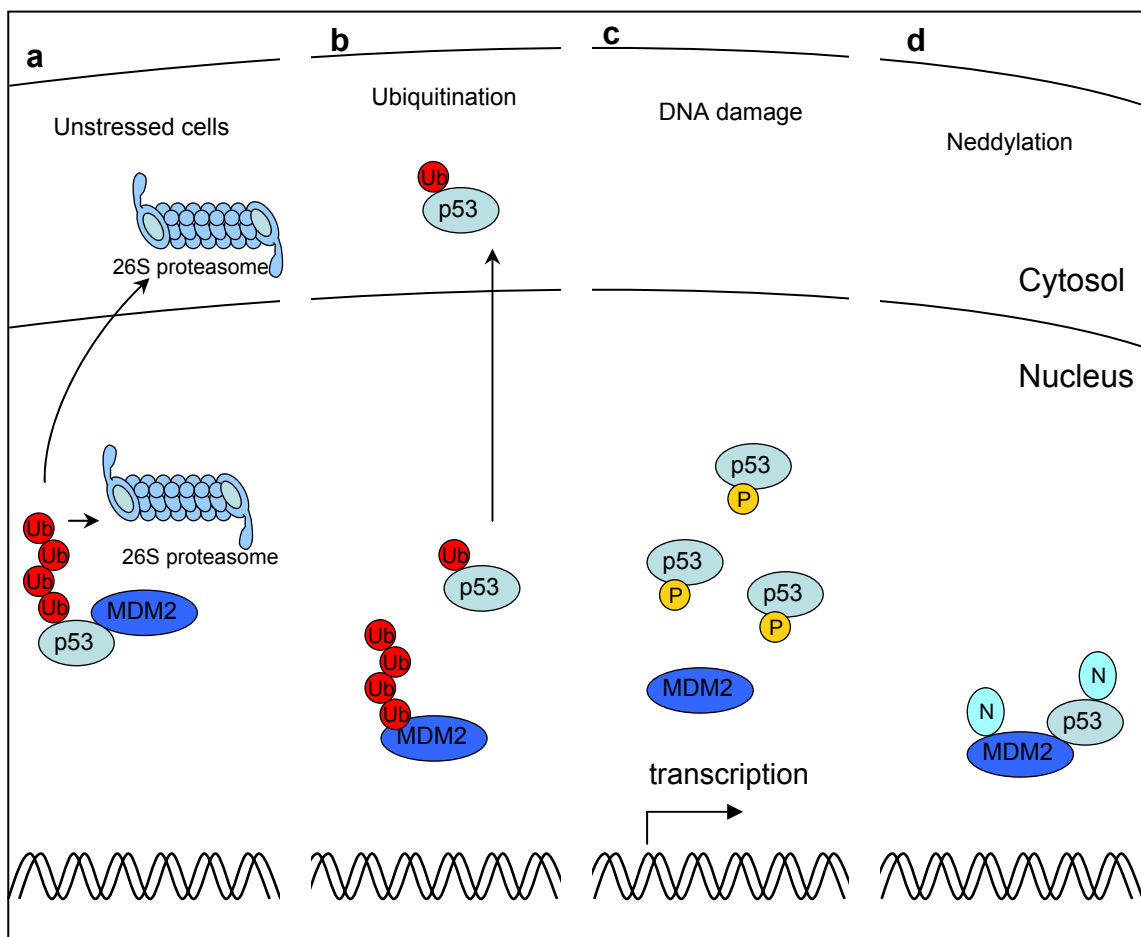
Figure 2.1 Different modification states of p53 and Mdm2
a) In unstressed cells a small amount of p53 is present in the nucleus, so that the level of transcriptional activity is low. This is due to different modification strategies: at high expression levels of Mdm2, p53 is polyubiquitinated (Ub) and degraded. Proteasomes both present in the nucleus and the cytosol are capable of degrading p53. **b)** If Mdm2 is present at low levels it can mono-ubiquitinate p53, thereby leading to the export of p53. In the cytosol, p53 monoubiquitination can be extended to polyubiquitination resulting in its degradation. It can also be deubiquitinated and shuttle back into the nucleus **c)** DNA damage activates several kinases that phosphorylate (P) p53 at its interaction surface with Mdm2. **d)** Mdm2 was shown to mediate its conjugation with Nedd8 (N), resulting in decreased transcriptional activity. Figure modified from Hoeller et al., 2006.

called auto-ubiquitination. Like ubiquitinated p53, Mdm2 is then degraded by the proteasome.

Recent reports have shown that Mdm2 not only acts as an E3-Ligase for Ubiquitin, but that it also mediates linkage of the neural cellular precursor developmentally downregulated 8 (Nedd8) to p53. Nedd8 is homologous to ubiquitin and exhibits an amino acid identity of 57% to ubquitin, thereby being its closest relative (reviewed in Watson and Irwin, 2006). Nedd8 has been implicated in cell cycle regulation and belongs to the family of ubiquitin-like modifiers. The conjugation of Nedd8 to its targets requires the E1 activating enzyme which consists of a heterodimer of the amyloid precursor binding protein 1 (APP-BP1) and the Uba3 protein, the E2-conjugating enzyme hUbc12 and a specific E3 ligase (Figure 2.2). While ubiquitination of p53 targets it for the proteasomal degradation, neddylation of p53 compromises its transcriptional activity. Neddylation occurs on at least three C-terminal lysine residues of p53 that are also subject to ubiquitination by Mdm2. The neddylating activity of Mdm2 is dependent on the same cysteine residue (C464) in the RING-finger domain as its ubiquitination activity. In analogy to the auto-ubiquitination of Mdm2, its auto-neddylation has been described, which in turn results in a mitigation of its repressive effect on p53 (Xirodimas et al., 2004).
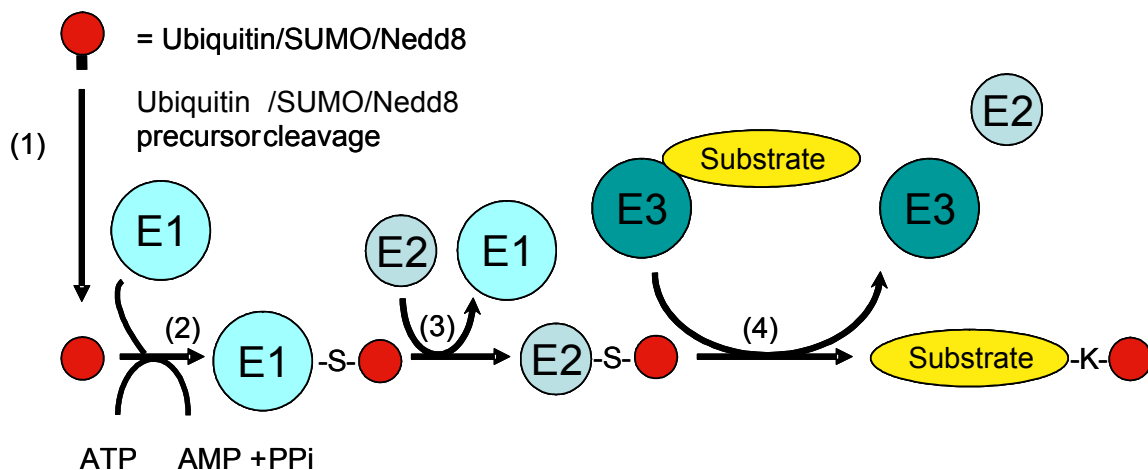
Figure 2.2: General overview of the ubiquitin and UBL protein conjugation pathways
(1) Ubiquitin, SUMO and Nedd8 are synthesised as precursors that are processed at a conserved C-terminal glycine residue by the hydrolase activity of deubiquitinating, desumoylating and deneddylating enzymes, generating an exposed Gly-Gly motif that serves as the attachment site to target substrates. **(2)** The exposed C-terminal glycine of ubiquitin/SUMO/Nedd8 is adenylated by an activating (E1) enzyme in an ATP dependent manner and is transferred to an active E1 cysteinyl side chain through a thiol ester linkage. **(3)** Activated ubiquitin/SUMO/Nedd8 is subsequently transferred to a conjugating (E2) enzyme, forming another thiol ester linkage. **(4)** A ligase (E3) transfers ubiquitin/SUMO/Nedd8 to the ε-amino group of a substrate lysyl residue of target substrates, resulting in the formation of an isopeptide bond. Taken from: Watson and Irwin, 2006.

2.2.1 Regulators of Mdm2

The activity of Mdm2 is regulated by its own abundance and also by interaction with other proteins. The levels of Mdm2 are regulated on the mRNA level and on the protein level. As one of the p53 target genes, Mdm2 is induced upon p53 activation. Newly synthesized Mdm2 itself binds p53 and targets it for degradation, thereby establishing a negative feedback loop (Wu et al., 1993). On the other hand, Mdm2 is regulated in its protein stability. Several kinases that phosphorylate p53, also exhibit this activity towards Mdm2. For instance, Mdm2 is phosphorylated at serine 395 by the ATM-kinase (ataxia telangiectasia-mutated) upon DNA damage. This results in the inhibition of p53 export to the cytoplasm and its subsequent degradation (Maya et al., 2001). Moreover, Mdm2 is acetylated by the CBP-complex, compromising the capability of Mdm2 to target p53 for degradation (Wang et al., 2004). Phosphorylation of Mdm2 at serine 166 and 186 by the Akt kinase, however, leads to a block of the Mdm2-p14arf interaction, thereby stimulating the degradation of p53 (Gottlieb et al., 2002).

p14arf is a small, nucleolar protein that is encoded by the INK4A/ARF locus. By directly interacting with Mdm2, p14arf is capable of inhibiting the Mdm2-mediated p53-degradation (Pomerantz et al., 1998). Binding of p14arf to Mdm2 results in a conformational change of Mdm2, thereby revealing a previously hidden signal sequence. This leads to the sequestration of Mdm2 to the nucleolus, freeing p53 from the impact of Mdm2 (Tao and Levine, 1999; Weber et al., 2000).

This mechanism leads to the disruption of the negative feedback loop, allowing p53 to activate its target genes (Weber et al., 1999).

Moreover, ribosomal proteins have been implicated in the regulation of Mdm2. Like p14arf, the ribosomal L11 protein binds Mdm2 and inactivates it, resulting in stabilization of p53 levels (Lohrum et al., 2003). Recently it was reported that L11 differentilally regulates the stability of Mdm2 and p53. Ubiquitinated Mdm2 accumulates due to an inhibition of a subsequent degradation step (Dai et al., 2006). Furthermore, the ribosomal proteins L5 and L23 interfere with the Mdm2 function and are found in complex with Mdm2. These proteins are capable of inducing a p53-dependent cell cycle arrest (Dai and Lu, 2004; Jin et al., 2004).

The Mdm2 homolog MdmX has also been described to regulate Mdm2 by inhibiting the Mdm2-mediated p53 export and degradation (Jackson and Berberich, 2000).

The PML protein is another regulator of Mdm2. It is a nuclear RING-finger protein that, together with several other proteins, forms nuclear structures that are called PML nuclear bodies (PML NBs) or PML oncogenic domains (PODs). Although their direct role in nuclear activity is unclear, PML NBs are implicated in the regulation of transcription, apoptosis, tumor suppression and the anti-viral response (reviewed in Dellaire and Bazett-Jones, 2004). An emerging view is that they represent sites where multi-subunit complexes form and where posttranslational modification of regulatory factors, such as p53, occurs in response to cellular stress. Following DNA damage, several repair factors transit through PML NBs in a temporally regulated manner implicating these bodies in DNA repair. PML has been shown to interact with p53 and Mdm2, resulting in inhibition of Mdm2-mediated p53-degradation. Moreover, PML neutralizes the inhibitory effects of Mdm2 by prolonging the stress-induced phosphorylation of p53 on serine 20, a site of the checkpoint kinase 2 (Chk2). PML recruits Chk2 and p53 into the PML nuclear bodies and enhances the p53/Chk2 interaction (Louria-Hayon et al., 2003). Another mechanism, by which PML protects p53, is the sequestration of Mdm2 to the nucleolus, thereby precluding it from p53 (Bernardi et al., 2004).

2.3   The histone acetyl transferase Tip60

The Tip60 protein was originally identified as an interacting protein of the HIV-tat protein (Kamine et al., 1996). It is a nuclear protein of 60 kDa size that is present in three different splice variants (reviewed in Sapountzi et al., 2006). Tip60 contains several conserved domains, the N-terminally located chromo-domain is required for the recognition of methylated histone tails. In the center/N-terminus of the protein the MYST domain is found. It defines the membership of Tip60 to the family of the MYST histone acetyl transferases and contains the catalytical HAT domain as well as a zinc-finger motif which is essential for the acetyltransferase activity and is required for protein-protein interactions (Barron et al., 2005; Hlubek et al., 2001; Nordentoft and Jorgensen, 2003; Xiao et al., 2003) (Figure 2.3). The MYST domain is the region of homology remarkably well conserved and common among all family members.

The exon 5 is deleted in one of the splice variants, called PLIP (cPLA2 interacting protein). PLIP interacts with $cPLA_2$, a cytosolic phosphatase that is activated by calcium ions and that is transported to the nuclear membrane and has been implicated in the apoptotic response (Sheridan et al., 2001).

Depending on the cellular process in which it participates, Tip60 forms distinct transient complexes with the appropriate binding partners. However, the majority of cellular Tip60 exists in a stable nuclear multiprotein complex, the evolutionary conserved NuA4 complex, that consists of at least 18 subunits and performs most transcriptional and DNA damage-related Tip60 functions. Central to the Tip60 stable complex is the scaffold protein TRRAP (transformation/ transcription domain associated protein) (Ikura et al., 2000), which is present in other acetyltransferase complexes, e.g. PCAF (p300/CBP associated factor complex). Moreover, the NuA4-Tip60 complex contains helicases as the RuvB-like proteins Tip48 and Tip49 (reviewed in Sapountzi et al., 2006). The NuA4 complex acetylates nucleosomal histones H4 and H2A by the addition of an acetyl group to the ε-amino group of specific lysines. Thereby it contributes to a loosening of the chromatin structure and facilitates the binding of further transcripton factors to the promoter, finally leading to the recruitment of the RNA polymerase II and activation of gene transcription (reviewed in Sapountzi et al., 2006).
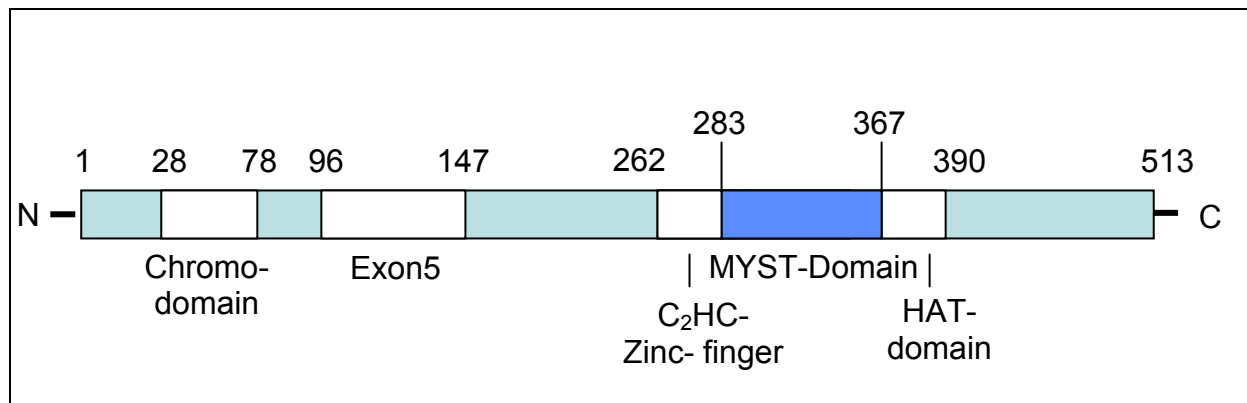
Figure 2.3 : Primary structure of Tip60
The figure shows the so far known domains of Tip60. In between the chromatin organising domain (aa 28-78) and the exon 5 (aa 96-147) a cyclinB/Cdc2 recognition site is found, with serine 90 as an acceptor residue.The MYST domain (aa 262-390) contains two more domains, a zinc-finger motif (aa 262-283) as well as the catalytic acetyl transferase domain (aa 367-390)

Recent work in different experimental systems implicated that Tip60 plays a role on several levels of the DNA damage response and repair. For example, it was observed that the acetylation of ATM by Tip60 is required for its activation by stimulating its autophosphorylation, which results in the ATM dimer dissociation (Sun et al., 2005). A major substrate of ATM is the histone variant H2AX, which becomes phosphorylated in nucleosomes adjacent to the double strand break (DSB) (reviewed in Wurtele and Verreault, 2006). Furthermore, histone 2Av acetylation by the

drosophila homolog of Tip60 is needed for the exchange of histones at sites of DNA damage (Kusch et al., 2004).

Also, it was found that the knockdown of Tip60 compromises the cellular response to UV irradiation (Tyteca et al., 2006). Moreover, the overexpression of a HAT-deficient Tip60 mutant led to inhibition of apoptosis after UV irradiation (Ikura et al., 2000). The functions of Tip60 in DNA damage response and transcriptional control are likely to contribute together and in a complex manner to the cellular response to genotoxic stress.

Apart from playing a role in tumor suppression, Tip60 has also been implicated in tumor promotion. This is in part due to its role as an activator of E2F-induced transcription, which is needed for cell cycle progression (Taubert et al., 2004). The transcription factor Myc has also been shown to rely on the HAT-activity of Tip60. In this case, the recruitment is mediated by the TRRAP protein (Frank et al., 2003). Furthermore, Tip60 was described to acetylate the tumor suppressor pRb (retinoblastoma protein), resulting in its accelerated degradation (Leduc et al., 2006).

2.3.1   The role of Tip60 in the p53 pathway

Experiments based on RNA interference showed that reduced Tip60 levels bypassed p53-induced cellcycle arrest in human cells, suggesting that Tip60 is rate limiting for the biological activity of p53 (Berns et al., 2004; Legube et al., 2004; Tyteca et al., 2006). In addition to preventing p53-dependent cell cycle arrest, Tip60 knockdown also prevented induction of the CDK inhibitor p21 (Berns et al., 2004; Legube et al., 2004; Tyteca et al., 2006). Furthermore, overexpression of Tip60 together with p53 enhanced p21 expression levels in 293T cells (Doyon et al., 2004). Given the fact that Tip60 is a *bona fide* histone acetyl transferase, these findings suggest a role of Tip60 as a transcriptional coactivator of p53. In fact, p53 induced histone H4 acetylation on its target promotors but it is unclear whether this is mediated by Tip60 (Kaeser and Iggo, 2004).

However, Tip60 was also found to bind the p53-antagonist Mdm2, which had initially been reported to result in the ubiquitination and subsequent degradation of Tip60. This Mdm2-mediated degradation was abolished after UV-irradiation, revealing a co-regulation of Tip60 and p53 upon DNA damage. Strikingly, this interaction did not only affect the Tip60 protein but in turn also led to inhibition of the Mdm2-dependent p53

degradation (Legube et al., 2004). Interestingly, Tip60 is not capable of inhibiting the Mdm2-mediated ubiquitination of p53.

Taking into account that Mdm2 not only affects p53 abundance by targeting it for degradation by ubiquitination, but also its transcriptional activity by Neddylation, this prompted us to ask whether Tip60 might additionally interfere with this activity.

In this work it should be investigated how Tip60 contributes to tumor suppression with the focus on the Mdm2-p53-pathway.

2.4 The cellular response to UV irradiation

UV light is electromagnetic radiation emitted from the sun (or an artificial source) and it is divided to three areas according to its wavelength: UV-A 315-380 nmn, UVB 280 – 315 nm and UV-C 190-280 nm. The ozone layer absorbs solar UV-C and most of UV-B, and it is estimated that 1-10% of UV radiation on the surface of Earth is UV-B and over 90% UV-A. However, the proportion of shorter wavelengths is increasing due to stratopheric ozone depletion (Lloyd, 1993).

UV irradiation damages the cell mainly by directly affecting the DNA and by the production of reactive oxygen species that then damage other cellular components. The most apparent types of UV-radiation induced DNA damage are cyclobutane-type pyrimidine dimers and (6-4)-photoproducts, which crosslink adjacent DNA bases (Ravant et al., 2001). The DNA damage induced by UV radiation triggers several signaling cascades to provoke a cellular response.

Cellular response to UV radiation depends on the cell type, the wavelength, and the dose of UV radiation inflicted on the cells. Several studies have used UV-C radiation. Although it is not a physiological wavelength, it serves as a good model to study the UV induced bulky DNA lesions.

After the DNA damage is recognized, the primary cellular DNA damage sensors are activated; these include the phosphoinoside-3-kinase (PI-3-kinase)-related proteins ATM and ataxia telangiactasia related (ATR), which have overlapping functions. ATM is essential for IR (ionizing radiation)-induced and ATR for UV-induced phosphorylation of several G1/S checkpoint kinases. The checkpoint kinases Chk1 and Chk2 phosphorylate among other subtrates also p53, leading to its activation and subsequent cell cycle arrest by induction of p21 (reviewed in Latonen and Laiho, 2005) and (see chapter 2.1).

Low doses of UV irradiation induce a transient cell cycle arrest with the transient induction of p53, whereas high doses of UV radiation induce apoptosis correlating with a slower, but more sustained and, perhaps, more pronounced induction of p53. The apoptotic p53 UV response involves the upregulation of apoptotic targets like *Bax* or *Noxa* (reviewed in Latonen and Laiho, 2005).

The repair of UV-induced DNA lesions is launched immediately after a UV insult. The helix-distorting DNA adducts induced by UV irradiation are repaired by nucleotide excision repair (NER) in mammalian cells (de Laat et al., 1999).

One of the proteins that is involved in the signal transduction of DNA damage signals is the p53BP1 protein, which functions as a sensor of DNA double strand breaks (reviewed in Adams and Carpenter, 2006).

Furthermore, UV radiation results in activation (phosphorylation) of the MAP kinases (mitogen activated protein kinases), the jun-N-terminal kinase (JNK) and the p38 kinase. The induction of MAP kinases depends on the dose, time, and wavelength of UV radiation, subsequently regulating cell growth control, survival, chromatin remodeling, and apoptosis (Bode and Dong, 2003). The JNK protein phosphorylates among other factors the transcription factor c-jun, leading to its activation (Derijard et al., 1994; Hibi et al., 1993).

As sensors of DNA damage and cellular stress the PML nuclear bodies also play a role in the response to UV irradiation. UV radiation causes rapid rearrangements of PML NBs and promotes PML-p53 and PML-Mdm2 complex formation, coincinding with p53 stabilization (Kurki et al., 2003). In addition, UV radiation leads to an increase in both PML protein levels and in the number of PML NBs (de Stanchina et al., 2004; Xu et al., 2003). Moreover, knockdown of PML sensitizes cells to UV-induced apoptosis.

One of the proteins that is associated with the PML NBs and interacts with the PML protein is the death domain associated protein (Daxx). Daxx was originally cloned as a CD95 (FAS)-interacting protein and modulator of FAS-induced cell death (reviewed in Salomoni and Khelifi, 2006). It has been implicated in the induction of UV-induced apoptosis by JNK (Khelifi et al., 2005; Wu et al., 2002).

UV irradiation moreover leads to a stabilization of Tip60 by interfering with the Mdm2-mediated degradation of Tip60 (Legube et al., 2002) (see chapter 2.3).

Following UV irradiation, knockdown of Tip60 compromises the ability of p53 to bind to its target sequences on the p21 promotor (Tyteca et al., 2006).

2.5 Questions to be addressed in this work

The following questions should be addressed in this work:

- Which impact does Tip60 have on the protein levels of Mdm2 and p53?

- Does Tip60 interfere with the E3 ligase activities of Mdm2, e.g. ubiquitination and neddylation actvities?

- Which domains on Tip60 are required for the regulation of Mdm2 and p53?

- Is the direct association of Tip60 with Mdm2 required for its impact on Mdm2?

- What role does Tip60 play in the transactivation of p53-responsive genes?

- By what mechanism does Tip60 contribute to the cellular response to ultraviolet irradiation?

3 MATERIAL

3.1 Chemicals

Agarose electrophoresis grade	Sigma
Ampicillin	Roche
Ammonium persulfat	BioRad
1,4-Diazobicyclo-[2.2.2]-oktan [DABCO]	Sigma
1,4-Dithiothreit [DTT]	Sigma
Bovine serum albumin (BSA)	New England Biolabs
Bromphenolblue	Serva
Calciumchloride	Merck Eurolab GmbH
Complete Mini-Protease inhibitor EDTA-free Tablets	Roche Applied Science
Complete Protease inhibitor EDTA-free Tablets	Roche Applied Science
Chelating Fast Flow sepharose	Amersham Bioscience
Cycloheximide	Sigma
Desoxycholate	Sigma
DNA-standard „1kb plus"	Invitrogen
dNTP-mix	Invitrogen
Dimethylsufoxide	Merck
Ethanol	Fluka
Ethylen diamin tetra acetate (EDTA)	Roth
Glycogen	Roche Applied Science
High performance Nickel sepharose	Amersham Bioscience
Fluoprep	bioMerieux
Isopropanol	Merck
Imidazole	Sigma
Iodacetamide	Sigma
Kanamycin	Roche
Methanol	Bie & Berntsen
MG132 (Proteasome inhibitor)	Sigma
Milk powder	Töpfer
N,N,N´,N´-Tetramethylendiamin (TEMED)	Bio-Rad
Protein A Sepharose (4 Cl-B)	Amersham
Protein-standard "SeeBlue® Plus 2"	Invitrogen

Protein-standard „Benchmark"	Invitrogen
Paraformaldehyde (PFA)	Merck Eurolab GmbH
Rotiphorese (30% acrylamide solution)	Roth
Sodiumhydrogendiphosphate	Sigma
Sodiumhydrogenphosphate	Sigma
Sodiumchloride	Riedel de Haen
Sodiumdodecylsulfate (SDS)	Merck Eurolab GmbH
Tetracyclin	Invitrogen
Traysol	Bayer
Triton-X100	Sigma
Trypsin-EDTA	Invitrogen
Trizol$^®$	Invitrogen
Urea	Bie & Berntsen

3.2 Enzymes

Alkaline phosphatase (from calf instestine)	Roche Applied Science
Expand HIFI polymerase system	Roche Applied Science
Pfu Turbo® [2,5U/µl]	Stratagene
Restriction endonucleases	New England Biolabs
T4-DNA-Ligase [30 Weiss units/µl]	MBI Fermentas

3.3 Kits

Pure Yield™ Midi Prep System	Promega
BIORAD Protein Assay	Bio-Rad
E.Z.N.A.® Plasmid Miniprep Kit II	peqlab
Lipofectamine™2000	Invitrogen
Firefly Luciferase Assay Kit	Promega
First strand cDNA synthesis kit	Roche Applied Science
QIAquick Gel Extraction Kit	Qiagen
LightCycler® DNA Master SYBR Green I	Roche Applied Science
SuperSignal® West Femto Maximum	Pierce
SuperSignal® West Dura	Pierce

3.4 Consumables

6/12/24-well cell culture dishes	Greiner
35mm cell culture plates	Greiner
sealing film for membranes	Krupp
1,5 ml and 2 ml reaction tubes	Eppendorf
1,5 ml sonication tubes "M5001-EX"	Laboratory Products
cryovials	Nunc
cell scraper	Sarstedt
sterile plastic pipettes	Costar
X-Ray films	Amersham Biotech
Gel-Blotting-Paper GB002 (Whatman-Papier)	Schleicher und Schuell
Chamberslides LabTEK®	Nalge Nunc Int.
PCR-tubes MicroAmp®	PE Biosystems
PVDF membrane (pore size: 0,45µm)	Schleicher und Schuell
PROTRAN® Nitrocellulose Transfer Membrane (pore size: 0,2µm)	Schleicher und Schuell
cell culture flasks (162 cm^2, 75 cm^2, 30 cm^2)	Greiner
100µl reaction tubes	Applied Biosystems
96 well frame with 8 well stripes	Nalge Nunc Int.
Optical adhesive Cover Starter Kit	Applied Biosystems
Lightcycler 20µl glass capillaries	Roche
MicroAmp™ Optical 96 well Reaction Plate with barcode	Applied Biosystems
8-16% Gradient Gels PAGEr Gold Standard	Cambrex
4-12% Gradient Gels PAGEr Gold Standard	Cambrex
7,5% PAGEr Gold Standard Gel	Cambrex
Syringes	BD-PlastiPak
Needles	BD-PlastiPak
nuclease free water	Ambion
Mini gel chamber	Invitrogen

3.5 Antibodies

Primary antibodies

name	dilution	application	species origin	manufacturer
anti-p53 (Ab-6) (DO-1)	1:3,000	WB	mouse monoclonal	Calbiochem
anti-p53 (Ab-2)(1801)	1:3,000	WB	mouse monoclonal	Calbiochem
anti-p53 (FL393)	1:300	IF	rabbit polyclonal	Santa Cruz Biotechnology
anti-Mdm2 (2A10)	1:100	WB	mouse monoclonal	Hydridoma-Supernatant
anti-α-Actin	1:50,000	WB	mouse monoclonal	Santa Cruz Biotechnology
anti-beta-Galactosidase	1:3,000	WB	mouse monoclonal	Promega
anti-p21=anti-WAF1(Ab-1) (clone EA10)	1:1,000	WB	mouse monoclonal	Oncogene
anti-EGFP	1:300	IF	rabbit polyclonal	Abcam
anti-p63 (4A4)	1:300	IF	mouse monoclonal	Santa Cruz Biotechnology
anti-SV40 LT-Ag (Pab419)	1:300	IP	mouse monoclonal	Hybridoma-supernatant
anti-HA-tag (HA.11)	1:1,000	WB/IF/IP	mouse monoclonal	Covance
anti-Phospho-JNK	1:1,000	WB	rabbit polyclonal	Cell Signalling Technology
anti-total-JNK	1:1,000	WB	rabbit polyclonal	Cell Signalling Technology
anti-PARP	1:2,000	WB	mouse monoclonal	Oncogene
anti-PML (PG-M3)	1:50	IF	mouse monoclonal	Santa Cruz Biotechnology
anti-gamma-H2AX(Ser139)	1:10,000	WB	mouse monoclonal	Upstate

Secondary antibodies

name	dilution	manufacturer
Peroxidase-conjugated Affinipure Goat Anti-mouse IgG (H+L)	1:15,000	Jackson ImmunoResearch
Peroxidase-conjugated Affinipure Rabbit Anti-mouse IgG (H+L)	1:15,000	Jackson ImmunoResearch
Alexa Fluor® 488 goat anti-mouse IgG (H+L)	1:500	Molecular Probes
Alexa Fluor® 488 goat anti-rabbit IgG (H+L)	1:500	Molecular Probes

Alexa Fluor® 594 goat anti-mouse IgG (H+L)	1:500	Molecular Probes
Alexa Fluor® 594 goat anti-rabbit IgG (H+L)	1:500	Molecular Probes

3.6 Cell culture media & supplements

Ciprofloxacin (Ciprobay®)	Bayer
Dulbecco`s Modified Eagle Medium (DMEM)	Invitrogen
Fetal bovine calf serum (FBS)	Invitrogen
L-Glutamine	Invitrogen
Penicillin/Streptomycin	Invitrogen
Tetracyclin	Invitrogen
Trypsin/EDTA	Invitrogen

DMEM (complete) contains:

10 µg/ml	Ciprobay
50 U/ml	Penicillin
50 µg/ml	Streptomycine
2 µg/ml	Tetracycline
10%	FCS
200 µM	L-Glutamine

Bacterial media and supplements

Ampicillin [ad 200 µg / ml]	Sigma
Kanamycin [ad 25 µg / ml]	Sigma

LB- Medium
- 10 g Peptone, pancreatic digest (or Tryptone)
- 5 g Yeast extract
- 5 g NaCl
- Fill up to 1000ml

2YT-Medium
- 16 g Peptone, pancreatic digest (or Tryptone)
- 10 g Yeast extract
- 5 g NaCl
- Fill up to 1000ml

3.7 Bacteria and human cells

Bacteria

Escherichia coli DH 10 B   Invitrogen

Human cells

H1299	cancer cells derived from a lung tumour, p53$^{-/-}$	A.J. Levine
U2OS	osteosarcoma cells, p53$^{+/+}$	ATCC
MEF *pml*$^{+/+}$	mouse embryonic fibroblasts	Marikki Laiho, Piero Pandolfi
MEF *pml*$^{-/-}$	mouse embryonic fibroblasts	Marikki Laiho, Piero Pandolfi

3.8 Oligonucleotides

All oligonucleotides were synthesized by MWG Biotech, Ebersberg.

(Orientation 5'→3'; restriction sites underlined, complementary sequences underlined twice)

oligo dT -Primer	oligo dT
GAPDH rev primer	GCA GAG ATG ATG ACC CTT TTG GCT C
GAPDH for primer	TGA AGG TCG GAG TCA ACG GAT TTG GT
HTATIP rev primer	GAG GAA AGG GTC TGT GTC ATA G
HTATIP for primer	CCG TAG TCT CAA GTG TCT TCA G
p21 for	CCT GGC ACC TCA CCT GCT CTG CTG
p21 rev	GCA GAA GAT GTA GAG CGG GCC TTT
His12for	CGC G<u>GG ATC C</u>GC CAT GCA TCA TCA TCA TCA T<u><u>GG AGC AGG TGC AGG C</u></u>
HisNedd8for	<u><u>GGA GCA GGT GCA GGC</u></u> CAT CAT CAT CAT CAT CAT ATG CTA ATT AAA GTG AAG AC
HisNedd8rev	CGC G<u>AG ATC T</u>AG TGA CGG ATT CTG GTG GAG G
HIsSUMO-1for	<u><u>GGA GCA GGT GCA GGC</u></u> CAT CAT CAT CAT CAT CAT ATG TCT GAC CAG GAG GCA AAA CCT
HisSUMO-1rev	CGC G<u>AG ATC T</u>GA TTT GAC AAC TTA CTG G

3.9 Plasmids and vectors

pcDNA3.1-HA-Tip60	Didier Trouché (Legube et al., 2002)
pEGFP-COP1	X.W. Deng (Yi et al., 2002)
pC1-EGFP-Mdm2	Claudia Lenz-Bauer
pcDNA3	Invitrogen
pCMV-Mdm2	Bert Vogelstein
pBP100-Luc	(Freedman et al., 1997)
pcDNA3-HA-Nedd8	Edward T.H. Yeh (Kamitani et al., 1997)
pcDNA3-HA-SUMO-1	Ronald T. Hay (Rodriguez et al., 1999)
pcDNA3-His12-Nedd8	see chapter 4.3.5
pcDNA3-His12-SUMO-1	see chapter 4.3.5
pCDNA3-His6-Ubiquitin	Dirk Bohmann (Treier et al., 1994)
pCMV2-flag-UbcH8	Dong Er-Zhang (Kim et al., 2004)
pcDNA3.1-His6-hUbc12	Aaron Ciechanover (Amir et al., 2002)
pCMVSPORT6-beta-Gal	Invitrogen
pcDNA3-Myc-p14arf	Yue Xiong (Zhang et al., 1998)
pRc-p53	A.J. Levine (Lin et al., 1994)
pcDNA3.1-HA-Tip60deltaMYST	Max Koeppel
pcDNA3.1-HA-Tip60deltaHAT	Max Koeppel
pcDNA3.1-HA-Tip60deltaExon5	Max Koeppel
pcDNA3.1-HA-Tip60_STOP263	Max Koeppel
pcDNA3.1-HA-Tip60_STOP390	Max Koeppel

3.10 siRNA

All siRNAs were purchased at Ambion, Inc.; 20nM, annealed,

target sequences are given in 5'->3' direction. All siRNAs were synthesised with a 3'-dTdT overhang.

siRNA name	siRNA target sequence	Reference
siRNA *TP53*	GACUCCAGUGGUAAUCUACtt	(Tiscornia et al., 2004)
siRNA *HTATIP* #1	GGUGGAGGUGGUUUCACCAtt	Ambion pre-designed siRNA
siRNA *HTATIP* #2	GGUGGUUUCACCAGCAACUtt	Ambion pre-designed siRNA
siRNA *HTATIP* #3	GGAGAAAGAAUCAACGGAAtt	Ambion pre-designed siRNA
siRNA Negative Control #1	sequence unknown (commercial)	Ambion
siRNA *TP53BP1* #1	GATACTGCCTCATCACAGTtt	(Brummelkamp et al., 2006)
siRNA *MDM2*	AAGCCAUUGCUUUUGAAGUUAtt	(Rodway et al., 2004)

3.11 Buffers

6x DNA Sample buffer: 0,25 % Bromphenolblue

                                                       40 % Sucrose

                                                       10 % Glycerol

EB buffer: 10mM Tris (pH 8,5)

6x Laemmli buffer: 0,35 M Tris pH 6,8

                                                       30 % Glycerol (v/v)

                                                       10% SDS (w/v)

                                                   9,3 % Dithiotreitol (w/v)

                                         0,015 % Bromphenolblue (w/v)

10x Buffer for Proteingels: 0,1 % SDS

                                                 25 mM Tris

                                         192 mM Glycine

Transfer buffer for Wet blot: 100 ml Western-Salts (10x)

                                                   700 ml dH$_2$O

                                                 150 ml Methanol

PBS^{++} (phosphate buffered saline)   236,9 mM NaCl

                                               2,7 mM KCl

                                               8,1 mM Na$_2$HPO$_4$

                                               1,1 mM MgCl$_2$

                                               1,5 mM KH$_2$PO$_4$

                                               1,2 mM CaCl$_2$

PBS^{deficient} : same as PBS^{++} , but without MgCl$_2$ and CaCl$_2$

RIPA-buffer: 0,1 % Triton X-100 (v/v)

                                               0,1 % Desoxycholate, DOC (v/v)

                                               0,1 % SDS (w/v)

                                               2 mM Tris / HCl pH 8,5

	9 mM	NaCl
	1 mM	EDTA
	1,4 %	Traysol
	18,5 %	Iodacetamide

50x TAE-buffer:	2 M	Tris
	1 M	Natriumacetate
	0,1 %	EDTA

10x TBE-buffer:	40 mM	Tris
	0,05 mM	EDTA
	0,89 M	Boric acid

Western-Salts (10x):	60,55 g	Tris
	288,1 g	Glycine
	4 ml	10 % SDS (equivalent to 0,02 %)
	ad 2000 ml	H_2O bidest.
		adjust pH to 8,3

Stripping buffer	628µl	beta-Mercaptoethanol
	62,5 mM	Tris-HCl pH 6.8
	2%	SDS
	ad 100ml	H_2O bidest.

Ponceau S solution	100 ml	H_2O bidest
	0,5g	Ponceau S
	1 ml	acetic acid (100%)

Nickel-Pulldown lysis-buffer	0,1 M	Na_2HPO_4/NaH_2PO_4
	0,01 M	Tris-HCl pH 8,0
	10 mM	Beta-Mercaptoethanol
	8 M	Urea

	1 tablet / 7ml	Mini-EDTA free protease inhibitor tablet
	20mM	Imidazole

Nickel-Pulldown washing buffer 1 (WB1)	as lysis buffer	but without Imidazole

Nickel-Pulldown washing buffer 2 (WB2)	0,1 M	Na2HPO4/NaH2PO4
	0,01 M	Tris-HCl pH 6,3
	10 mM	Beta-Mercaptoethanol
	8 M	Urea
	0,2%	Triton-X100

Nickel-Pulldown washing buffer 3 (WB3)	as WB2	but without Triton-X-100
	20 mM	Imidazole

Nickel-Pulldown elution buffer	as WB2	but with
	500 mM	Imidazole

co-IP buffer	300 mM	NaCl
	0,5%	Nonidet P-40
	5 mM	$MgCl_2$
	10% (v/v)	Glycerol
	50 mM	Tris-HCl pH 8.0
	1 tablet /50 ml	Protease-inihibitor EDTA-free tablet
	ad to 100ml	PBS[def.]

3.12 Instruments

Name	*Manufacturer*
Gel Doc 200	BioRad
GeneQuant Pro	Amersham Biotech
PCR Cycler "Primus"	MWG Biotech
PCR Cycler „Gene Amp PCR System 2400"	Perkin Elmer

Gene Pulser II (Electroporation)	Bio-Rad
Western Blot Chamber	Bio-Rad /Invitrogen
X-Ray Developing-Machine „Optimax2010"	Protec
Incubator „Hera Cell"	Heraeus
Heat block " Thermomixer comfort"	Eppendorf
Lightcycler 2.0®	Roche Applied Science
Realtime-PCR-system 7300	Applied Biosystems
Table Cooling centrifuge "MIKRO 22 R"	Hettich
Cooling centrifuge "Rotina 35R"	Hettich
Table centrifuge "Biofuge Pico"	Heraeus
Rotator „PTR-30"	Grant-Bio
UV Crosslinker „UVC-500"	Hoefer Inc.
Luminometer „Lumistar"	BMG Labtech
Power supply for electrophoresis	Invitrogen / E-C Apparatus Corporation
Freezer -80°C	Siemens
Freezer -20°C	Siemens
Vortexer „Vortex Genie2"	Scientific Industries
Incubator for bacteria "Innova 44"	New England Biolabs
Microwave	Panasonic
PCR thermo cycler "Primus"	MWG Biotech
Shaker	Labnet
pH-meter "PHM210"	Radiometer analytics
Pipetting Aid „Pipettus"	Hirschmann Laborgeräte
Film-sealing device „Quick Seal"	Möllerström AB
Sterile bench	Holten /Heraeus
Research Pipettes	Eppendorf
Sonicator "Bioruptor"	Diagenode

4 METHODS

4.1 Methods in cellular biology

4.1.1 Cell culture

The adherent cells were grown in cell culture flasks with a filter closure in a 37°C incubator at 5% CO_2 and 95% humidity. All cell lines were maintained in Dulbecco's modified eagle media supplemented with 10% fetal bovine serum, L-glutamine, penicillin/streptomycin, ciprofloxacin and tetracyclin. Cell culture work was done in a laminar flow.

Passaging of cells

Passaging of cells was performed by removing the medium followed by washing twice with PBS[def.] to remove remaining dead cells and the rests of FBS that would neutralize the trypsin. Finally, 3 ml Trypsin were added and cells were incubated for a few minutes in the incubator until the adhesion between the cells and the cell culture flask was abolished. The trypsin was then neutralized by adding 10 ml of fresh medium, and the cells were carefully resuspended. After this step, the cells were counted and seeded for following experiments, just diluted and passed to new culture flasks (passage), or frozen.

Counting of cells

The number of cells in a suspension was determined by using a Neubauer chamber. A drop of the cell suspension was transferred to the chamber. The cells in the 4 fields (each with 16 smaller ones) were counted. The number obtained was divided by four and multiplied by 10^4, yielding the number of cells per ml of the cell suspension.

Freezing and thawing of cells

For freezing, a 182-cm^2 – culture flask with confluent cells was used to obtain 3 aliquots. Cells were washed with PBS[def], trypsinized, resuspended in new medium and centrifuged 5 min at 800 rpm. The supernatant was removed and the cell pellet was resuspended in a cold solution of 10% DMSO in FBS. 1ml aliquots were distributed into cryovials. After 1-3 minutes on ice, the cryotubes were wrapped into paper towels, which then were transferred into 50ml centrifuge tubes. The so

prepared tubes were then frozen in the -80°C freezer over night and subsequently transferred to the liquid nitrogen tank.

For thawing cells, a culture flask with new warm medium was prepared first. An aliquot was removed from the liquid nitrogen, thawed in the hand, and the cells were transferred quickly into the flask and incubated at 37°C. On the next day, the culture medium was changed.

4.1.2 Transient transfection of Eukaryotic Cells

Depending on the nucleic acid to be transfected, the cells were seeded at concentrations of 60-70.000 cells per ml for siRNA transfection or 100.000 cells per ml for DNA transfection. Cells were seeded into different cell culture plates, 6/12 well dishes or 4well/8well chamber slides. The total amount of plasmid DNA and siRNA to be used was optimized for the transfection reagent. If necessary, the empty vector pcDNA3 or the control-siRNA was added to achieve the ideal amount of DNA or siRNA. For each cell line, the choice of the method to be used was done according to the transfection efficiency and toxicity of the different transfection reagents. All transfections were perfomed with Lipofectamine 2000™.

Transfection with Lipofectamine 2000™

The following table shows the amount of transfection reagent and media used for the transfection of DNA and siRNA:

Reagent	Nullmedia for reagent	DNA	siRNA	Null media for nucleic acids
8µl	200µl	2,4 µg	-------	200µl
4µl	200µl	-------	80pmol	200µl

Procedure	Time
Add nucleic acid to null media	
Add Lipofectamine to null media	
Vortex	
Incubation at room temperature (RT)	5 min
Mix both preparations and vortex	
Incubation at RT	20 min
Add 400µl Lipofectamine 2000™-nucleoacid-mixture to one 6 well and rock gently	

4.1.3 UV irradiation of cultured cells

For the irradiation of cultured cells with UV-C light (254 nm), using the UV-crosslinker, the cells were seeded in 6well or 12well dishes and transfected or treated and 36 h post transfection the cells were washed once with PBS^{def.} to ensure no liquid or proteins would impair the UV-irradiation. After carefully removing all PBS^{def.}, the cell culture dishes (without lid) were put into the UV-crosslinker and the irradiation was performed (lasting a few seconds). The non-irradiated control cells were treated in the same way but were left under the sterile bench. After irradiation, fresh medium was added and the cells were incubated for a specific time until harvesting.

4.1.4 Cycloheximide (CHX) treatment of cultured cells

In order to study the half-life of a protein of interest, a cycloheximide chase experiment was performed. To this end, the cells were grown in 12well cell culture dishes and transfected after 24 h. After further 24 hours, the medium was removed and fresh medium with 50 µg/ml cycloheximide was added, followed by harvesting at different time points after treatment as described in chapter 4.2.2.

4.1.5 Treatment of cultured cells with proteasome inhibitor

For Nickel histidine pulldown assays of ubiquitinated proteins by coexpressing His-6-Ubiquitin, the proteasome inhibitor MG132 (Sigma) (based on a small peptide) was added to the the cell culture medium 36 h post transfection at a concentration of 40µM after removing the old medium. MG132 protects ubiqitinated proteins from degradation by the proteasome, allowing their detection in the immunostaining after the his-tag pulldown procedure (chapter 4.2.5).

4.2   Biochemical and immunological methods

4.2.1   Indirect immunofluorescence

For the protein analysis by indirect immunofluorescence, 5×10^4 cells were seeded into each well of a 4well chamberslide. For 8well chamberslides, half the amount was used. On the next day, the cells were transfected with different plasmids. Twenty-four

hours after transfection, the medium was carefully removed and the cells were washed with PBS^{++}, fixed with 4% paraformaldehyde in PBS^{++} for 15 min at RT or overnight at 4°C, washed again with PBS^{++}, permeabilized with 0,2% Triton-X-100 in PBS^{++} for 15 min and washed three times with PBS^{++}. The cells were then blocked with 10% FBS in PBS^{++} (blocking solution) for 10 min. This was followed by the incubation with the primary antibody (protein specific, diluted in blocking solution, usually 1:300) for 1 h. The cells were then washed twice shortly and once for 5 min with PBS^{++}. Afterwards, the secondary antibody (species specific, diluted 1:500 in blocking solution) was added, followed by 30 min incubation in the dark. For the additional staining of the nuclei, DAPI (10 mg/ml) was diluted 1:5,000 in the secondary antibody mixture. After incubation the cells were washed (2x shortly and once for 5 min with PBS^{++} and the preparation was mounted using Fluoprep (0,2% DABCO). All incubation steps were performed at room temperature. After at least 30 min drying time, the slides were observed under the microscope and pictures were taken, using a digital camera.

4.2.2 Western Blot Analysis

<u>Cell harvest and sample preparation</u>

For protein analysis by Western Blot, the cells were harvested by scraping, transferred into a reaction tube and centrifugated at 3000 rpm at RT for 5 min. After removing the supernatant, the cell pellets were dry vortexed and immediately 100 µl of ice-cold RIPA buffer was added followed by repeated vortexing. For the detection of cleaved PARP, Nickel-Pulldown lysis buffer was used. Depending on the kind of comb and the size of the pockets, 15 µl (17er comb), 20 µl (15er comb), 25 µl (12er comb) or 40µl of the sample (10er comb) were loaded.
25 µl of 6x Laemmli buffer was added and the samples were heated at 96ºC for 5 min. The tubes were then vigorously rocked for 15 min at 4ºC (to shear the DNA) and centrifugated for 10 min at 14.000 rpm (to remove cell debris). If the samples were not directly analyzed by SDS-PAGE, they were frozen at -20 ºC.

<u>SDS-PAGE (sodium dodecyl sulfate-polyacrylamide gel electrophoresis)</u>

The denatured and negatively charged proteins were separated in a SDS-PAGE. For some applications, which required an increased range of good separation, ready-to-

use gradient gels were used that were purchased at Cambrex (USA). For the rest of the experiments, the gels were poured, using the BioRad or Invitrogen system. The gels were either 8, 10 or 12% acrylamide. The stacking gel was always 5%. The two parts of the gel were prepared as follows:

Resolving gel (for 20ml total volume)			
	8%	**10%**	**12%**
30% acrylamide	9,3 ml	7,9 ml	6,6 ml
dH$_2$O	5,3 ml	6,7 ml	8,0 ml
1,5 M Tris-HCl pH 8,8	5,0 ml	5,0 ml	5,0 ml
10% SDS	200 µl	200 µl	200 µl
10% APS (ammonium persufate)	200 µl	200 µl	200 µl
TEMED	12 µl	8 µl	8 µl

After pouring, 100% Isopropanol was carefully added to obtain an equally horizontal surface.

Stacking gel (5%)(for 5 ml total volume)	
30% acrylamide	830 µl
dH$_2$O	3,4 ml
1 M Tris-HCl pH 6,8	630 µl
10% SDS	50 µl
10% APS (ammonium persufate)	50 µl
TEMED	5µl

The protein marker "Benchmark prestained" (Invitrogen) or "SeeBlue® Plus 2 prestained" (Invitrogen) and 25µl of sample were used. The electrophoresis was performed at 80, 120 and 150 V subsequently, in 1x SDS-PAGE running buffer, until the desired separation was obtained.

Western Blot (Wet Blot)

As the method of protein transfer onto membranes, the Wet-Blot procedure was chosen (Nitrocellulose or PVDF). This required one Western Blot buffer (transfer buffer, chapter 3.11). The PVDF membrane first had to be activated by incubation in 100% methanol for 15 s, 2 min in dH$_2$O and 5 min in transfer buffer.

The sponges and whatman papers were soaked well with transferbuffer and the nitrocellulose membrane was put in water for a few minutes before soaking it with transferbuffer. Before blotting, the stacking gel was removed using a scapel.

setup:

Cathode

Sponge
2 Layers Whatman-Paper
Polyacrylamide gel
Nitrocellulose membrane
2 Layers Whatman-Paper
Sponge

Anode

The proteins were transferred using a constant voltage of 90V for 2h (or 37V over night) (BioRad system) or 25V for 2h (or 18V over night) (Invitrogen system).

Protein detection (Immunostaining)

After blotting, the membrane was immediately stained with Ponceau S to check wether equal amounts of proteins had been transferred onto the membrane. The side that was in contact with the gel was marked. The nitrocellulose was then blocked in a solution of 5% milk powder and 0,1% Tween in PBS$^{def.}$ („milk") for 30 min, followed by incubation with the protein-specific antibody (diluted in milk). To save antibody, the membrane was sealed in a plastic film with approx. 4-5 ml milk and incubated for 2 h at room temperature or over night at 4ºC on a shaker at 60 rpm. After this, the membrane was washed several times: twice 3x shortly with PBSdef. and 15 min in milk. The species specific antibody was added (a horseradish-peroxidase coupled IgG or Fab-fragment, usually diluted 1:20.000 in milk) followed by 1 h incubation on the shaker.

Finally, the proteins were detected using enhanced chemiluminescence. A 1:1 mixture of the components A (Luminol/Enhancer) and B (Peroxide solution) of SuperSignal West Dura (Pierce) was added to the membrane (in a polyethylene-sealing-bag). If a higher sensitivity was required, SuperSignal West Femto Maximum (Pierce) was used. The excess of substrate was removed, and a sensitive film

(Amersham Biosciences) was exposed to the membrane and developed. The time of exposure necessary was dependent on the protein to be analysed and on the antibody dilutions used.

Ponceau S-staining of Western Blots

Using Ponceau S solution (0,1% Ponceau S (w/v) in 1% acetic acid) proteins can be visualised unspecifically. To this end, the membranes were washed with H_2O and incubated for 1 min with the Ponceau S solution. After that, the membrane was rinsed with water until the protein bands became clearly visible. The staining was documented by wrapping the blot into sealing film and scanning. In order to reverse the staining, the blot was washed in $PBS^{def.}$ /0,1% Tween.

Removing antibodies from a membrane

If a membrane had to be stained against different proteins after each other, it sometimes was required to reverse the previous staining in order to exclude cross-stainings. To this end, the membrane was incubated with stripping buffer in a closed 50 ml plastic tube for 30 min and 50°C. After that, the membrane was washed several times with $PBS^{def.}$/0,1% Tween at RT.

4.2.3 Co-immunoprecipitation

Co-immunoprecipitation was used to study the association of Tip60 and its mutants with the Mdm2 protein.

The cells were scraped off in culture medium and centrifuged in sterile 15 ml tubes for 5 min at 1500 rpm (RT). After taking off the medium, the cells were resuspended in 150 µl of $PBS^{def.}$ and transferred into a 1,5 ml tube followed by centrifugation at 3000 rpm for 5 min at RT. Next, the supernatant was removed and the cell pellet was resuspended in 300 µl ice-cold co-IP buffer (freshly prepared and supplemented with protease inhibitor (Roche)) and transferred into a 1,5 ml sonication tube made of very rigid plastic to ensure efficient sonication. The sonication was performed at 4°C for 10 min in intervals at high-energy settings to shear the DNA in the sample. After sonication, the tubes were shortly spinned down and the cell suspension was transferred into a new eppendorf tube followed by centrifugation for 10 min at 14.000 rpm and 4°C to pellet the cell debris. Thereafter, 10 µl of the supernatant was taken

off as an input control and mixed with 10 µl of 6x Laemmli buffer while the rest of the sample was split into new tubes according to the number of antibodies used to immunoprecipitate. Antibodies were added as follows: anti-Mdm2 (2A10): 80 µl per sample; anti-HA-tag (HA.11): 2µl of a 1:6 dilution in dH$_2$O; anti-SV40 LT-Ag (Pab419): 20µl. The total volume of the samples was adjusted to 500 µl including the antibody and the tubes were rotated gently at 4°C over night. After incubation with the antibodies, the samples were centrifuged for 3 min at 14.000 rpm to pellet potentially disturbing precipitates and transferred into new tubes. Next, 30 µl of the protein A sepharose (50% slurry in co-IP buffer) was added, which had been equilibrated before by incubation in co-IP buffer for 30 min on the rotator followed by two wash steps in the same buffer. To ensure an equal dsitribution of protein A sepharose, the 100 µl pipette tips were cut to enlarge the opening. After 1 h incubation at 4°C on the rotator, the samples were washed 6 times with ice-cold co-IP buffer with one washing step consisting in the centrifugation for 2 min at 4°C and 7500 rpm, removing the medium with a syringe (RT) and addition of 500 µl ice-cold co-IP buffer and rotation for 5 min at RT.

Finally, the samples were centrifuged for 1 min at 14.000 rpm and 20 µl of 6x Laemmli was added after taking off the supernatant. For protein separation by SDS-PAGE, the whole sample was loaded.

4.2.4 Luciferase assay

This assay was used to study the impact of Tip60 on the transcriptional activity of overexpressed p53. 2 x 10^5 H1299 cells were seeded into 6well dishes. After 24 h, the cells were transfected with different expression plasmids encoding for the activating gene (p53) and the factors to be studied (Tip60 and p14arf). A reporter construct containing a portion of the murine *mdm2* intron that confers transcriptional response to p53 upstream of the luciferase coding region (pBP100luc) was cotransfected. Again, after 24 h post transfection, cells were harvested in the medium, transferred to a 1,5 ml tube and centrifugated for 5 min at 3000 rpm (RT). The medium was removed and each pellet was resuspended in 150 µl of reporter lysis buffer (Promega, 1:5 in H$_2$O), followed by 15 min incubation at RT with vortexing from time to time. During this procedure only the cell membrane was disrupted leaving the nucleus intact. The tubes were centrifugated at 13,000 rpm and 4°C for 3 min, to remove the intact nuclei and organelles. Thereafter, the supernatant was

directly frozen or instantly used. For the measurement of chemiluminescence (luciferase activity), 20 µl of cell lysate were transferred into a 96 well plate (Nunc) and measured in the luminometer (LUMIstar, BMG Biolabs), using the software LUMIstar 3.00-0, according to the manufacturers instructions. As a blank, 20µl of the diluted reporter lysis buffer were used. The luciferase firefly substrate was prepared by solving a luciferase substrate tablet in the freshly thawed luciferase assay buffer. The luminometer was set to inject 100µl of the substrate to each well, yielding 120 µl volume in total. Finally, the protein concentrations of the lysates were measured using the Bradford assay to normalize the luciferase activity (see chapter 4.2.5).

4.2.5 Nickel-histidin-tag-pulldown assays

The Nickel-Histidine-Tag-pulldown method is based on the Nickel-chelating characteristic of a 6x or 12x histidine strech in a polypeptide. By adding a repeat of histidines to a protein of interest, either on the N-or C-terminus, it can be used to specifically extract ("pull down") this protein by using specially modified and "Ni^{2+}loaded" sepharose. Here, this method was used to extract proteins from a cell lysate that had been modified with ubiquitin-like proteins as SUMO-1, Nedd8 or Ubiquitin itself.
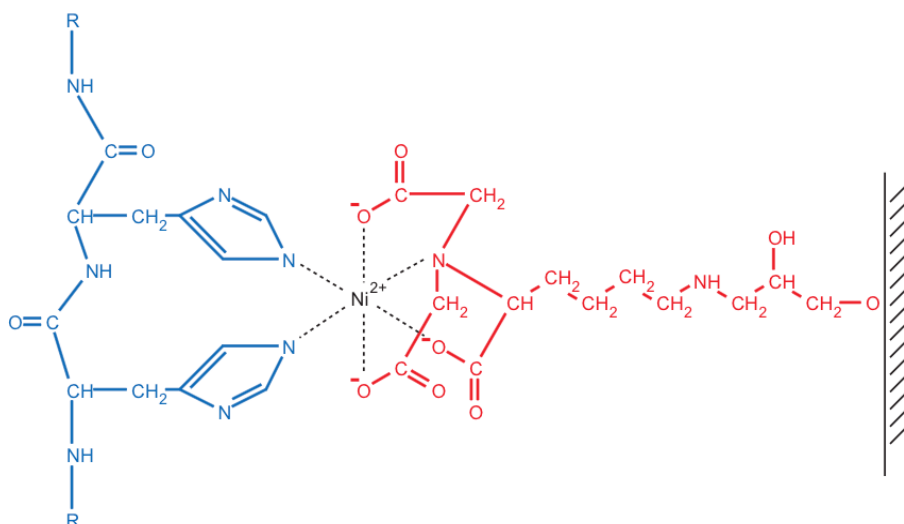

Figure 4.1: Nickel-His-tag pulldown principle
Chelate complexes between adjacent histidine side chains and Ni-ions, immobilized at a NTA-matrix (taken from the handbook „the QIAexpressionist[TM]" from Qiagen, 2003).
4 out of 6 ligand binding sites of the Ni2+ (black) are bound by nitrilo tri acetic acid (NTA; red), which is coupled to the sepharose. The remaining 2 sites are complexed by 2 histidine side chains (blue).

Cells were harvested 36 h post transfection and lysed in lysis buffer (8 M Urea, 0,1 M Na2HPO4/NaH2PO4, 0,01 M Tris-HCl pH 8.0 and 10 mM beta-mercaptoethanol

supplemented with 20mM imidazole + protease inhibitor mini tablets EDTA-free (Roche), the cell debris was pelleted by centrifugation at 14.000 rpm for 15 min at RT and the supernatant was subjected to preclearing with chelating fast flow sepharose (Amersham Bioscience). The fast flow sepharose was equilibrated first, by centrifugation at 500x g followed by a washing step with dH_2O and resuspension in one volume of lysisbuffer + protease inhibitor.

Subsequently the lysate was incubated for two hours with High Performance Nickel sepharose (Amersham Bioscience) (equilibrated as the fast flow sepharose) on a rotator, followed by one 5 min washing step with 500 µl washing buffer 1 (WB1) (lysisbuffer without imidazole), 2 washing steps with WB2 (8 M Urea, 0,1 M Na2HPO4/NaH2PO4, 0,01 M Tris-HCl pH 6.3, 10 mM beta-mercaptoethanol suppl. with 0,2% triton X-100) and 2 washing steps with WB3 (WB2 without triton X-100 + 20mM imidazole). The His-tagged proteins were eluted with 100 µl elutionbuffer (WB2 without triton X-100 + 500mM imidazole), 6x Laemmli buffer was added and the samples were subjected to SDS-PAGE and Western blot analysis. All steps were carried out at RT.

4.2.6 Measurement of protein concentrations

<u>Bradford method</u>

5µl cell lysate were transferred to a 1 ml plastic cuvette and mixed with 1 ml Bradford-reagent (BioRad, 1:5 in H_2O). The absorbances were measured at 595 nm against a blank containing no lysate but equivalent amounts of lysis buffer and Bradford reagent. The absorbances correlated with the protein concentration and were used to normalize the values obtained in the luciferase assays.

4.3 Methods in molecular biology

4.3.1 Transformation of *E. coli*

The introduction of plasmid DNA into bacteria (transformation) to produce a high number of plasmid copies was performed by using chemo- or electrocompetent bacteria.

Preparation of chemocompetent *E.coli*

5 ml LB medium were inoculated with one single colony of *E.coli* DH10B and incubated overnight at 37°C with shaking. 200 ml LB were then inoculated with 0,5 ml of the overnight culture and shaken at 37°C until the optical density (590nm) achieved 0,6 (log phase of bacterial growth). The culture was chilled on ice for 10 min and cells were harvested by centrifugation at 3,000 rpm, 5min at 4°C. The bacteria were resuspended in 50 ml of ice-cold, sterile 0,1 M $MgCl_2$, followed by 20 min incubation on ice. The suspension was centrifugated again and the cells were resuspended in 5 ml of sterile 0,1 M $CaCl_2$, followed by one hour incubation on ice. The suspension of competent cells was then brought to 15% in glycerol, distributed in 50µl aliquots, frozen in liquid nitrogen and stored at -80°C.

Chemical transformation of competent *E.coli*

Chemocompetent bacteria were transformed by the temperature-shock method. 1µl plasmid was transferred to a 1,5 ml tube together with 20µl of bacteria suspension. The tube was incubated on ice for 30 min, then for 2 min at 42°C and again on ice for 1 min. For selection with ampicillin (that inhibits the synthesis of the cell wall), the mixture was directly distributed over an ampicillin-LB plate. For selection with kanamycin (inhibitor of the 30S ribosomal subunit) the bacteria suspension was first incubated in 500 µl LB-medium at 37°C for 1 h (to enable the transcription and translation of the kanamycin inactivating enzyme), before spreading onto a kanamycin-LB-agar plate. The agar plates were incubated overnight at 37°C.

Electroporation of *E.coli*

This method is more efficient than the chemical transformation and was used for ligated DNA, during the cloning procedure.

0,5µl of the ligation sample was gently mixed with 8 µl electrocompetent *E.coli* (ElectroMAX DH10B, Invitrogen) in a pre-chilled 0,1 cm Gene-Pulser-Cuvette (BioRad). The cuvette was immediately transferred back on ice. The electroporation was perfomed using the the Gene-Pulser-Controller at 1,7 kV, 200 Ω and 25 µF followed by the addition of 250 µl LB-Medium to the bacterial suspension and treated as described above.

After striking out the bacteria on an agar plate, the plates were incubated at 37°C overnight.

4.3.2 Isolation of plasmid DNA

For the purification of plasmid DNA from a 2 ml bacterial suspension, the E.Z.N.A.® Plasmid Miniprep Kit I (peqlab) was used. For the preparation of higher amounts of DNA, 15-30 ml bacteria-suspensions and the E.Z.N.A. Plasmid MiniPrep Kit II or the Pure Yield™ Midi Prep System (Promega) were used. All kits were used according to the manual's instructions.

The procedure is based on the alkaline lysis of bacterial cells, cleaning and preparation of the lysate, adsorption of DNA to silica membranes in the presence of high salt, washing and elution of DNA with EB (elution buffer; 10 mM Tris-HCl, pH8,5).

4.3.3 Measurement of DNA/RNA concentration

To determine the concentration of a DNA or RNA preparation, 400µl of a 1:100 dilution (in water) was transferred into a quartz cuvette and the absorbance (260nm) was measured using the GeneQuantProII-photometer (Pharmacia Biotech). The concentration of dsDNA sample was calculated using a factor of 50 (1 absorbance unit corresponded to 50 µg/ml) and a factor of 40 was used for the RNA samples.

4.3.4 Polymerase chain reaction (PCR)

The PCR is used to specifically amplify a DNA sequence that is located in between two oligonucleotide fragments (Primer), which bind complementary to DNA. First, the template DNA is denatured by the application of heat (>90°C) into single strands. This phase is followed by annealing of the primers to their target sequences, which subsequently is amplified by the DNA-Polymerase through elongation of the Primers. This sequence of reactions is repeated several cycles. The new products are themselves used as new templates leading to an exponential amplification of DNA-fragments. For the amplification of larger DNA-fragments, the Expand-HIFI polymerase (EHF) system was used. The polymerase mix contained in this system allows even the amplification of long sequences of DNA (>1kb) with a relatively low error rate.

PCR-sample: 5,0 µl   10x reaction buffer

                         0,5 µl   dNTP-Mix [20 mM each]

                         1,0 µl   Forward primer [50 ng / µl]

                         1,0 µl   Reverse primer [50 ng / µl]

                      200 ng   DNA-template

                         1,0 µl   EHF Enzyme-Mix [3,5 U / µl]

                ad 50 µl dH_2O

The PCR was performed in programmable PCR machines in special thin wall PCR tubes (Applied Biosystems)

PCR-Program:

		94°C	3 min.	Denaturing
		94°C	30 s	Denaturing
40x		55°C	30 s	Annealing
		70°C	2,5 s	Elongation
		70°C	7 min	Elongation
		4°C	∞	End of reaction, storage

4.3.5 Cloning of pcDNA3-His-12-Nedd8 and pcDNA3-His-12-SUMO-1

His12-Nedd8 was amplified from pcDNA3-HA-Nedd8 in a first step with the primers HisNedd8for 5'-CGC GGG ATC CGC CAT GCA TCA TCA TCA TCA TCA TGG AGC AGG TGC AGG C-3' and HisNedd8rev 5'-CGC GAG ATC TAG TGA CGG ATT CTG GTG GAG G-3' followed by an amplification from the first product with the primers His12for GGA GCA GGT GCA GGC CAT CAT CAT CAT CAT CAT ATG CTA ATT AAA GTG AAG AC and HisNedd8rev. The PCR product containing the His-tagged Nedd8 was cloned into pcDNA3 using *Xba*I and *Bam*HI.

His12-SUMO-1 was generated by amplifying the SUMO-1 sequence from pcDNA3-HA-SUMO-1 with the primers His-SUMOfor 5'-GGA GCA GGT GCA GGC CAT CAT CAT CAT CAT CAT ATG TCT GAC CAG GAG GCA AAA CCT-3' and SUMO-1rev 5'-CGC GTC TAG AGA TTT GAC AAC TTA CTG G-3'. After that, the product was used for another amplifcation with the primers His-for and SUMO-1rev and purified and cloned into pcDNA3 using *Xba*I and *Bam*HI. The plasmids were checked by sequencing.

4.3.6 DNA restriction digest

The treatment of DNA with restrictionendonucleases represents a fast and simple method to check or modify plasmids during the construction of new vectors. An analytic sample is used for the fast check of plasmids. The complete sample is loaded onto an agarose gel after the incubation at 37°C and addition of 2µl DNA-sample buffer (6x).

The preparative sample is used to produce suitable fragments of DNA that are later inserted into a new vector. In some cases, the DNA fragment of interest has to be purified by separation on a agarose gel followed by its extraction.

Analytical sample: 7µl   plasmid-DNA from mini-prep ($\cong$ 1-2µg DNA)

                            2µl   BSA (bovine serum albumin)

                            2µl   10x buffer

                            1µl   restriction endonuclease(s)

                   ad 20µl   dH$_2$O

Preparative sample: 10µg   plasmid-DNA from mini-prep ($\cong$ 1-2µg DNA)

                           10µl   BSA (bovine serum albumin)

                           10µl   10x buffer

                           10µl   restriction endonuclease(s)

                  ad 100µl   dH$_2$O

The restriction endonucleases are provided with an adequate 10x reaction buffer and if applicable, with BSA which stabilizes the enzymes. In case, two enzymes exhibit different temperature optima, the treatment has to be perfomed sequentially.

4.3.7 Fill-in reaction of non-compatible, overhanging DNA ends

If two DNA molecules cannot be treated with restriction endonucleases in a way enabling them to be ligated together, it is possible to fill in the overhanging DNA ends with single nucleotides to yield blunt ends.

sample: 43 µl   purified DNA in EB-Buffer

                           (after Phenol/Chloroform-Extraction: 4.3.10)

                  5 µl   10x Pfu-Buffer

            1 µl   dNTP-Mix [20mM each]

            1 µl   Pfu-Polymerase [2,5U/µl]

Incubation 30 min. at 70°C.

4.3.8   Dephosphorylation of vector-DNA

In order to avoid the religation or oligomerization of vectors that exhibit compatible ends following a restriction digest, the 5'-ends of the linearized vectors were treated with alkaline phosphatase (calf intestine phoshatase, CIP). To this end, 2µl CIP (20U/µl) were added to the restriction digest sample after 1 h incubation. The sample was incubated for 1 h more and purified in analogy to insert-DNA by Phenol/Chloroform extraction.

4.3.9   Ligation

The T4-DNA ligase was used to form a phospodiester bond between the 3'-OH and the free 5'-phosphate residues of the cohesive ends of insert and vector DNA. This allows the insertion of an additional DNA-fragment into an existing vector. Here, it is of advantage to shift the molar ratio of the different DNA molecules towards the insert.

sample: 6 µl insert-DNA (ca. 1,5µg)

                          1 µl vector-DNA (ca. 0,3 µg)

                          1 µl ATP [100 µM]

                          1 µl T4-DNA-Ligase

                          1 µl 10x ligation buffer

In order to estimate the ratio of religated vectors to ligated plasmids, a control ligation with only the vector was perfomed in parallel. Ligations were incubated over night at 16°C or for 2 h at RT.

4.3.10 Electrophoretic separation of DNA in an agarose gel

DNA fragments can be separated electrophoretically based on their size and dependent on the agarose concentration. For the gel electrophoresis performed in this work, 0.8 – 2 % agarose gels were used, depending on the DNA fragment to be

separated. The gels contained ethidium bromide at a concentration of 0,1µl /ml (1% stock solution). The DNA-samples were loaded on the gel after adding 6x DNA-sample buffer. To identify the size of the DNA fragments, a DNA-size-marker was loaded on the gel. After the electrophoretic separation of the DNA fragments (30 min at 120V), the gel was observed under UV irradiation in a gel doc system (BioRad), showing the DNA that incorporated the ethidium bromide.

4.3.11 Isolation of DNA from agarose gels

For the isolation of DNA-fragments from agarose gels, the desired DNA fragments were first cut out under UV light using a scapel and subsequently transferred to a 1,5 ml tube. After weighing the gel piece, the purification was performed with the QIAquick™ gel extraction kit according to the manual. In the last step, the DNA was eluted from a silica column using EB-buffer.

4.3.12 Phenol Extraction of DNA

During cloning and after digestion of the DNA (and dephosphorylation of the vector), phenol extraction was performed to purify the DNA from enzymes and buffers. One volume of phenol (Roth) was added to the DNA solution to be purified, followed by vigorous mixing and centrifugation (13,000 rpm, 3 min at 4°C). The upper aqueous phase, containing the DNA, was transferred to a new tube and mixed with a volume of CIA (chloroform/isoamyl-acohol 24:1) This mixture was shortly centrifuged (in a table centrifuge) and the upper aqueous phase was transferred to a new tube. This was followed by an ethanol precipitation.

4.3.13 DNA Ethanol Precipitation

To precipitate and purify DNA after a phenol-extraction (during cloning), the following components were added to the DNA solution and mixed:

      1 µl gycogen (used as carrier; 10 mg/ml)

      1/10 volume 3 M sodium acetate (pH 6,2)

      2,5x volume 100% ethanol

This solution was centrifuged for 30 min at 13,000 rpm and 4°C, the pellet was washed in 250 µl 70% ethanol, dried, and resuspended in 10 µl EB (elution buffer, 10mM Tris-HCl, pH 8,5). This purified DNA was then used for ligation.

4.3.14 DNA sequencing

For DNA sequencing the dideoxy chain termination technique (Sanger et al., 1977) was used. This method is based on the cyclic polymerization of the DNA of interest with a specific primer and a mixture of dNTPs and ddNTPs (labelled with four different fluorescent groups). The incorporation of a ddNTP causes the termination of the DNA polymerization due to its lack of the 3'-OH group. In this way, DNA fragments of different sizes are obtained and separated in a electric field.

For DNA sequencing, 1-2 µg of DNA was precipitated by ethanol precipitation and the dried DNA pellet was sent to MWG Biotech, Ebersberg, Germany, together with the appropiate sequencing primer in an extra tube.

4.3.15 Phenol Extraction of RNA

The RNA was extracted from the cells 36 h after transfection with plasmids or siRNA using the Trizol® reagent (Invitrogen).

The cells were scraped in culture medium and centrifuged in a sterile 15 ml tube for 5 min at 1500 rpm. The cell pellet was resuspended in 150 µl PBS$^{def.}$ and transferred into a 1,5ml tube. The tube was centrifuged for 5 min at 3000 rpm (RT), the PBS$^{def.}$ was removed and 700 µl Trizol® reagent (a mixture of phenol and guanidine isothyocyante) was added after dry vortexing the tube. The pellet was resolved by carefully pipetting up and down, followed by another vortexing step. After 5 min incubation at room temperature, 150 µl chloroform were added and the tube was shaked very vigorously for 15 sec, followed by 3 min incubation at room temperature. After centrifugation at 10.000 g, for 15 min at 4°C, different phases were separated: an organic phase containing proteins, an interphase containing DNA and an aqueous upper phase containing the RNA. The latter was transferred into a new tube and the RNA was precipitated by adding 500 µl isopropanol, mixing incubating for 10 min at RT and centrifugating at 10.000 g, for 10 min, at 4°C. The pellet was washed with 1ml 75% ethanol and resuspended in 20 µl nuclease free water (Ambion).

The RNA concentration was measured as described in 4.3.3. The RNA was distributed in aliquots and stored at -80°C or directly used for reverse transcription (for qRT-PCR)

4.3.16 Reverse transcription

For reverse transcription, the First strand synthesis Kit from Roche was used. After measuring the RNA concentration, 1µg of RNA was used for reverse transcription. As primers, oligo-dT- primers were used that unspecifically bind to the polyA-tail of all cellular polyadenylated mRNA species.

Reverse transcription reaction (for Applied Biosystems and Roche Lightcycler):

RNase inhibitor	1µl
RT-Primer	1µl
Total RNA	1µg
10x First strand synthesis buffer	2µl
AMV Reverse transcriptase	0,8µl
$MgCl_2$	2µl
Sterile H_2O	ad 20µl
Total volume	**20 µl**

Reverse transcription program

25ºC	10 min
42ºC	60 min
99ºC	5 min
4ºC	∞

4.3.17 Quantitative realtime-PCR (qRT-PCR)

The use of conventional PCR methods to quantify the amount of a certain mRNA species or other nucleic acids has the disadvantage of being not very accurate and laborious. This weakness has been overcome by the advent of the new quantitative Real-time PCR methods that make up an increasing percentage of PCR applications. The SYBR Green method exploits the characteristic of the SYBR green molecule to specifically bind to doublestranded DNA molecules that form upon amplification of a certain template (reviewed in Zipper et al., 2004). When bound to doublestranded

DNA, the SYBR Green molecule emitts green light (λ_{max} = 522 nm), when it is excitated by a specific wavelength (λ_{max} = 498 nm). With each PCR cycle, the number of doublestranded products increases and more SYBR Green can bind to the DNA (Figure 4.2). The Realtime PCR machine tracks the amount of fluorescence at the end of each PCR cycle and plots these values against the cycle number, allowing the user to determine the logarithmic phase of amplification. In this phase, conclusions can be drawn from the time the fluorescence exceeds a certain threshold to the initial amount of template in the sample. Usually, two kinds of Realtime PCR quantification are distinguished; the relative quantification and the absolute quantification. A disadvantage of the SYBR Green method is the unspecific binding of SYBR green to all dsDNA, including potential unspecific PCR products. Therefore, a melting curve has to be performed to control the melting temperatures of the PCR products. Furthermore, the identity of the PCR products were checked on an agarose gel.

A

B

C
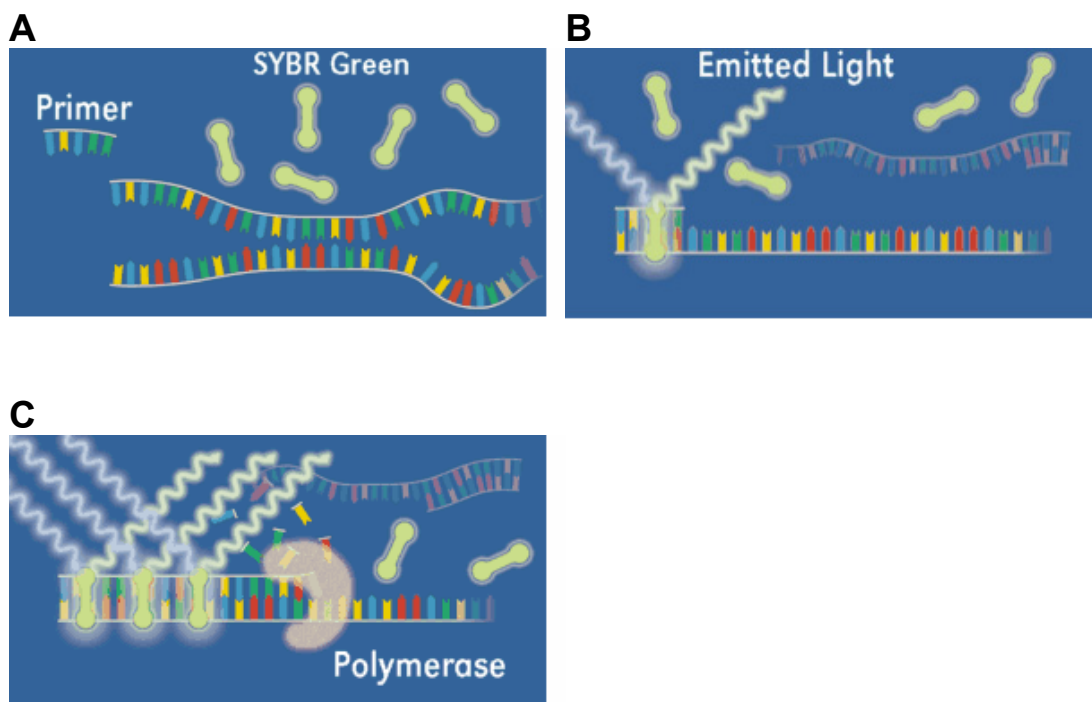
Figure 4.2 : Mechanism of SYBR green based Realtime PCR
(A) Step 1: Free SYBR green molecules and denatured DNA molecules (Template and Primers)
(B) Step 2: Upon Primer binding, the first SYBR green molecules can bind and are now capable of emitting light when excited.
(B) Step 3: Amplification of the template leads to proportionally increased binding of SYBR green molecules to the DNA and increase of fluorescence. (Pictures taken from the homepage of Roche Applied Science, www.roche-applied-science.com)

The quantitative Realtime analysis was performed on two different systems:

        1) Lightcycler 2.0 (Roche) (Marburg)

        2) 7300 Real time PCR system (Applied Biosystems) (Odense)

The Realtime PCRs that were run on the Lightcycler were performed using capillaries in a carousel.

The machine of Applied Biosystems is based on a 96well plate basis.

Capillary preparation (Lightcycler)

The mastermix (18 µl) was pipetted into the precooled capillaries (in a metal-cooling block). After that, the template was added to the capillary (2 µl), followed by sealing with a plastic lid and centrifugation at 3000 rpm for 5 s at 4°C. The samples were introduced into the light cycler carousel without applying force and were pressed carefully into it. The carousel was subsequently put into the light cycler and the machine was started.

To check the Realtime PCR products on an agarose gel, the capillaries were opened, and put upside down into a 1,5 ml tube followed by short centrifugation (20-30 s) at 500 rpm.

Mastermix for quantitative Realtime PCR (Roche Lightcycler)

Mastermix 5x	4,0 µl
forward-Primer (1:20)	1,3 µl
reverse-Primer (1:20)	1,3 µl
dH$_2$O	8,4 µl
total volume	**18,0 µl**

The Primers had a final concentration of 500 nM.

PCR-program (*GAPDH/p21*):

Program:	Temperature (°C)	Hold (h:min:s)	Ramp (C°/s)	Aquisistion Mode
Denaturation:	95	00:10:00	20	none
Amplification:	95	00:00:10	20	none
	60	00:00:08	20	none
	72	00:00:30	20	single
Melting Curve	95	00:00:00	20	none
	65	00:00:20	20	none
	95	00:00:00	0,1	continuous
Cooling	37	00:00:00	20	none

The special construction of the lightcycler and the thin capillary walls allowed very short program steps.

Plate preparation for Realtime PCR (Applied Biosystems):

First, the plate was put on ice and the mastermix was prepared. The cDNA was diluted 1:10 and then 2,5 µl were used as template per well. For the standard curve, the cDNA was first diluted 1:2 and then in 4 serial dilution 1:4 :

6µl cDNA + 6µl H_2O -> 3µl + 9µl H_2O ->…

The cDNA was pipetted into the plate, then the mastermix was added followed by the application of a sealing adhesive cover to avoid evaporation of reagents from the reaction. Finally, the plate was centrifugated shortly to spin down drops of reagent.

Mastermix for quantitative Realtime PCR (Applied Biosystems)

Applied Biosystems Mastermix	12,5µl
Nuclease free Water	3,5µl
Forward-Primer (5µM)	3,25µl
Reverse-Primer (5µM)	3,25µl
End Volume:	**22,5µl**

PCR program used for the amplification of GAPDH/p21 (Applied Biosystems)

Degree	Time	Comments	Cycles
95°C	10 min	DNA Polymerase Activation	1
95°C	15 sec	DNA melting	40
60°C	15 sec	Primers annealing	
72°C	1 min 15 sec	Extension	
		Dissociation stage	1

Data analysis at the computer (Roche Lightcycler)

The quantification was performed using the Lightcycler® 2.0 software, with the relative quantification setup (calibrator normalized relative quantification without efficiency correction) according to the manual.

Data analysis at the computer (Applied Biosystems)

The quantification was performed using the SDS-Program (Applied Biosystems). A relative quantification was performed, but the amounts of PCR product were correlated to a standard curve, derived from different dilutions of one sample.

4.3.18 Suppression of gene expression by RNA interference

The overexpression of proteins in the cells often does not lead to mRNA and protein levels that really reflect the actual physiological level of the protein of interest. Apart from that it is also very important to study the effect in the absence of a particular protein. To overcome this problem, several methods have been developed to abrogate the expression of a gene of interest. The gene knockout, a deletion of one or both allels of a gene of interest in live animals with subsequent cultivation of the cells, is a very laborious and time-consuming method. Over the past decade a new method emerged, termed RNA interference (RNAi). This method exploits a naturally occurring phenomenon that was originally discovered in plants in the year 1990 (Napoli et al., 1990). In the last few years, it has become clear that RNAi occurs in both plants and animals and has roles in viral defense and transposon silencing mechanisms.

The short interfering RNAs are transfected by Lipofection (Lipofectamine 2000™), using the protocol and siRNA amounts decribed in 4.1.2. After entering the cell, the duplex molecule is unwound by a helicase and integrated into the RNA induced Silencing complex, called RISC. After its integration into RISC, the siRNAs anneal to their target mRNA and the RISC component Argonaute protein cleaves the mRNA, thereby preventing its translation (reviewed (Mittal, 2004).

For the design of a highly efficient siRNA that does not provoke too many unspecific effects, certain rules have to be considered. Here only a few are mentioned:

> 1) The siRNA target sequence shoud not exhibit sequence similarity with any other known mRNA, e.g. longer strechtes of identical bases. This is checked for with the BLAST for short, nearly exact matches at NCBI.
> 2) The siRNA sequence should have an overall low to medium G+C content (30-50%).
> 3) Internal repeats or palindromes should be avoided.

The siRNA used in these experiments were either designed by a special algorithm that was developed by Ambion Inc. that incorporates several rules, or taken from publications that had already proven their efficacy.

Chemically synthesized short RNA moleclues of 19-21 bases that are self-complementary and form a RNA-duplex are now used for the specific suppression of

gene expression (Elbashir et al., 2001). Moreover, the siRNAs exhibit a 2 nucleotide overhang (typically: dTdT) at the 3' end.

The efficiency of the siRNA was evaluated by qRT-PCR and Western Blot analysis if applicable.

5   RESULTS

5.1   Tip60 as a modulator of p53 and Mdm2 protein levels

A large scale siRNA screen has identified the Tip60 protein as an essential factor for the p53-dependent cell cycle arrest (Berns et al., 2004). This finding, together with the fact that Tip60 acts as a histone acetyl transferase, implicates that Tip60 functions by virtue of its activity as a transcription cofactor. However, it has recently been shown that Tip60 interacts with Mdm2, leading to the degradation of Tip60 (Legube et al., 2002). This prompted us to ask, whether Tip60 might also contribute to p53 activity by directly antagonizing the activity of Mdm2 towards p53.

5.1.1   Overexpression of Tip60 leads to increase in p53 and Mdm2 protein levels

The Mdm2 oncoprotein and its target p53 are very unstable proteins, which is mainly due to the E3-Ubiquitin-ligase activity of Mdm2 towards p53 and itself. Since Tip60 and Mdm2 can form a complex (Legube et al., 2004), we sought to further investigate the role of Tip60 in the regulation of Mdm2. First, we overexpressed Tip60 in U2OS (derived from an osteosarcoma; $TP53^{+/+}$) cells and performed immunoblot analysis to determine the endogenous protein levels of Mdm2 and p53 under these circumstances (Fig. 5.1A). Tip60 overexpression led to an increase of Mdm2 and p53 protein levels (compare lanes 1+2). However, in comparison, p14arf was more potent in elevating the levels of Mdm2 and p53 (lane 3).

5.1.2   Tip60 overexpression results in an increased protein half-life of Mdm2

Next, we were interested in how Tip60 overexpression was capable of stimulating the accumulation of Mdm2 and p53. Principally, there are different scenarios that could be envisioned to explain the increase in Mdm2 and p53 protein levels. Tip60 could either act to induce the transcription of these genes or affect their protein stability. Since p53 and Mdm2 are mainly regulated at the protein level, cycloheximide (CHX) chase experiments were performed to reveal the impact of Tip60 on the half-life of Mdm2 (see chapter 4.1.4). Cycloheximide is an antibiotic, produced by *Streptomyces griseus,* that specifically inhibits the translation of mRNAs, thereby stalling the cellular protein biosynthesis. H1299 cells ($TP53^{-/-}$) were transfected either with empty vector, Mdm2, or a combination of Mdm2 with Tip60 or p14arf. While no more Mdm2 protein was visible after 3 hours of CHX treatment in the cells transfected with the vector

alone (Figure 5.1B, lane 1-6), the coexpression of Tip60 as well as p14arf led to a strong stabilisation of Mdm2 (lanes 7-12). We conclude that Tip60 is capable of blocking the degradation of Mdm2.

5.1.3 Tip60 reverses the destabilization of p53 by Mdm2

The next question was, whether Tip60 could specifically interfere with the Mdm2-mediated degradation of p53. For this purpose, p53 was coexpressed in H1299 cells ($TP53^{-/-}$) either alone with Mdm2 or in addition with Tip60 and p14arf. H1299 cells are derived from a human adenocarcinoma of the lung and are particularly well suited for the study of the Mdm2-p53 system, as they do not contain p53 and only very low levels of Mdm2, which could interfere with the effectors to be studied.

As expected, the coexpression of Mdm2 and p53 led to a reduction of p53 protein levels due to Mdm2-mediated degradation of p53 (Figure 5.1C, compare lane 2 and 5). However, upon coexpression of Tip60, p53 levels were partially restored while Tip60 overexpression in the absence of Mdm2 had no effect (lanes 2+3 and 5+6). p14arf expression led to an even stronger increase of p53 levels. Moreover, the Mdm2 levels were strongly increased when Tip60 was coexpressed as in the case of p14arf (lanes 5-7). These data imply that Tip60 is capable of inhibiting the Mdm2-mediated degradation of p53. This is supported by the fact that Tip60 overexpression in the absence of Mdm2 does not alter the p53 protein levels (lanes 2 and 3).

5.1.4 Tip60 mRNA levels are strongly reduced upon siRNA-mediated knockdown of *HTATIP* expression

The overexpression of proteins to study their role in the cell is initially very helpful but does not necessarily reflect the physiological situation. Therefore, we studied the effect of specific siRNA-mediated *HTATIP* knockdown. To this end, three different siRNAs were designed and subsequently tested in regard to their efficiency in suppressing the expression of *HTATIP*. The siRNAs suppress the expression of all Tip60-mRNA species to avoid interference between the splicing variants. U2OS cells were transfected with equal amounts of siRNA followed by RNA extraction after 48 h, reverse transcription and qRT-PCR analysis (chapter 4.3.16 and 4.3.17). As shown in Figure 5.2, the siRNAs differ in their knockdown effiency. Tip60-siRNA#3 had the most pronounced effect on Tip60-mRNA levels, leading to a reduction of over 80%. Therefore, knockdown experiments were were carried out with Tip60-siRNA#3.
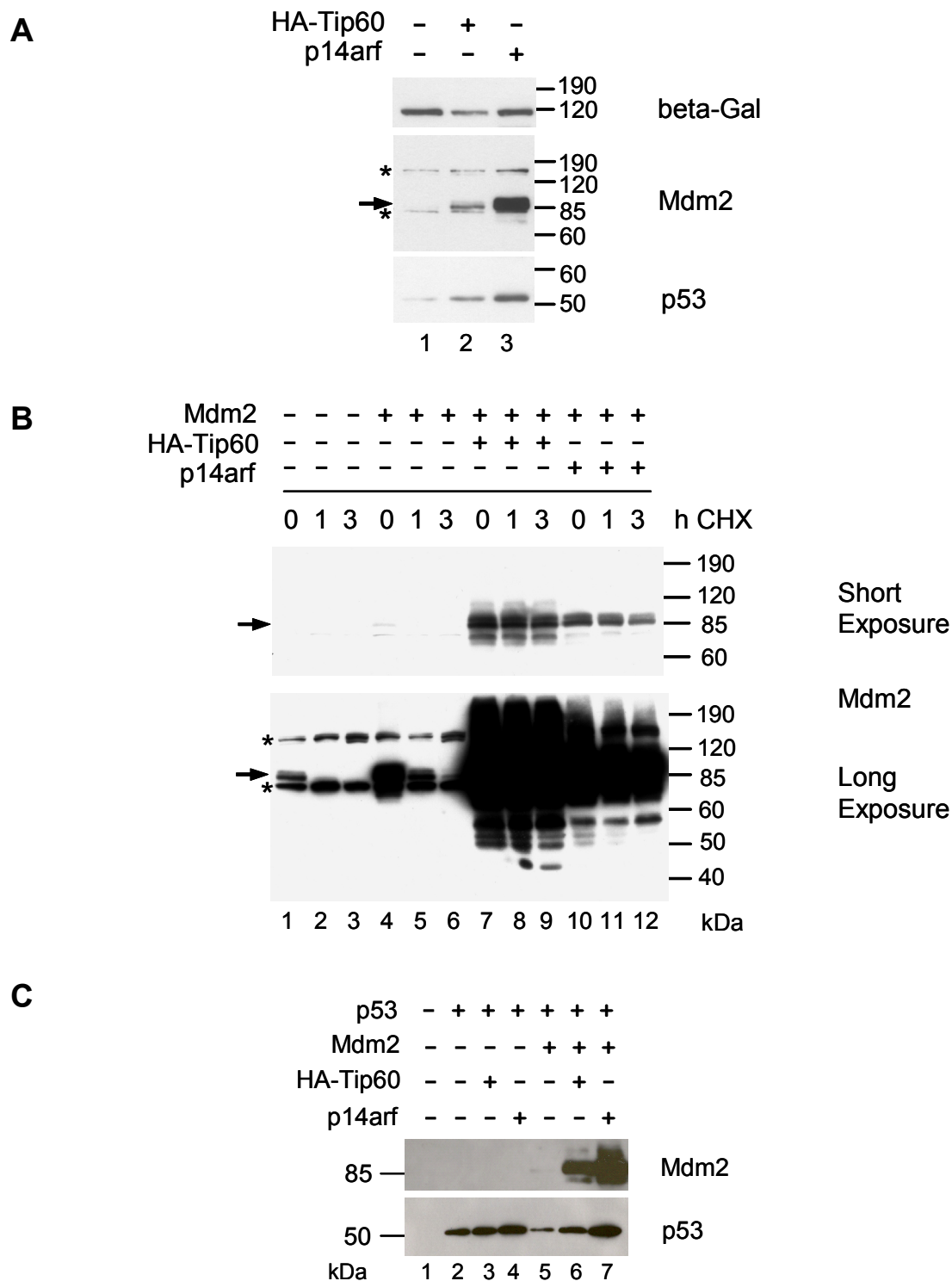
Figure 5.1 Impact of Tip60 on Mdm2-mediated degradation of p53.
(A) Impact of Tip60 on endogenous p53 and Mdm2 protein levels. U2OS cells were transfected either with empty vector or expression plasmids for HA-Tip60 and p14arf. Twenty-four hours post transfection, the cells were harvested by scraping, lysed in RIPA buffer, supplemented with Laemmli buffer and subjected to SDS-PAGE followed by protein detection by immunoblot analysis. The position of Mdm2 is shown by an arrow; non-specific bands observed independently of Mdm2 are labelled by asteriks. **(B)** Impact of Tip60 on the protein half-life of Mdm2. H1299 cells were transfected with the indicated plasmids; 24 h post transfection, the cells were treated with 50µg/ml cycloheximide to inhibit protein translation. The cells were then harvested at the indicated time points after cycloheximide addition and further processed as described in **(A)**. A longer exposure is shown to reveal the stability of endogenous Mdm2. **(C)** H1299 cells were transfected with the indicated plasmids and processed as in described in **(A)**.
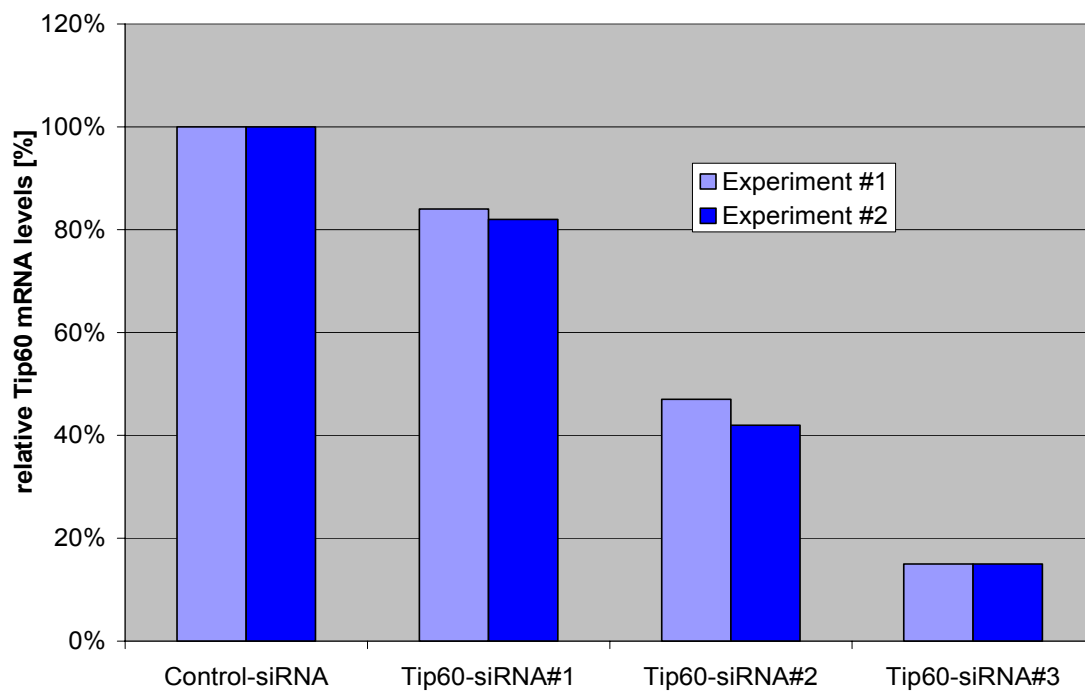
Figure 5.2: Comparison of different Tip60 siRNAs in their knockdown efficiency.
U2OS cells were transfected with a Control siRNA and three different siRNAs against Tip60. After 48h, the cells were harvested followed by RNA extraction and specific reverse transcription of GAPDH (control gene) and Tip60 mRNAs. To determine the amount of Tip60 mRNA, a quantitative Realtime PCR was performed. The values for *HTATIP* were set in relation to *GAPDH* and the control siRNA was set to one. The results of two independent experiments are shown.
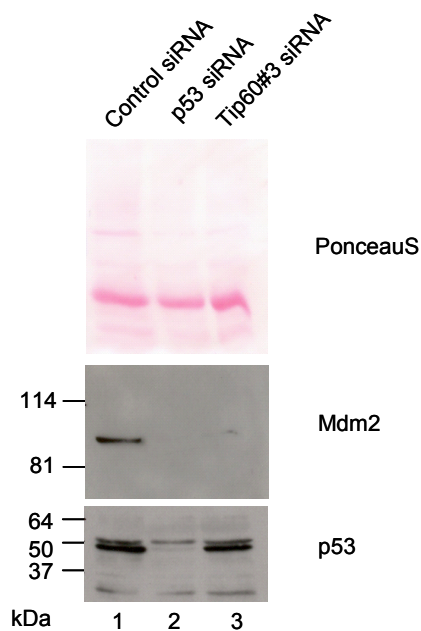
Figure 5.3: Impact of Tip60-siRNA on the levels of Mdm2 and p53 in U2OS cells.
U2OS cells were transfected with the indicated siRNAs and harvested 36h later in RIPA/laemmli buffer. The proteins were separated by SDS-PAGE and detected by immunoblot.

5.1.5 siRNA-mediated knockdown of *HTATIP* expresssion decreases the protein levels of Mdm2

Next, we were interested in whether the removal of endogenous Tip60 by siRNA-mediated gene knockdown would have the opposite effect on the Mdm2 and p53 levels as its overexpression. Therefore, U2OS cells were transfected with siRNAs targeting Tip60- and p53-mRNA (positive control) as well as a randomized siRNA preparation (negative control). While the siRNA against Tip60 led to a reduction of endogenous Mdm2 protein levels, the p53 protein levels remained unaltered (Figure 5.3, lane 3). siRNA targeting the p53-mRNA also led to a reduction of Mdm2 protein levels which is most likely due to a lack of transcriptional activation of *MDM2*-promoter by p53 (lane 2). These results suggest that endogenous Tip60 is indeed required for the maintenance of basic Mdm2 protein levels. However, the experimental conditions used here did not allow us to see a negative effect of Tip60-siRNA on p53 levels.

5.2 Impact of Tip60 on posttranslational modifications of p53 and Mdm2

5.2.1 The stabilization of p53 by Tip60 is not due to inhibition of Mdm2-mediated ubiquitination of p53

It appeared conceivable that the stabilization of Mdm2 and p53 by Tip60 is due to interference of Tip60 with the ubiquitination of Mdm2 and p53. To test this, we performed a Nickel-His-Tag-pulldown after coexpressing the E2-conjugating enzyme UbcH8 and His-tagged Ubiquitin (later termed Ubiquitin-CS for "conjugating system") together with Mdm2 and p53. As shown in Figure 5.4, the coexpression of the Ubiquitin-CS with p53 and Mdm2 led to the occurrence of slower migrating bands, corresponding to the ubiquitinated forms of p53 (lane 4). As p14arf has been described to inhibit the ubiquitination of p53 (Honda and Yasuda, 1999), we used it as a positive control. Indeed, a change in the ubiquitination pattern of p53 with fewer slower migrating bands was observed (lane 5). However, parallel overexpression of Tip60 did not influence the appearance of ubiquitinated p53 (lane 6). From these data, we conclude that, unlike p14arf, Tip60 does not interfere with the Mdm2-mediated ubiquitination of p53, at least in the system under study here. The stabilization of Mdm2 and p53 therefore appears to occur at a step between the ubiquitination and the proteasomal degradation.
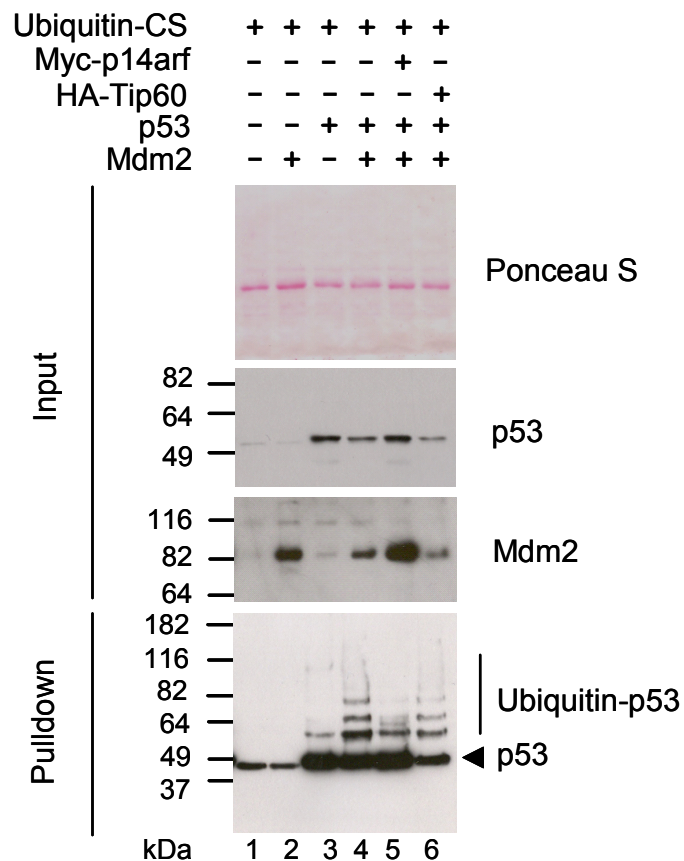
Figure 5.4: Impact of Tip60 and p14arf on Mdm2-mediated Ubiquitination of p53.
U2OS cells were transfected with the indicated combinations of expression plasmids. Thirty-six hours post transfection, the cells were treated with 40 µM of the proteasome inhibitor MG132 for 4 h. Subsequently, the cells were harvested, followed by a Nickel-His-tag pulldown. The samples were subjected to SDS-PAGE with subsequent protein detection by immunoblotting.

5.2.2 Tip60, but not p14arf inhibits the Mdm2-mediated neddylation of p53

Mdm2 not only acts as an E3-ligase for Ubiquitin, but also mediates the neddylation of p53, thereby inhibiting its transcriptional activity (Xirodimas et al., 2004). So far, the mechanisms regulating the neddylation activity of Mdm2 are unknown. Therefore, we asked whether Tip60 might affect p53-neddylation by Mdm2. To test this, p53 was coexpressed together with the conjugating enzyme for Nedd8, hUbc12 and His-tagged Nedd8 (later called Nedd8-CS). This led to the occurrence of a slower migrating p53 band, which corresponds to neddylated p53 (Figure 5.5, lane 6). Addition of Mdm2 to the system resulted in a visible increase in the neddylation of p53, as represented by the four slower migrating bands of p53 (Figure 5.5, lane 5). This Mdm2-dependent neddylation of p53 was completely abrogated by the simultaneous coexpression of Tip60. In addition to inhibition of p53-neddylation,

Tip60 inhibited the neddylation activity of Mdm2 towards itself (Figure 5.5, compare lanes 2 and 3).

Next, we sought to investigate the role of p14arf in p53- and Mdm2-neddylation in comparison to Tip60. We therefore expressed p14arf together with p53 and the Nedd8-CS, with or without Mdm2. Coexpression of p14arf also decreased p53-neddylation, but to a far lesser extent than Tip60 (Figure 5.6, compare lanes 4 + 7).

Concluding, Tip60 and p14arf are capable of inhibiting the Mdm2-dependent conjugation of Nedd8 and Ubiquitin, respectively, in a specific manner. While p14arf preferentially inihibits ubiquitination, Tip60 interferes with Mdm2-mediated neddylation.
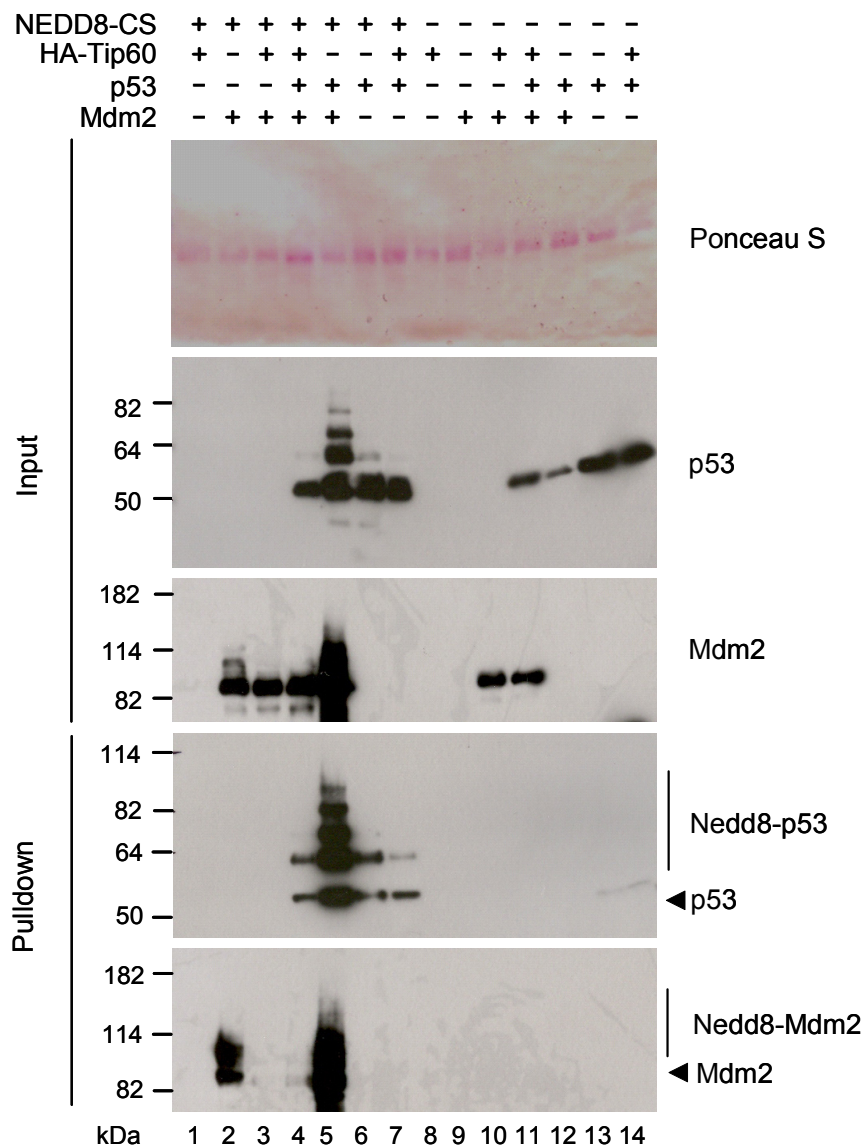
Figure 5.5 : Impact of Tip60 on Mdm2-mediated Neddylation of p53.
Impact of Tip60 on Mdm2-mediated neddylation of p53. U2OS cells were transfected with different combinations of the indicated plasmids, harvested 40 h post transfection and processed as in Figure 5.4.
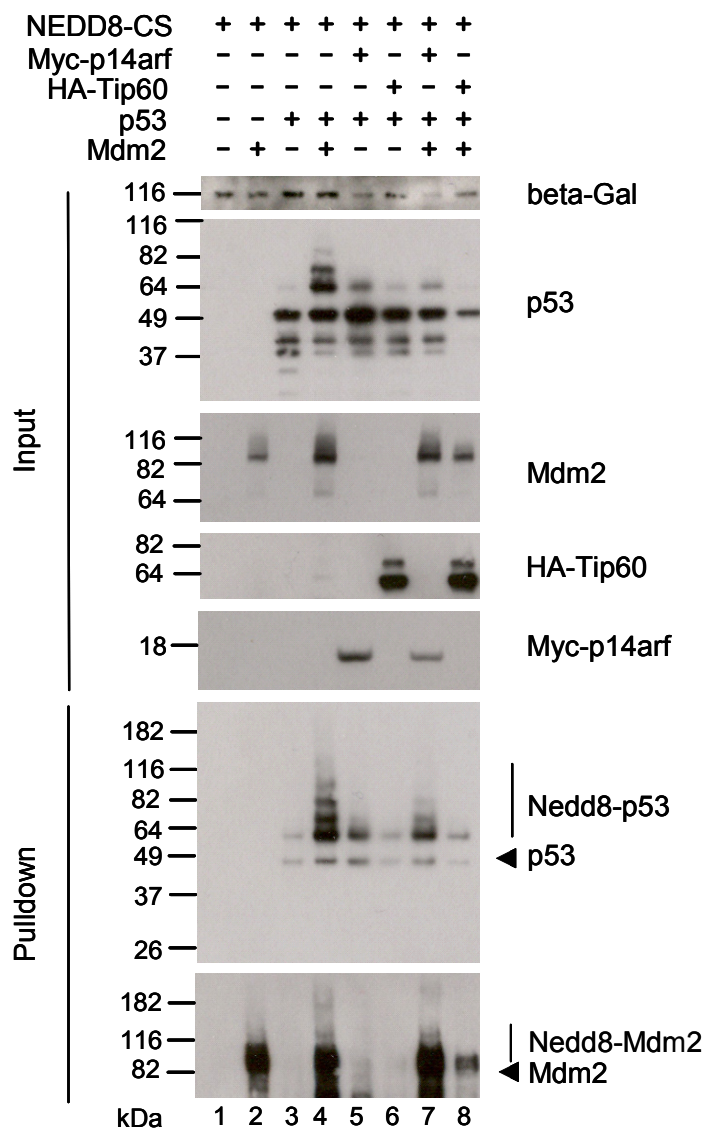
Figure 5.6: Impact of Tip60 and p14arf on Mdm2-mediated Neddylation of p53.
Comparison of Tip60 and p14arf in their effect on Mdm2-mediated neddylation of p53. U2OS cells were transfected with different combinations of the indicated plasmids and harvested 40 h post transfection. Thereafter, the cells were processed as described in Figure 5.5.

5.3 Interaction of Tip60 and Mdm2

5.3.1 Mapping of the Mdm2-Tip60 interaction by co-immunoprecipitation

Mdm2 and Tip60 physically interact (Legube et al., 2002; Legube et al., 2004). Co-immunoprecipiation of wildtype Tip60 and Mdm2 is shown in Figure 5.7. Reciprocal co-immunoprecipitation also revealed the complex (lanes 5-12), whereas precipitation with the control antibody (anti-SV40-large T-antigen) did not yield a signal (lanes 1-4).

To narrow down the mechanism by that Tip60 inhibits neddylation, we performed mutational analysis and asked to what extent the following activities of Tip60 co-segregate: Mdm2-binding, Mdm2-relocalization, and the inhibition of Mdm2-mediated neddylation. We used mutants of Tip60, harbouring deletions of the MYST domain and the smaller catalytic HAT domain within MYST (mutants constructed by Max Koeppel; described in his diploma thesis). Exon 5 was deleted separately to mimic a naturally occurring splice variant of Tip60, termed PLIP (Sheridan et al., 2001). Furthermore, STOP-codons were introduced to yield C-terminally truncated forms of Tip60 (Figure 5.8 A).

As shown in Figure 5.8 B, the Tip60 mutants under study still associated with Mdm2. We conclude that the portion corresponding to residues 1-262 in Tip60 is sufficient to bind Mdm2. In seeming contrast to this, it was previously reported that a fragment consisting of residues 1-258 did not co-precipitate Mdm2 (Legube et al., 2002). However, the latter fragment accumulated to extremely high levels, raising the possibility that squelching precluded co-precipitation despite interaction. Nonetheless, it remains possible that more than one domain of Tip60 is capable of forming a complex with Mdm2. In any case, our further studies (below) together indicate that Tip60-Mdm2-interaction can be separated from functional interference by mutational analysis.
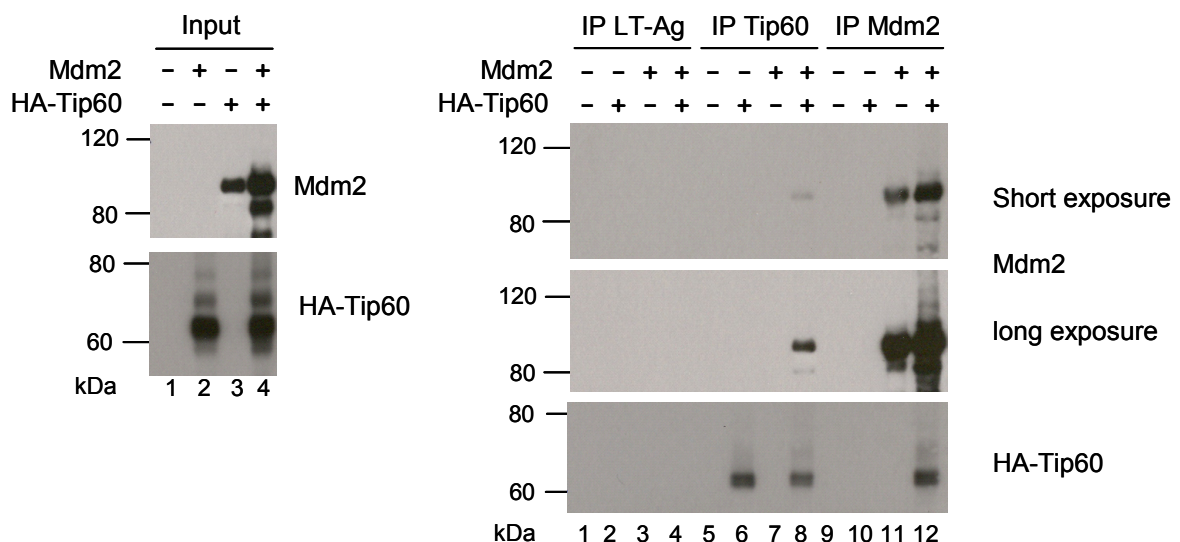
Figure 5.7: Co-immunoprecipitation of Tip60 and Mdm2.
U2OS cells were transfected with expression plasmids for HA-Tip60, Mdm2, and empty vector in the combinations indicated and harvested after 24 h. The cells were lysed and the proteins were immunoprecipitated with an anti-HA-tag antibody (HA.11), an Mdm2-antibody (2A10) and a control antibody against SV40 large T antigen (PAb419). The proteins were eluted in 6x Laemmli buffer and separated by SDS-PAGE followed by detection of the proteins by immunoblot.
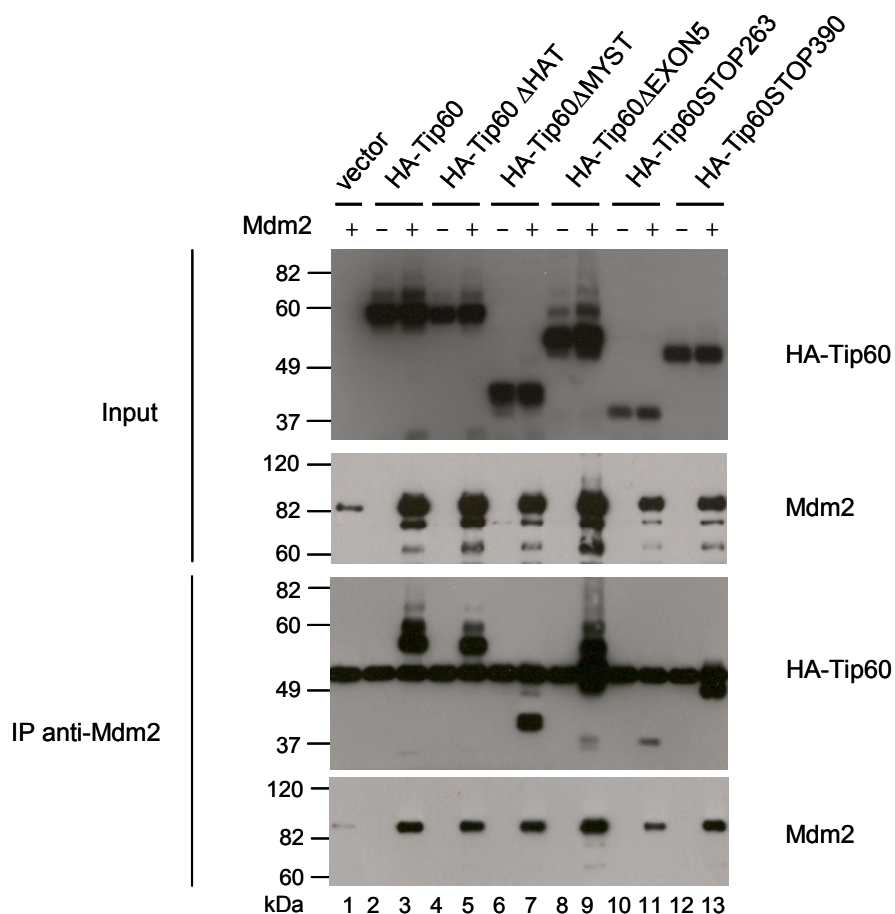
A
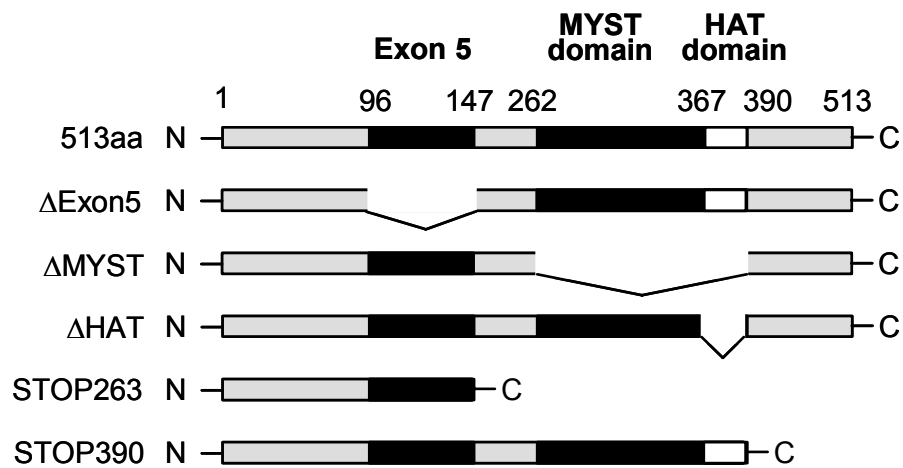
B

Figure 5.8: Mapping of the Tip60-Mdm2 association by Co-immunoprecipitation
(A) Overview of the different Tip60 deletion mutants. The figure shows the domain structure of Tip60 and the amino acids at the boundaries that are still present in the mutants.
(B) U2OS cells were transfected with different expression plasmids for Tip60 mutants together with Mdm2 in the indicated combinations, followed by co-immunoprecipitation with the anti-Mdm2 antibody (2A10). The samples were further processed as described in Figure 5.7.

5.3.2 The MYST domain of Tip60 is required for the inhibition of Mdm2-mediated neddylation

In order to map the domains on Tip60 that are required for the inhibition of neddylation, the Tip60 mutants were coexpressed with p53, Mdm2 and the Nedd8-CS.

In contrast to Tip60wt (Figure 5.9, lane 11) and Tip60dHAT (lane 13), Tip60dMYST was not capable of inhibiting the occurrence of slower-migrating forms of p53 (lane 12). The mutant lacking the Exon 5 (PLIP) was still able to inhibit the neddylation of p53 (lane 14), albeit less efficiently than Tip60wt (lane 11). The C-terminally truncated Tip60-mutants also depended on the presence of the MYST domain in their inhibitory effect on neddylation. While the Tip60STOP390 mutant (lane 16) still reduced Mdm2-mediated neddylation to a substantial extent, the Tip60STOP263 mutant (lane 15) did not. The influence of the Tip60 mutants on the neddylation of Mdm2 itself reflected the situation of p53-neddylation.
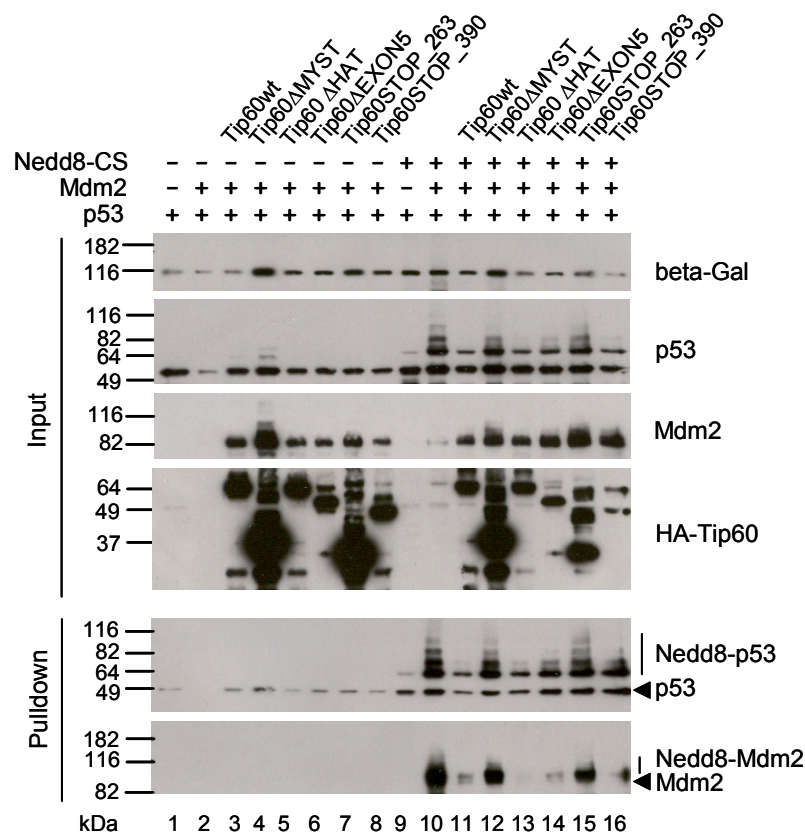
Figure 5.9: Impact of the deletion of different Tip60 domains on its inhibition of Mdm2-mediated p53-neddylation
U2OS cells were transfected with different combinations of the indicated plasmids. Forty hours post transfection the cells were processed as described in Figure 5.5.

5.4   Impact of Tip60 on the intracellular localization of Mdm2 and p53

In order to study the underlying mechanisms for the stabilization of Mdm2 and p53 by Tip60 and the inhibition of neddylation, the intracellular localization of Tip60, Mdm2 and p53 was examined by co-immunofluorescence experiments.

5.4.1   Coexpression of Mdm2 and Tip60 leads to the occurrence of nuclear dots

To study the intracellular localization of Mdm2 and Tip60, H1299 cells were transfected with expression plasmids for HA-Tip60 and EGFP-Mdm2 and a co-immunofluorescence was performed. Due to the lack of suitable antibodies to Tip60, we had to use an overexpression system with tagged Tip60, to study the localization. While the sole expression of Mdm2 or Tip60 led to a diffuse nuclear staining pattern of the proteins (Figure 5.10 A, first two rows), the coexpression of both proteins resulted in the appearance of nuclear dot-like structures (Fig.5.10 A, third row). Therefore, Tip60 is capable of relocalizing Mdm2 to nuclear structures.

5.4.2   The MYST domain of Tip60 but not the HAT domain is required for the relocalization of Mdm2

To study the role of the different domains in the relocalization of Mdm2 by Tip60, we coexpressed the different Tip60 mutants with Mdm2 followed by co-immunofluorescence (Figure 5.10 A, rows 4-8)

To quantify the impact of different Tip60 domains on the colocalization with Mdm2, the cells were counted and divided into three groups: cells exhibiting a diffuse nuclear Mdm2 staining pattern, cells with an intermediate phenotype between even distribution and colocalization, and cells that show a colocalization of both proteins exclusively in the nuclear dots.

As shown in Figure 5.10 B, only the Tip60 mutants lacking the MYST domain show a clear shift of their phenotype towards an even distribution in the nucleus, strongly suggesting a function of this domain in the mutual relocalization of both proteins. In addition, the C-terminally truncated form, which lacks only the last 121 aa yields a phenotype with an equal distribution between the diffuse and the dot-like staining
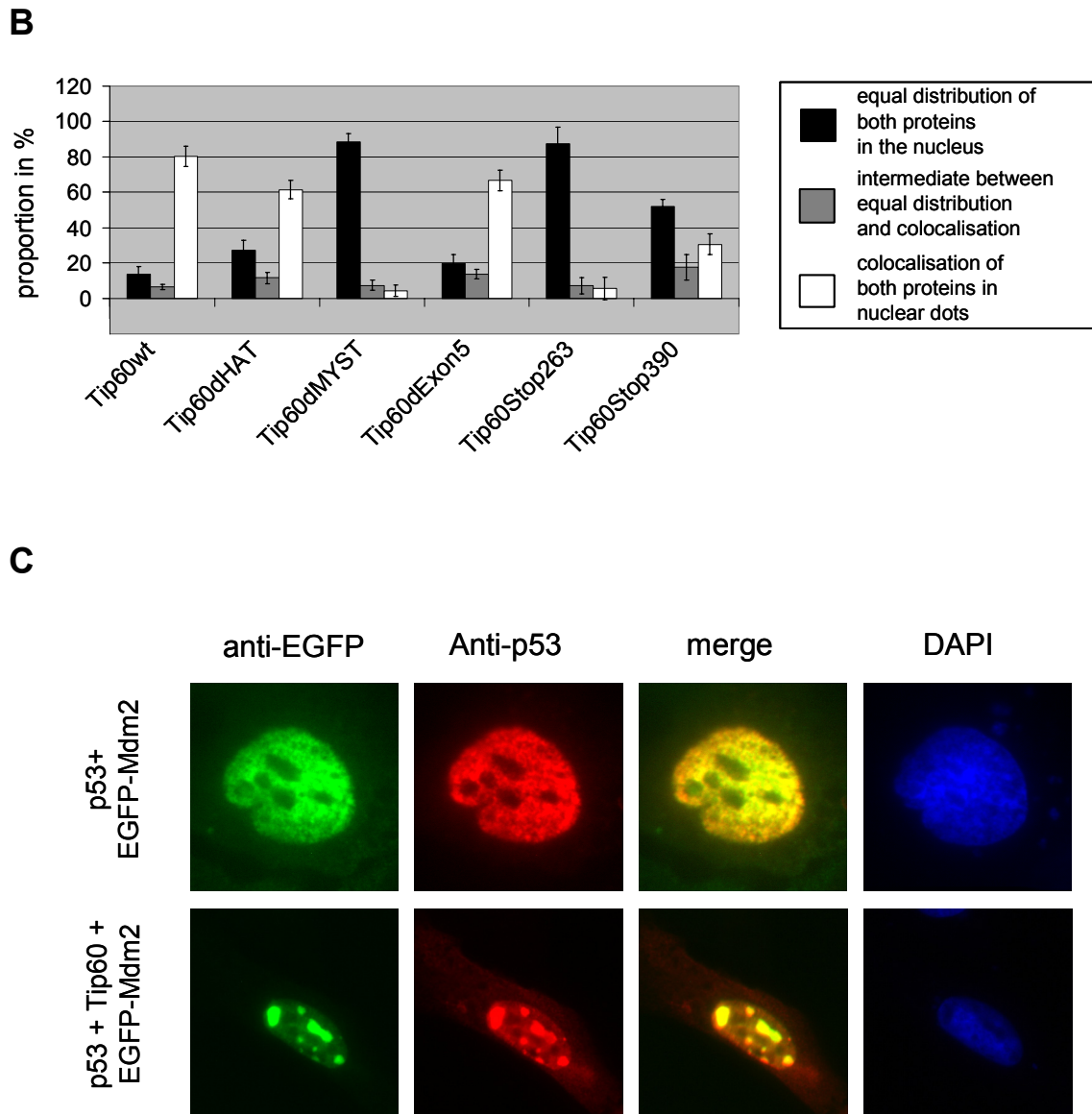
A

B

C
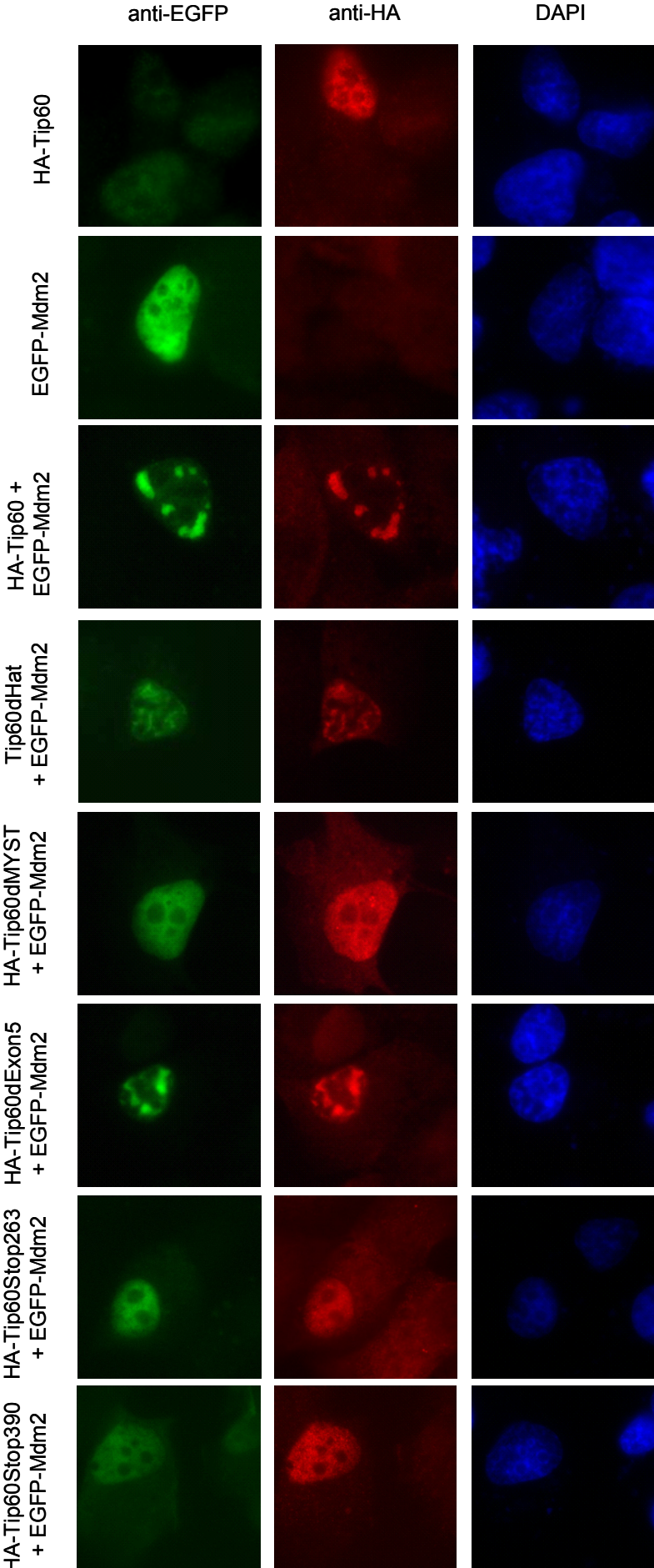
Figure 5.10: Mapping of the Tip60 domains required for relocalization of Mdm2 into nuclear dots

(A) Impact of the deletion of different Tip60 domains on the colocalization with EGFP-Mdm2. H1299 cells were transfected with equal amounts of the indicated expression plasmids. After 24 h, the cells were fixed and stained with antibodies against the HA-tag and EGFP. Nuclei were visualized wih 4,6'-Diamidino-2-phenylindole (DAPI).

(B) Statistical analysis of the immunofluorescence results, obtained as in **(A)**. 150 cells showing a green staining were evaluated by an observer who was unaware of the identity of the samples and divided into three groups; those with a clear colocalization of both proteins in nuclear dots (white columns), those with a diffuse nuclear staining pattern (black columns) and those with an intermediate phenotype (grey columns). The graph shows the percentage of cells with a particular staining pattern. The error bars show the standard deviation from three independent experiments.

(C) Colocalization of p53 with Mdm2 and Tip60. U2OS cells were transfected with the indicated plasmids and a co-immunofluorecence was performed with the antibodies anti-EGFP and anti-p53 (FL393) as described in **(A)**

The experiments shown in panel **(A)** and **(B)** were performed by Max Koeppel during his Diploma thesis under supervision of Matthias Dobbelstein and Christoph Dohmesen.

pattern. This suggests that the C-terminal region of Tip60 is needed for the relocalization of Mdm2, although it is not required for Mdm2 binding.

5.4.3 p53 also colocalizes to Tip60-Mdm2 nuclear dots

Since the intracellular localization of p53 is tightly linked to its activity, the next question was, whether the localization of p53 was also affected upon the coexpression of Tip60 and Mdm2. U2OS cells were transfected with expression plasmids encoding for Mdm2 and p53 and additionally Tip60. While the coexpression of Mdm2 and p53 yielded a diffuse nuclear staining pattern (Figure 5.10 C upper panel), the additional expression of Tip60 led, as with Mdm2 alone, to a relocalization of p53 and Mdm2 to nuclear dots (Figure 5.10 C, lower panel). This finding suggests that Tip60, Mdm2 and p53 may be found in one complex upon coexpression.

5.4.4 Mdm2, Tip60 and p53 localize to PML oncogenic domains

The occurrence of nuclear dots upon coexpression of Tip60, Mdm2 and p53 prompted us to study the identity of these nuclear structures. The nucleus contains various proteins that are frequently associated with dot-like structures. Our primary suspects were the PML nuclear bodies, because it had been shown before that Mdm2 and also p53 associate with these structures that contain several proteins involved in tumor suppression and transcriptional regulation (reviewed in Dellaire and Bazett-Jones, 2004). Since PML nuclear bodies can be visualized by staining of the PML protein, we performed a costaining of PML and EGFP-Mdm2 or p53 in the presence of Tip60. As shown in Fig.5.11A, a part of the nuclear dots observed by staining of EGFP-Mdm2, colocalize with PML nuclear bodies. The same observation was made for p53 and PML (Figure 5.11 B). This finding implies that PML might play a role in the relocalization of Mdm2 and p53 by Tip60 and potentially in the activity of Tip60 towards Mdm2 and p53.

5.4.5 Mdm2 and Tip60 still localize to nuclear dots in *pml* minus MEFs

Our next question was, whether the PML protein as a major component of the PML nuclear bodies is actually required for the Tip60-mediated relocalization of Mdm2.

For this purpose, we used mouse embryonic fibroblasts (MEFs) that are derived from PML wildtype (*pml*$^{+/+}$) and PML knockout (*pml*$^{-/-}$) mice, where both alleles of *pml* had been deleted by recombination. This system allowed us to study the role of PML in the relocalization of Mdm2 by Tip60. The staining of Mdm2 and Tip60 in *pml*$^{+/+}$ MEFs exhibited the same pattern as observed before in H1299 cells (Figure 5.11B). Strikingly, this pattern did not change in *pml -/-* MEFs (Figure 5.11C) . Tip60 was still found in nuclear dots together with Mdm2, indicating that the PML protein is not required for the formation of these structures.
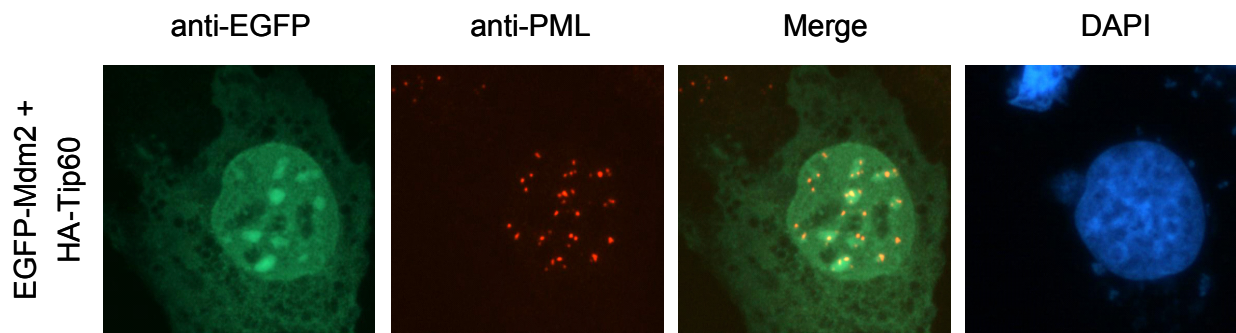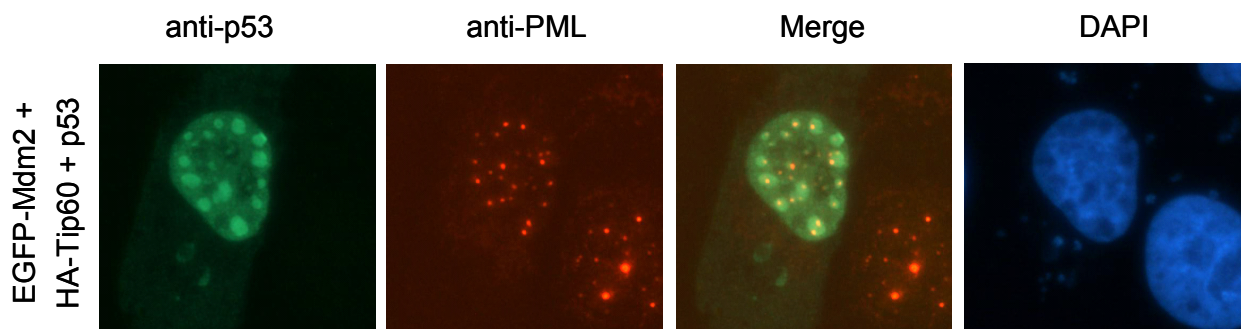
Figure 5.11: Colocalization of Mdm2, Tip60 and p53 with PML nuclear bodies
(A) Tip60-EGFP-Mdm2 nuclear dots colocalize with PML nuclear bodies. U2OS cells were transfected with the indicated expression plasmids and fixed after 24 h with 4% PFA, followed by permeabilization and immunostaining of EGFP-Mdm2 and PML. Nuclei were visualized by DAPI staining.
(B) Tip60, EGFP-Mdm2 and p53 colocalize with PML nucelar bodies. U2OS cells were transfected with the indicated expression plasmids and 24 h post transfection processed as described in **(A)**, but stained with antibodies against p53 and PML.
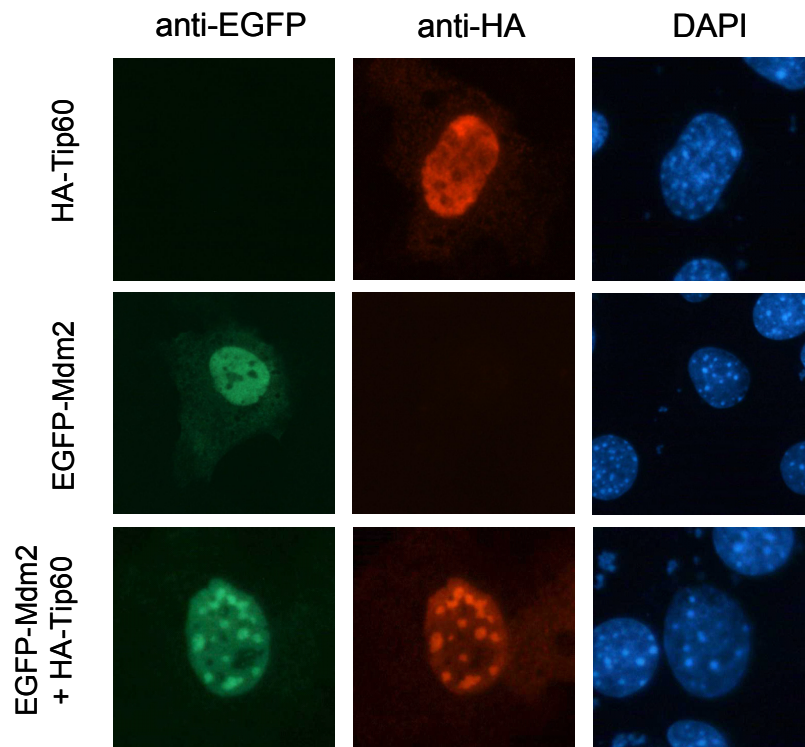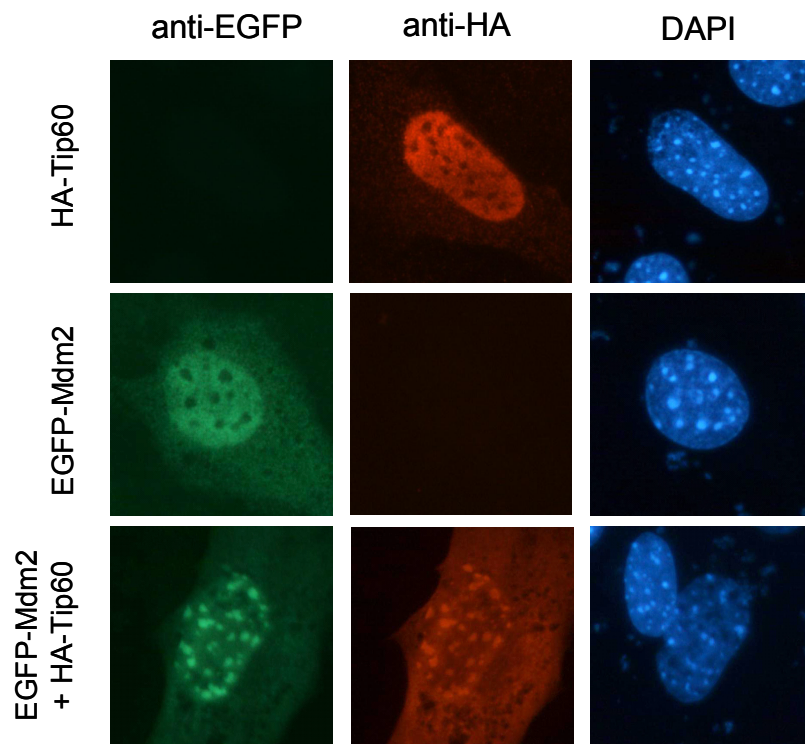
A

B

Figure 5.12: Comparison of Tip60- Mdm2 colocalization in *pml*^{+/+} and *pml*^{-/-} MEFs.
pml^{+/+} MEFs **(A)** and *pml*^{-/-} MEFs **(B)** were transfected with the indicated combinations of plasmids using Lipofectamine 2000 and 24 h post transfection the cells were fixed with 4% PFA followed by permeabilization and immunostaining with the indicated antibodies. The nuclei were visualized by DAPI staining. The cells were observed under microscope and pictures were taken.

5.5 Impact of Tip60 on p53 transcriptional activity

Intrigued by the findings that Tip60 is capable of stabilizing p53, at the same time inhibiting its Mdm2-mediated neddylation, we were interested in the effect of Tip60 on the transcriptional activity of p53.

5.5.1 Overexpression of Tip60 does not lead to transcriptional activation of p53

To study the impact of ectopically expressed Tip60 on the transcriptional activity of p53, we first performed a luciferase assay. To this end, H1299 cells were transfected with a p53-responsive reporter plasmid, containing a portion of the *mdm2*-intron in front of the luciferase gene, and different combinatons of plasmids encoding p53, Mdm2, Myc-p14arf and HA-Tip60, followed by a luciferase assay (chapter 4.2.4).

As expected, the expression of p53 led to a strong induction of luciferase activity (Figure 5.13). The coexpression of Tip60 or p14arf did not alter the p53-dependent luciferase activity, but the coexpression of p53 and Mdm2 resulted in a strong reduction of the luciferase activity. The simultaneous expression of p14arf led to partial rescue of p53-activity, which was expected, because p14arf disrupts the Mdm2-p53 complex. However, when Tip60 was expressed together with p53 and Mdm2 this did not result in a rescue of luciferase activity.

Since the luciferase assay is based on the measurement of p53-mediated transactivation of promoters that are not integrated into the cellular chromatin but located in the reporter plasmid DNA, this assay exhibits limitations. To overcome this limitation, we chose the approach of the quantitative realtime PCR (qRT-PCR) to determine the impact of Tip60 on the transcriptional activity of p53 on the endogenous *p21/CDKN1A* promoter. To this end, expression plasmids, encoding for p53, Mdm2, p14arf and Tip60 were transfected in different combinations in H1299 cells followed by RNA extraction, reverse transcription and analysis of *p21*-gene expression. As shown in Figure 5.14 A, the expression of p53 strongly stimulated the p21-mRNA synthesis. The coexpression of Mdm2 and p53 led, as expected, to a pronounced reduction of p53 activity on the endogenous *p21* promoter (Figure 5.14 A). This inhibition of p53-induced *p21*-expression by Mdm2 could be counteracted by p14arf, nearly restoring the original p53-activity.
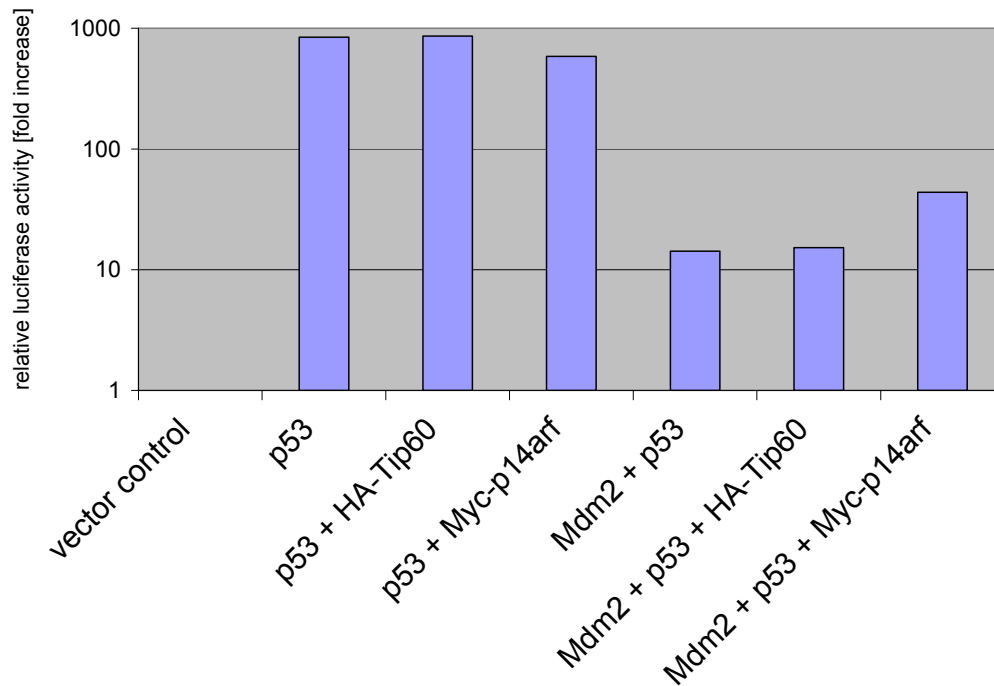
Figure 5.13: Comparison of Tip60 and p14arf in their impact on p53 transcriptional activity in a luciferase assay.
H1299 cells were transfected with a p53-responsive reporter plasmid (encoding a firefly luciferase) and the indicated combinations of expression plasmids for p53, HA-Tip60, Mdm2 and Myc-p14arf. After 24 h, the cells were harvested in reporter lysis buffer and a luciferase assay was performed. The protein amount of the samples was measured by a Bradford assay and the values of the luciferase activity were corrected accordingly.

The simultaneous expression of Tip60 however, did not lead to a rescue of p53-activity, thereby confirming the results obtained in the luciferase assay. The expression of p14arf and Tip60, in the presence of p53 but absence of Mdm2, even slightly decreased the levels of p21-mRNA while no effect was observed in case of the sole expression of p14arf and Tip60.

These findings suggest that Tip60 overexpression does not affect the activity of overexpressed p53, at least in the system tested here.

Next, we sought to investigate the impact of overexpressed Tip60 on the activity of endogenous p53. To test this, U2OS cells were transfected with expression plasmids encoding for p14arf, Tip60 and p53. Subsequently, a qRT-PCR was performed as described in 4.3.17. While the expression of p14arf led to a two fold increase in the p21-mRNA levels, Tip60 expression even led to a slight decrease of p53-transcriptional activity (Fig. 5.14B). p53 expression did not result in a strong increase of p21-mRNA levels, perhaps because its activity was blocked by endogenous regulators.

A
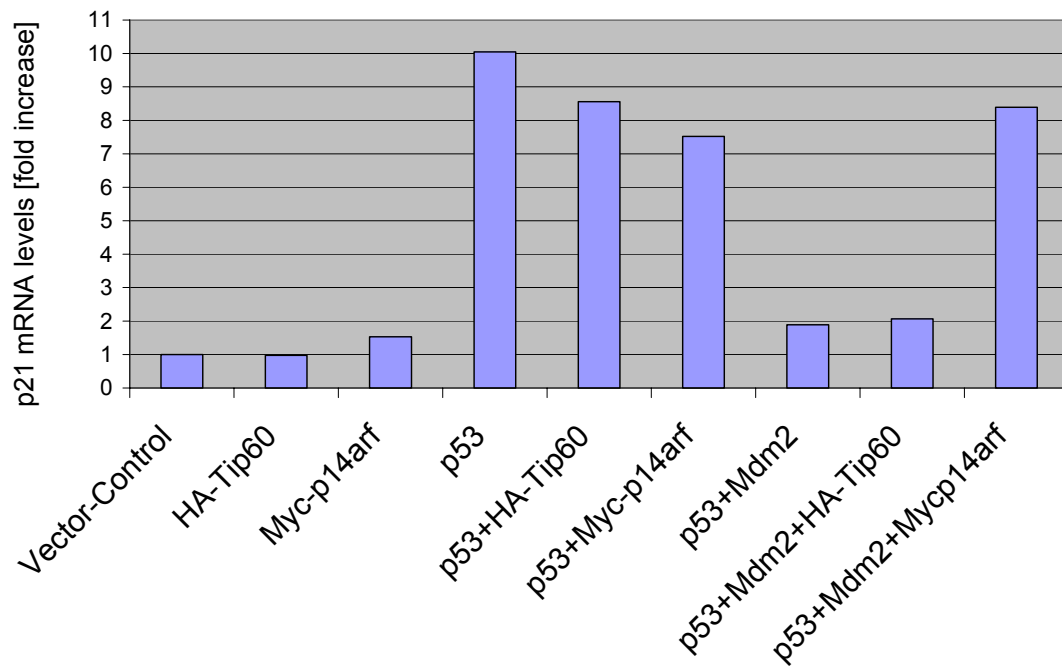
B
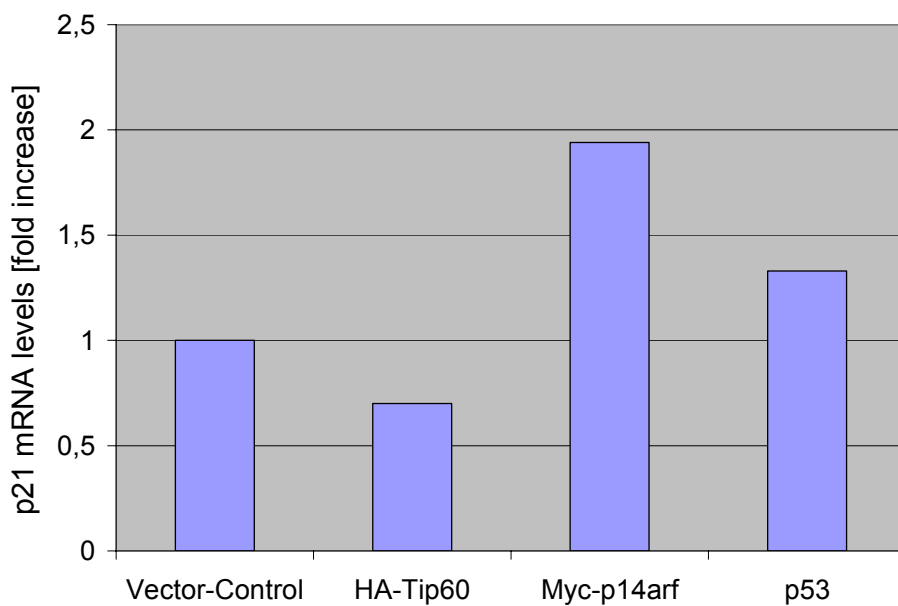
Figure 5.14: Impact of Tip60 on endogenous p21-mRNA levels
(A) Impact of Tip60 on the activity of overexpressed p53 to transactivate the endogenous *p21-*promoter. H1299 cells were transfected with the indicated combinantions of expression plasmids encoding for p53, Mdm2, HA-Tip60 and Myc-p14arf. After 24 h, the cells were harvested followed by a RNA extraction, reverse transcription and quantification of GAPDH-mRNA (control gene) and p21-mRNA levels by qRT-PCR.
**(B)** U2OS were transfected with the indicated expression plasmids and the cells were harvested 24 h post transfection and further processed as described in **(A)**

5.5.2 siRNA-mediated knockdown of *HTATIP* expression leads to slightly reduced p21-mRNA synthesis

Since the overexpression of Tip60 most probably results in Tip60 protein levels that significantly exceed its physiological levels, we also sought to determine the effect of *HTATIP*-gene knockdown on the transcriptional activity of endogenous p53. To this end, U2OS cells were transfected with siRNA directed against *HTATIP*, *TP53* and *MDM2* followed by qRT-PCR analysis of the *p21/CDKN1A* gene.

However, we were not capable of obtaining consistent results regarding the effect of *HTATIP* knockdown on p53 target gene expression whereas the knockdown of the *TP53* gene readily reduced the p21-mRNA levels. The knockdown of *MDM2* expression led to a four fold increase of p21-mRNA levels, since the repression of p53 was releaved. Our results differed in four different experiments from an effect of about 25% reduction of p21-mRNA levels to about 55%. This was also dependent on the location the experiments were performed and the Real time PCR system used. However, the *HTATIP* knockdown effiencies were very similar (about 10% remaining Tip60 mRNA levels; data not shown). Also, the effect of the siRNA targeting *TP53* on the p21-mRNA levels was more or less comparable in both cases with 11% and 16% remaining p21 mRNA (first two experiments) and 12% and 36% (last two experiments).

These results suggest that Tip60 is required only to a small extent for the p53-dependent transactivation, at least in our hands and in the system under study here.

A
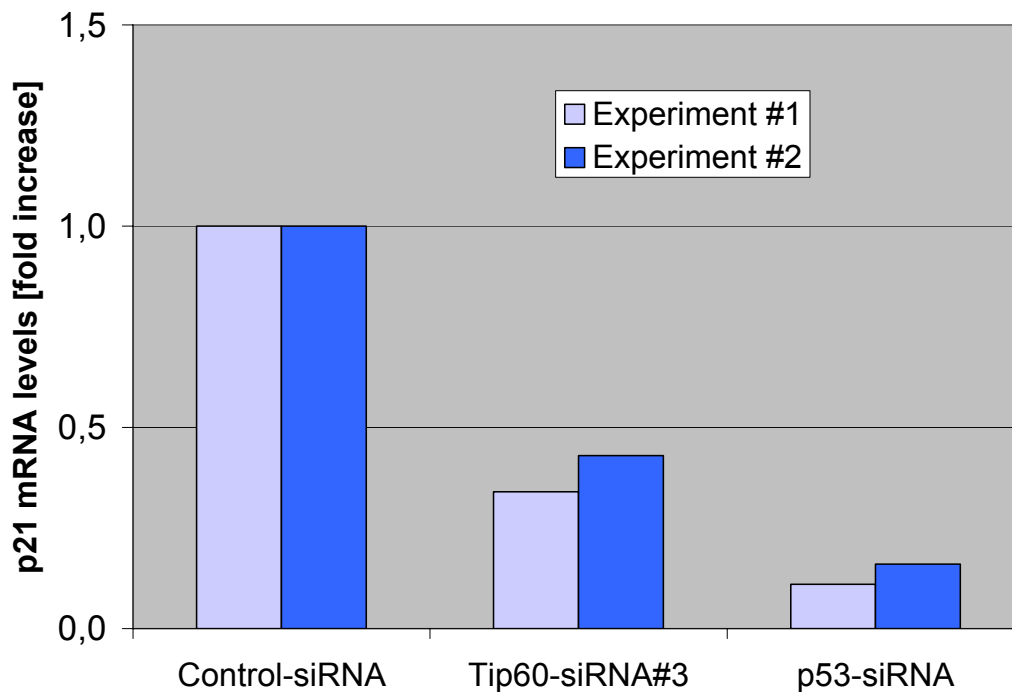
B
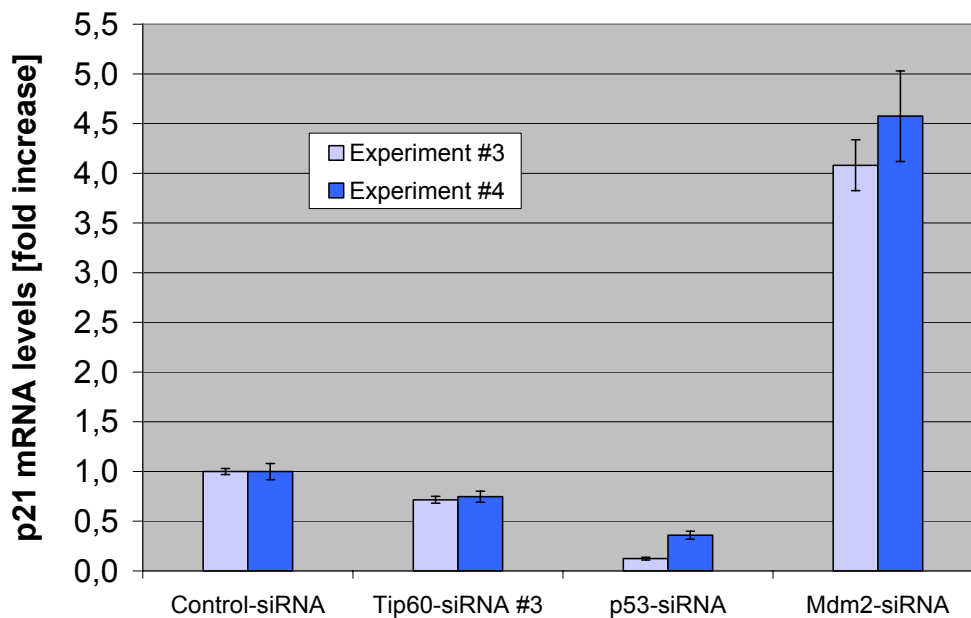
Figure 5.15: Impact of siRNA-mediated *HTATIP* knockdown on endogenous p21-mRNA levels
(A) U2OS cells were transfected with an control siRNA and siRNAs targeting *HTATIP* and *TP53*. After 48 h, the cells were harvested followed by a RNA extraction, reverse transcription and quantification of GAPDH-mRNA (control gene) and p21-mRNA levels by qRT-PCR (Roche Lightcycler 2.0, Marburg). **(B)** U2OS cells were transfected with a control siRNA and siRNAs targeting *HTATIP*, *TP53 and MDM2*. After 48 h, the the cells were processed as described in **(A),** but run on the Real time PCR system 7300 (Applied Biosystems, Odense). The samples were loaded in triplicates on the 96well reaction plate. The error bars show the standard deviation from one experiment.

5.6 The role of Tip60 in UV-induced apoptosis

Since we were not able to detect a consistent impairment of p53-dependent transcription after removal of Tip60 under non-stress conditions, we sought to investigate the role of Tip60 and p53 after UV-irradiation. It had been described previously that Tip60 plays a role in UV-induced apoptosis (Legube et al., 2002; Legube et al., 2004; Tyteca et al., 2006).

5.6.1 siRNA-mediated knockdown of *HTATIP* expression results in inhibition of UV-induced apoptosis

To study the effect of *HTATIP* knockdown on UV-induced apoptosis, U2OS cells were transfected with siRNA targeting the expression of *HTATIP*, *MDM2*, *TP53BP1* and *TP53* followed by UV-irradiation 36 h post transfection. After 4 more hours, the cells were harvested and a Western Blot was performed. As shown in Figure 5.16, the knockdown of *HTATIP* in unirradiated cells did not result in an effect on PARP cleavage (lane 2). However, in cells that were UV-irradiated with 20J/m^2 UV-C, *HTATIP* knockdown led to a reduction of PARP cleavage as indicated by less cleaved PARP (lower band; lane 7). Even at an UV radiation intensity of 80 J/m^2, *HTATIP* knockdown impaired PARP cleavage. Surprisingly however, *TP53* knockdown did not lead to a decrease of PARP cleavage (lane, 4 hours after irradiation. siRNAs against *TP53BP1* and *MDM2* were used as positive controls. As a result of *MDM2* knockdown, p21 protein accumulated, most likely leading to cell cycle arrest. Presumably, this is the reason for our observation that *MDM2* knockdown inhibits the UV-induced apoptosis. *TP53BP1* encodes for a well-known mediator of DNA damage that is required for a proper DNA damage response (reviewed in Adams and Carpenter, 2006) and its knockdown resulted in similar inhibition of PARP cleavage as *HTATIP* knockdown (lanes 10+15). Knockdown of *HTATIP* did not only impair the cleavage of PARP but also led to decreased gamma-H2AX protein levels after irradiation with 20 J/m^2, but not after 80 J/ m^2 (lane 7 and 12). This finding suggests that Tip60 is required in the immediate early response to UV irradiation as the accumulation of phosphorylated histone 2AX constitutes one of the first steps in the DNA damage response. Moreover, the short time after UV irradiation makes it unlikely that this effect is based on Tip60 influencing the transcriptional activation of apoptosis-related genes. As opposed to PARP cleavage and gamma-H2AX-levels, *HTATIP* knockdown did not alter the expression of the p21-protein.
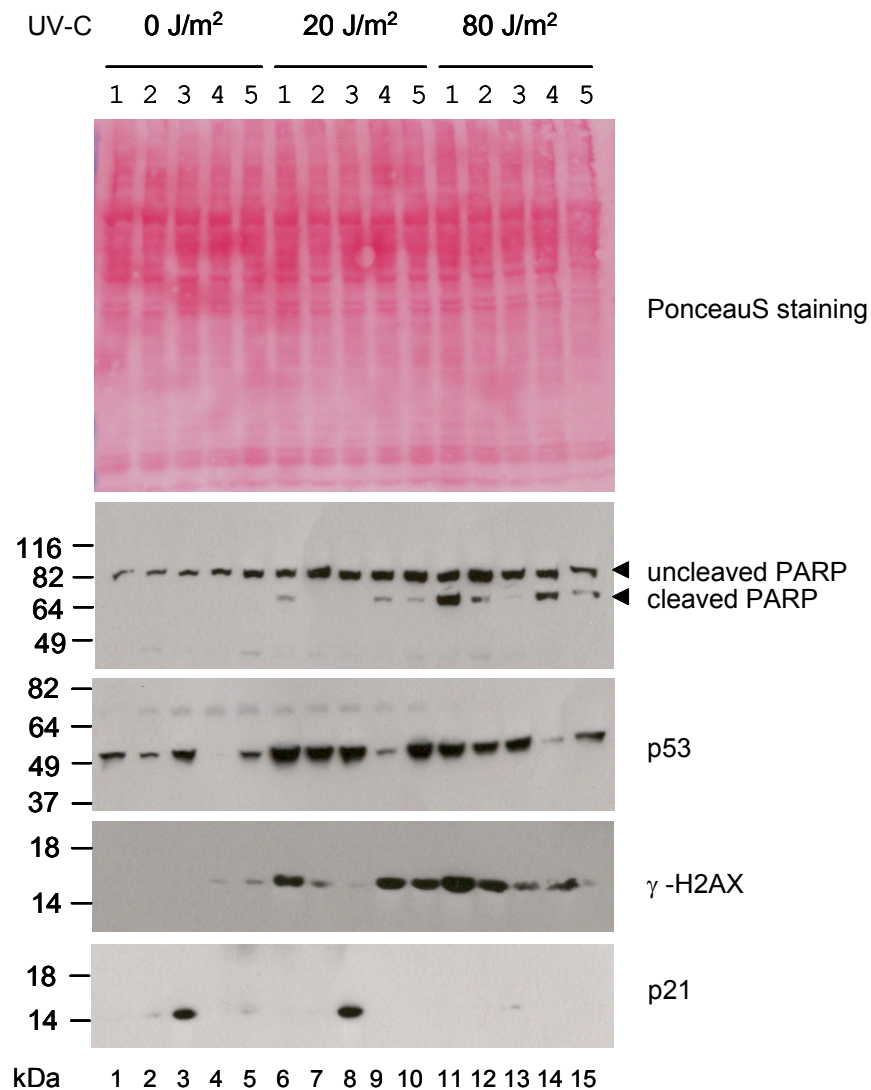
Figure 5.16: Impaired response to UV-irradiation upon removal of Tip60
(A) U2OS-cells were transfected with control-siRNA (1) as well as siRNA against *HTATIP* (2), *MDM2* (3), *TP53* (4) and *TP53BP1* (5). After 24 hours, the cells were irradiated with UV-C light (20 J/m2). After 4 more hours of incubation, the cells were harvested, followed by immunoblot detection of PARP (cleavage by caspases and the concomitant occurrence of a band with higher electrophoretic mobility indicate apoptosis), gammaH2AX (phosphorylation of H2AX indicates DNA-damage response), as well as p53 and p21.

5.6.2 siRNA-mediated knockdown of *HTATIP* expression results in decreased JNK-phosphorylation

Given the fact that *HTATIP* knockdown leads to an early inhibition of UV-response in the cells, we were interested in the levels of the jun N-terminal kinase (JNK) that is one of the kinases, apart from ATR and ATM, which is activated immediately after DNA damage and also required for the phosphorylation of histone 2AX (Burma et al., 2001; Lu et al., 2006; Ward et al., 2004). To study the impact of *HTATIP* knockdown

on JNK activation (measured by JNK phosphorylation) after UV irradiation, U2OS cells were treated either with siRNA against *HTATIP* and negative control siRNA. The protein expression was determined at different time points after irradiation by immunoblotting. As shown in Figure 5.17, phospho-JNK accumulation started 30 min after UV-C irradiation. *HTATIP* knockdown led to a reduction of JNK-phosphorylation already soon after exposure to UV light (lane 4), while the protein levels of total JNK remained unaltered. As observed before (Figure 5.16), the PARP cleavage was inhibited by *HTATIP* specific siRNA (lanes 9+10).

This result stresses the role of Tip60 in the immediate early response to UV, establishing a role of Tip60 in another kinase pathway in addition to involvement in ATM regulation.
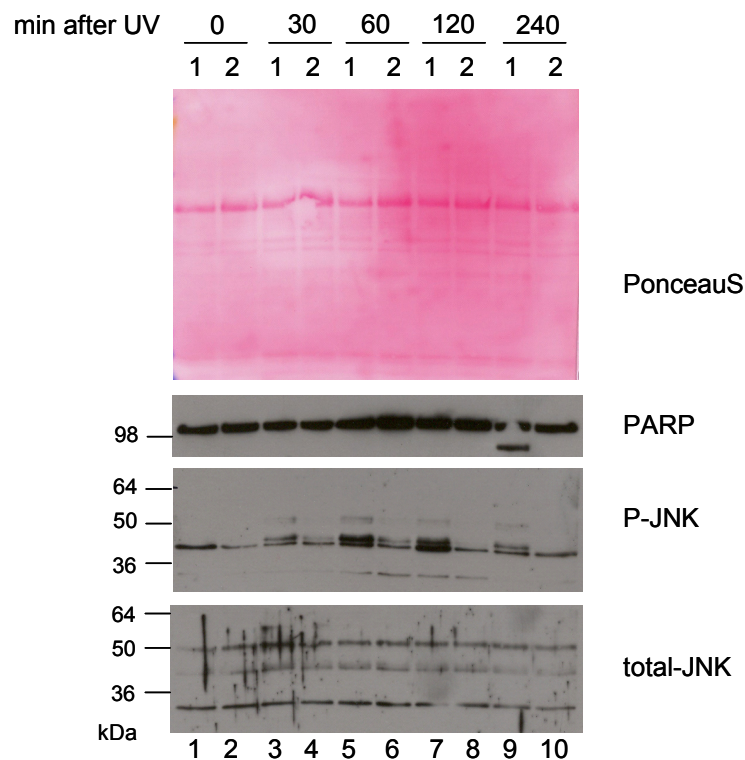

Figure 5.17: Impact of Tip60 knockdown on the phosphorylation of JNK
U2OS were transfected with either control siRNA (1) or Tip60 siRNA (2). Twenty-four hours later, the cells were UV-irradiated (20 J/m^2) as described in Fig.5.16. Harvesting of the cells was performed at the indicated time points after UV-C-irradiation, followed by immunoblot detection of phosphorylated JNK, total JNK and PARP.

6 Discussion

6.1 Differential regulation of the Mdm2 E3 ligase activity by Tip60

The results presented in this work suggest that Tip60 can act as a specific inhibitor of Mdm2-mediated neddylation. This concept reconciles three previous findings:

i) Tip60 turned out to represent an essential cofactor of p53, based on a genome-wide siRNA screen (Berns et al., 2004); ii) Tip60 was found to interact with Mdm2 but failed to block Mdm2-mediated ubiquitination (Legube et al., 2004); and iii) Mdm2 can antagonize p53 not only by ubiquitination, but also by neddylation (Xirodimas et al., 2004). In the light of these three previous notions, and based on the results shown here, we suggest that a plausible role of Tip60 in p53 regulation consists in an antagonism of Mdm2-mediated neddylation. In contrast, p14arf appears as the principal antagonist of ubiquitination by Mdm2.

At first glance, it seems surprising that the two E3 ligase activities of Mdm2 can be differentially regulated. After all, both activities require the intact RING domain near the carboxyterminus of Mdm2, and the disruption of this structure by mutation of residue Cys 464 abolishes both of them (Xirodimas et al., 2004). Also, neddylation and ubiquitination affect an overlapping set of lysine residues within the carboxyterminal domain of p53 (Xirodimas et al., 2004). The exact mechanisms that nonetheless allow the selective regulation of each activity remain to be determined. However, a few possibilities can be addressed by the results shown here. For instance, a functional acetyl transferase domain of Tip60 is not required for antagonizing Mdm2-mediated neddylation, arguing that Tip60 does not interfere with neddylation by acetylating one of the involved components. The acetylation of Mdm2 by CBP, for instance, had been shown to inhibit its ubiquitination activity towards p53 (Wang et al., 2004).

Further, by mutational analysis, the ability of Tip60 to bind Mdm2 could be separated from its ability to block neddylation.

Our results indicated that all Tip60 mutants studied still interact with Mdm2. Therefore, we conclude that the portion corresponding to residues 1-262 in Tip60 is sufficient to bind Mdm2. In seeming contrast to this, it was previously reported that a fragment consisting of residues 1-258 did not co-precipitate Mdm2 (Legube et al., 2004). However, the latter fragment accumulated to extremely high levels, raising the

possibility that squelching precluded co-precipitation despite interaction. Nonetheless, it remains possible that more than one domain of Tip60 is capable of forming a complex with Mdm2.

We therefore speculate that Tip60 does not simply act by binding Mdm2 but might in addition interact with a third partner to inhibit the ligation of Nedd8. Such a partner could also mediate the relocalization of Tip60 and Mdm2 to nuclear bodies, since relocalization and blocked neddylation co-segregated in our mapping experiments on Tip60 (Table 1).

	Association with Mdm2 in Co-IP	Relocalisation of Mdm2	Inhibition of Mdm2-mediated p53-Neddylation	Inhibition of Mdm2-Auto-Neddylation
Tip60 wild type	+ + +	+ + +	+ + +	+ + +
Tip60dHAT	+ + +	+ + +	+ + +	+ + +
Tip60dMYST	+ + −	− − −	− − −	− − −
Tip60dEXON5	+ + +	+ + −	+ + −	+ + −
Tip60STOP263	+ + −	− − −	− − −	− − −
Tip60STOP390	+ + +	+ − −	+ + −	+ + −

Table 1: Contribution of the Tip60 domains to the different effects of Tip60 on Mdm2

The finding that Mdm2 stimulated p53-neddylation *in vitro* only very weakly in comparison to p53-ubiquitination which was readily induced by Mdm2 (Xirodimas et al., 2004), may also be interpreted as a hint towards an unknown factor that might be required for Mdm2-mediated neddylation to occur.

The protein Cul4A, a member of the Cullin protein family, could represent a potential third factor, targeted by Tip60, that already was implicated in the Mdm2-mediated degradation of p53 by stimulating its polyubiquitination by Mdm2. Furthermore, Cul4A binds to Mdm2 (Nag et al., 2004). The inactivation of Cul4A leads to accumulation of p53 and its target gene p21 (Higa et al., 2006). As other Cullin proteins, Cul4A is neddylated and its neddylation is required for its proper activity. Although no cofactors have been described that are required for the Neddylation of p53 by Mdm2, Cul4A might be such a candidate. Tip60 might disrupt the binding of Cul4A to Mdm2, thereby interfering with its neddylation activity. Furthermore, recent work revealed a role of Cul4A in the DNA damage response, where it is engaged in a complex that ubiquitinates the histones H2A, H3 and H4 (Kapetanaki et al., 2006; Wang et al., 2006), two of which already have been described to be substrates of Tip60 acetylation (Ikura et al., 2000). However, the study of the Mdm2-mediated p53

neddylation in TS-41 cells that carry a temperature-sensitive neddylation pathway, show that the E3 ubiquitin ligase activity of Mdm2 is not regulated through neddylation of cullins (Xirodimas et al., 2004).

Since p14arf and Tip60 not only affect different E3 ligase activities of Mdm2 but also relocalize Mdm2 to distinct intranuclear structures (nucleoli vs. nuclear bodies), it is conceivable that the differential relocalization at least contributes to differential E3 ligase regulation. PML nuclear bodies have been reported to be sites of posttranslational modifications of proteins upon cellular stress like DNA damage but they have not been implicated yet in the regulation of protein-neddylation. The relocalisation of Mdm2 by p14arf to nucleoli has been described to play a role in the inhibition of Mdm2-activity. However, there are reports demonstrating that the relocalisation is not required for p53 stabilization (Llanos et al., 2001).

The only known regulators of cellular neddylation so far are the ASPP2 (apoptosis stimulating protein of p53) protein which had been implicated in the inhibition of APP-BP1 leading to decreased neddylation of cullins (Chen et al., 2003). Furthermore the enzyme Nedp1 and the COP9 signalosome regulate the levels of neddylated proteins by cleavage of Nedd8 (Mendoza et al., 2003; Min et al., 2005).

At present, the exact biological purpose of two distinct E3 ligase activities on Mdm2 and their separate regulation is unkown. Earlier reports have identified Tip60 as an essential cofactor for p53, showing that the knockdown of *HTATIP* by siRNA severely impairs the ability of p53 to transactivate its target genes (Berns et al., 2004; Legube et al., 2004). It is therefore tempting to speculate that a reduction in endogenous Tip60 levels might increase Mdm2- mediated neddylation of p53. In such a concept, increased p53 neddylation would then compromise transcriptional activity (Xirodimas et al., 2004). However, we were unable to observe such an effect directly . At least in the cells under study here, efficient knockdown of *HTATIP* gene expression (more than 80%) only led to a very moderate reduction in the expression of the p53 target gene *p21* (typically less than 30%) (discussed in 6.1.3), and the stable overexpression of exogenous Tip60 was compatible with continued cell proliferation, even in U2OS cells that carry wildtype p53 (data not shown). We therefore propose that Tip60, and possibly its ability to block Mdm2-mediated p53 neddylation, may activate p53 only under specific circumstances or cell species that still await their identification.

Nonetheless, our results do show that, in principle, two different Mdm2 E3 ligase

activities can be individually regulated, at least suggesting the evolution of tunable and independent mechanisms that differentially affect the stability and transcriptional activity of p53.

In the other characterized system for Nedd8 conjugation, Rbx1, the RING finger component of the SCF complex, which is required for ubiquitin ligase activity, can also act as an E3 Nedd8 ligase for cullins (Gray et al., 2002; Kamura et al., 1999; Morimoto et al., 2003). However, unlike in the case of Mdm2, studies of Rbx1 mutants suggest that some Rbx1 mutations preferably affect ubiquitylation, whereas others more affect neddylation (Megumi et al., 2005; Xirodimas et al., 2004).

The differential regulation of Mdm2-mediated ubiquitination and neddylation by Tip60 are in line with findings of Xirodimas et al. (2004), that p53 ubiquitination and neddylation are differentially regulated by UV-induced DNA damage. They demonstrated, by using stably-transfected MCF-7 cells (derived from carcinoma of the breast), that while the ubiquitinaton of p53 was inhibited 4 h post UV-irradiation and sustained 8 h post UV, p53 neddylation was transiently increased 4 h post UV but could not be detected by 8 h after UV irradiation. Taking this into account, UV irradiation would reduce Tip60 and p53 ubiquitination and thereby block their degradation, allowing Tip60 to inhibit additionally Mdm2-mediated Neddylation of p53, thereby further stimulating its transcriptional activity. An increase of Tip60 protein after UV irradiation would then lead to an inhibition of p53-Neddylation. Tip60 is probably only the first of several factors to be identified that can regulate the decision of ubiquitination versus neddylation.

It is somewhat puzzling that Tip60 also inhibited Mdm2-autoneddylation, thereby depressing its antagonising activity towards p53. However, an analogous observation has been reported for p14arf, which blocks p53 ubiquitination but also Mdm2 autoubiquitination.

6.1.1 The role of PML and the PML nuclear bodies

It is somewhat surprising to see that Tip60 and Mdm2 relocalize each other to nuclear bodies even in *pm l-/-* cells (Fig. 5.12). However, it should be noted that nuclear bodies have previously been observed in the absence of PML. An example is provided by the human homeodomain-interacting protein kinase (HIPK) 2. HIPK2 not only interacts with and phosphorylates p53 (D'Orazi et al., 2002; Hofmann et al.,

2002) but also localizes to nuclear bodies. These HIPK2 nuclear bodies coincide, at least in part, with the pattern of PML localization, but they are observed even when PML is absent (Moller et al., 2003). Hence, nuclear bodies can form in the absence of PML. The identity of scaffold proteins that allow the accumulation of Mdm2 and Tip60 in nuclear bodies independently of PML is currently under investigation.

It remains to be determined what role the PML protein plays in the inhibition of Mdm2-mediated neddylation of p53 by Tip60. Due to very low transfection efficiencies in the *pml* wild type and *pml* null MEFs, this issue could not be addressed in this work.

PML and the PML nuclear bodies have been implicated as an important player in the regulation of p53 stability and activity. Inhibition of PML expression was reported to have no detectable effect on the expression of endogenous p53 at the mRNA level; but led to a significant decrease of p53 protein (Bao-Lei et al., 2006). Moreover, an increase in the p53-Mdm2 complexes was observed, which may facilitate p53 protein degradation by the ubiquitin-proteasome pathway, also in irradiation treated cells. Furthermore, it was reported that p53 transcriptional activity was attenuated both in unstressed and gamma-irradiated cells upon removal of PML. Also, inhibition of PML expression in MCF-7 cells significantly reduced the expression of p53 downstream genes like *p21/CDKN1A* and *Bax* (Bao-Lei et al., 2006).

Mdm2, PML and p53 form temporal complexes in response to DNA damage (Kurki et al., 2003). Following UV irradiation, p53 forms a complex with PML, but only at a kinetically narrow window between 1-3 hours after the damage; Mdm2 complex formation with PML is also transient, peaking at 3 hours.

Although, Legube et al. (2004) also found that Tip60 relocalizes Mdm2 and p53 to PML nuclear bodies, it cannot be ruled out that part of the nuclear dots observed are due to the high protein levels after transient transfection. The protein levels of Tip60 and Mdm2 were usually very high in the transfected cells. As a consequence, Tip60 and Mdm2 might accumulate to such high levels that insoluble protein aggregates form. Therefore, it would be conceivable that a part of these complexes actually contain chaperones and proteasomes, which associate with clusters of unfolded proteins. In fact, it has been shown that Mdm2 and p14arf accumulate in extra-nucleolar bodies that are targeted by the PML protein and show an association with proteasomes and the stress protein HSP70 (Kashuba et al., 2003). There are also

hints that PML bodies are involved in the regulation of protein degradation of nuclear proteins. For instance, misfolded influenza nucleoprotein accumulates in PML nuclear bodies in cells where proteasome mediated degradation is inhibited suggesting that PML bodies function as the nuclear analogues of the cytoplasmic aggregosome (Anton et al., 1999).

6.1.2 Mechanism of p53 and Mdm2 stabilization by Tip60

Our results suggest that Tip60 does not interfere with the Mdm2-mediated ubiquitination of p53, but stabilizes it by inhibiting a subsequent step in the degradation process (Fig. 5.4). Mdm2 is required for both ubiquitination and degradation of p53. Consistent with our findings, Legube et al. (2004) reported that Tip60 overexpression results in the accumulation of ubiquitinated p53 forms in the presence of Mdm2.

The finding that siRNA against *HTATIP* leads to a decrease of Mdm2 protein levels at the same time leaving the p53 levels unaltered, points to a stronger dependence of Mdm2 stability on Tip60 than p53. Legube et al. (2004) only found a very weak reduction in p53 protein levels upon knockdown of Tip60. This effect may also strongly depend on the cell line under study.

Although the mechanism is not fully characterized, a post-ubiquitination role has been proposed for Mdm2 in the p53 degradation pathway (Brignone et al., 2004; Glockzin et al., 2003; Kulikov et al., 2005) (Figure 6.2 A). Also, it recently has been demonstrated that Mdm2 directly binds to the C8 subunit of the 20S proteasome and promotes Rb protein degradation in a proteasome-mediated manner (Sdek et al., 2005). Therefore, Mdm2 may function as a post ubiquitination adaptor for its ubiquitinated substrates, with assistance of other proteasome-interacting proteins like the human homolog of Rad23 (hHR23) (Brignone et al., 2004; Glockzin et al., 2003). Other proteasome interacting proteins that deliver ubiquitinated substrates to the 19S regulator subunit of the 26S proteasome, potentially targeted by Tip60, are Dsk2 (dominant suppressor of Kar2) and Ddi1 (DNA damage molecule 1) (reviewed in (Welchman et al., 2005). Thus, Tip60 could either directly interfere with the Mdm2-proteasome interaction or manipulate the activity of proteasome-interacting proteins, explaining its ability to stabilize p53.

The small ribosomal protein L11 has recently been shown to inhibit Mdm2 degradation by a postubiquitination mechanism (Dai et al., 2006), supporting this hypothesis.

Given that Tip60 relocalizes Mdm2 and p53 to PML nuclear bodies (Figure 6.2 C), it is also conceivable that p53 and Mdm2 stabilization is in part due to an inhibition of nuclear export. Such a mechanism has already been described for p53 stabilisation by p14arf (Tao and Levine, 1999).

Besides p53, it was recently shown that its homologue p73 (and specifically its isoforms containing an aminoterminal transactivation domain) can also be neddylated in an Mdm2-dependent manner (Watson et al., 2006). We therefore assume that Tip60 not only affects posttranslational modifications on p53 but also on p73 and possibly p63.

Taken together, the results presented here strongly suggest that the Mdm2 oncoprotein not only carries out two distinct E3 ligase activities but that these activities can also be regulated individually by different factors. In perspective, this suggests an unexpected versatility of Ubiquitin ligases. With hundreds of Ubiquitin conjugating enzmes of the E3 type expressed by the human genome (Ciechanover, 2005), the targeting of Ubiquitin conjugation has already reached enormous complexity (Figure 6.1). If even a small fraction of these ligases turned out to carry out additional and individually regulated conjugation of several Ubiquitin-like modifiers, this would even further increase the flexibility of the system. Mdm2 may only represent the first example of such an E3 ligase that not only integrates multiple regulatory inputs but can also respond with individual combinations of at least two different output activities.

6.1.3 Impact of Tip60 on the transcriptional activity of p53

Given the fact that Tip60 has been described previously to play a role in the transcriptional activation of p53 target genes like *p21/CDKN1A,* revealed both by knockdown and overexpression experiments (Berns et al., 2004, Legube et al., 2004), it is astonishing that the overexpression of Tip60 did not result in an increase of p53 activity measured both by luciferase assay and qRT-PCR analysis. In our experiments, the protein levels of p53 did not correlate with its transcriptional activity. Legube et al. (2004) have reported that Tip60, Mdm2 and p53 coprecipitated when overexpressed.
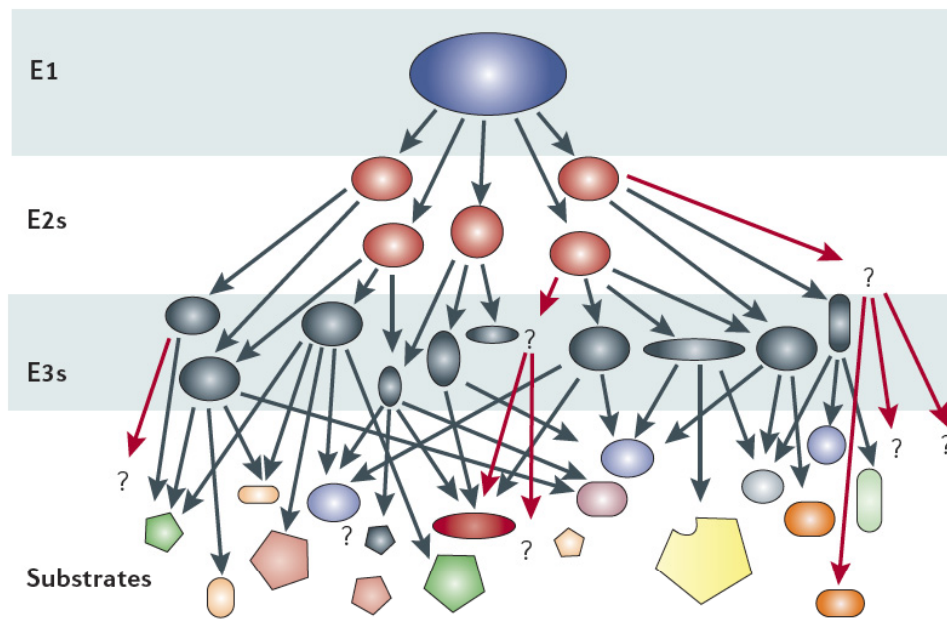
Figure 6.1: Complexity of the ubiquitin cascade
The ubiquitin cascade is pyramidal in design. A single E1-activating enzyme transfers ubiquitin to roughly three dozen E2s, which function together with several hundred different E3 ubiquitin ligases to ubiquitylate thousands of substrates. The differential regulation of different E3-ligase activities (e.g. ubiquitination versus neddylation) would add even another level to this complexity. Taken from Nalepa et al., 2006.

Therefore, it is conceivable that p53 is stabilized by Tip60 but still is impaired in its transcriptional activation by Mdm2 binding to its N-terminal transactivation domain while p14arf sequesters Mdm2 away from p53, thereby stimulating the transcriptional activity of p53 (Tao and Levine, 1999; Weber et al., 1999). Moreover, overexpression of proteins involved in transcription has been described to provoke so called squelching effects. In such a case, a transcription factor or coactivator binds in a saturating fashion to the binding sites of proteins involved in transcription, thereby disrupting the integrity of the complex in question.

In fact, Tip60 has been described to repress the activity of a reporter plasmid responsive to the Fe65 protein (Scheinfeld et al., 2003). While the interaction domain of Mdm2 with p14arf is mapped (Weber et al., 2000), very little is known about the binding site of Tip60 on Mdm2 (Legube et al., 2002; Legube et al., 2004). Unlike Tip60, p14arf was capable of partially rescuing the transcriptional activity of p53 in luciferase assays as well as in qRT-PCR analysis.
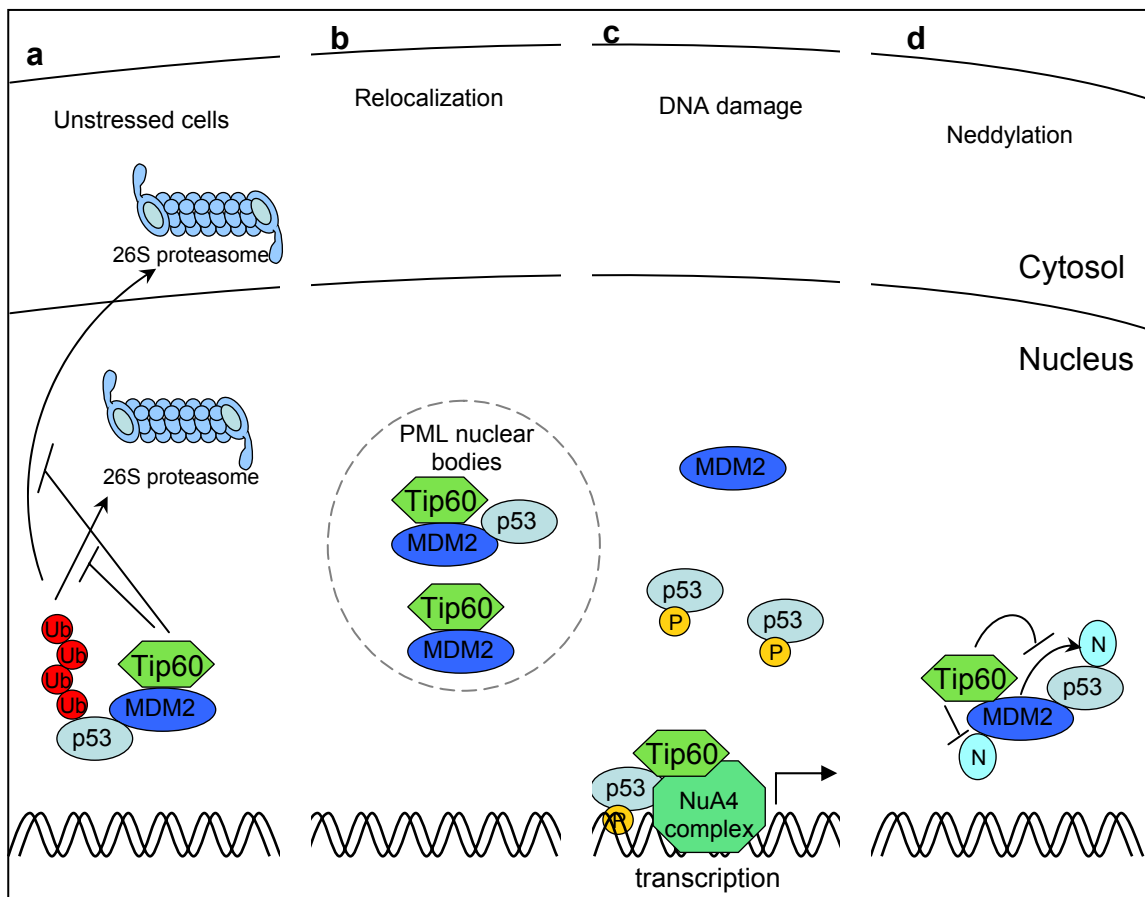
Figure 6.2: The role of Tip60 in the p53 pathway
(A) Tip60 inhibits the degradation of p53 and Mdm2, but not their ubiquitination, probably also under non-stress conditions. Therefore it most likely inhibits the degradation at a step between ubiquitination and degradation by the proteasome. **(B)** Tip60 colocalizes with Mdm2 and p53 to PML nuclear bodies, thereby potentially inhibiting their nuclear export. **(C)** Tip60 is involved in the transactivation of transcription by p53, possibly as a part of the HAT complex NuA4. **(D)** Tip60 inhibits the Mdm2-mediated conjugation of Nedd8 to p53 and towards Mdm2 itself. Figure modified from Hoeller et al., 2006.

The fact that Tip60 does not inhibit the Mdm2-mediated ubiquitination of p53 (Figure 5.4), but rather interferes with a subsequent step, is consistent with the finding that overexpression of Tip60 does not rescue p53 transcriptional activity. Ubiquitinated p53 might still be associated with Mdm2 and thereby kept inactive.

Furthermore, our results stand in contrast to the findings of Berns et al., Legube et al. and Tyteca et al. that found a strong reduction in the p21-mRNA levels upon Tip60 knockdown whereas our experiments only showed a light effect of Tip60 knockdown on p53 transcriptional activity in exactly the same cell line (U2OS). So far, we cannot explain this discrepancy. However, it is possible that the differences are at least in part due to slightly different experimental setups, and although the same cell line was used, certain genetic alterations in the cell lines, resulting in a different experimental outcome cannot be ruled out completely.

However, the sole knockdown of *HTATIP* expression by siRNA does not allow to draw conclusions on the mechanism of reduced *p21*-expression. Tip60 could act on multiple levels as discussed before, e.g. inhibition of Mdm2 neddylation, and also function as a p53 cofactor in transcription. To elucidate the mechanisms, it would be conceivable to perform rescue experiments where different siRNA-resistant Tip60-mutants are reintroduced into the cell by transfection after knockdown of endogenous *HTATIP* expression, followed by analysis of gene expression.

6.1.4 Tip60 and p14arf

It remains to be determined, what roles Tip60 plays in the p14arf-p53 pathway. The impact of p14arf on Tip60 can be most probably neglected as U2OS cells, which were mainly used in these studies, do not contain the p14arf protein due to methylation of its gene promoter at the *INK4A/ARF* locus (Park et al., 2002).

However, two recent reports highlighted new functional interactions between Tip60, p14arf and pRb, independently from p53. First, Tip60 was shown to bind and acetylate pRb, resulting in increased pRb degradation (Leduc et al., 2006). Overexpression of p14arf prevented pRb acetylation, hence stabilizing pRb. Furthermore it was shown that p14arf and Tip60 can form a complex in cells (Eymin et al., 2006). p14arf overexpression induced an ATM-ATR-dependent DNA damage response in p53-null cells, in a Tip60-dependent manner. Genotoxic stress led to p14arf dependent accumulation of pRb, as well as Arf- and Tip60-dependent activation of ATM. Thus, ARF appears to antagonize Tip60 in terms of pRb degradation, whereas the two proteins work together in the DNA damage response and p53 phosphorylation.

6.2 The role of Tip60 in the UV-induced apoptosis

Tip60 was recently identified as an essential cofactor in UV-mediated apoptosis (Tyteca et al., 2006), and consistent with this, we found that UV-mediated cleavage of poly ADP ribose polymerase (PARP), a substrate of caspases, was attenuated when Tip60 was removed by siRNA prior to irradiation (Fig. 5.16 and 5.17). Strikingly, we observed that the removal of p53 did not confer such protection against

apoptosis in a parallel experiment, arguing that the knockdown of *HTATIP* does not exert its effect through attenuating the p53 response.

Furthermore, studies in the Drosophila eye revealed that p53 knockdown increases the UV sensitivity (Jassim et al., 2003).

Even more surprisingly, however, it turned out that the removal of Tip60 not only interfered with caspase activation, but also with the phosphorylation of histone 2AX (measured by the accumulation of γ-H2AX). This argues that Tip60 is required for the early response triggered by UV-induced genotoxicity. H2AX phosphorylation has long been known to be induced by the classical signalling kinases ATM/Chk2 and ATR/Chk1, the latter being particularly implied in the UV response.

Also, Tip60 and histone 2AX have previously been shown to be linked, e.g. by the finding that the Tip60 homologue in drosophila is required fo the exchange of phosphorylated H2Av, the homolog of mammalian H2AZ isoform (which is not phosphorylated by ATM) but contains the same PIKK-target (phosphatidylinositol 3-kinase-related kinase) residue as H2AX (Ser 139 in both cases). Here, the acetylation of H2Av by the Tip60 complex initiates its exchange, performed probably by another member of the Tip60 complex, the p400 protein (Kusch et al., 2004).

In our hands, *HTATIP* knockdown not only led to a reduction of H2AX-phosphorylation upon UV irradiation, but also reduced the phosphorylation of the jun-terminal kinase JNK at a very early timepoint (30 min post UV irradiation). It was found more recently that H2AX phosphorylation in response to UV light requires the induction of JNK (Lu et al., 2006), perhaps as a result of daxx (death domain associated protein) relocalization. Daxx is found associated with the PML NBs where also Tip60 has been found (Khelifi et al., 2005). Recent reports suggest that UV irradiation induces the ubiquitination and degradation of Daxx, releasing its interaction partner RASSF1C (Ras association domain family 1C) from the nucleus (Kitagawa et al., 2006). This in turn leads to the activation of the SAPK/JNK (stress activated kinase/ jun-N-terminal kinase) pathway. It is conceivable that Tip60 is needed for the ubiquitination and degradation of Daxx, maybe by acetylating it. The lack of Tip60 would then result in a block of Daxx degradation and retention of RASSF1C in the nucleus. Furthermore, Daxx has been reported to play a critical role in regulating Mdm2 by stabilizing it and stimulating its ubiquitination towards p53 (Tang et al., 2006).

In summary, Tip60 can favor p53 activity through several independent and possibly additive mechanisms. In this work, two additional roles of Tip60 have been unveiled that potentially contribute to tumor suppression. First, Tip60 can inhibit the Mdm2-mediated conjugation of the Nedd8 protein to p53, thereby possibly releaving it from transcriptional inhibition by Mdm2. Moreover, Tip60 apparently is required for the proper activation of the UV-induced JNK-signaling pathway, thereby ensuring an efficient response to DNA damage and apoptosis induction.

7 REFERENCES

Adams, M.M. and Carpenter, P.B. (2006) Tying the loose ends together in DNA double strand break repair with 53BP1. *Cell Div*, **1**, 19.

Amir, R.E., Iwai, K. and Ciechanover, A. (2002) The NEDD8 pathway is essential for SCF(beta -TrCP)-mediated ubiquitination and processing of the NF-kappa B precursor p105. *J Biol Chem*, **277**, 23253-23259.

Anton, L.C., Schubert, U., Bacik, I., Princiotta, M.F., Wearsch, P.A., Gibbs, J., Day, P.M., Realini, C., Rechsteiner, M.C., Bennink, J.R. and Yewdell, J.W. (1999) Intracellular localization of proteasomal degradation of a viral antigen. *J Cell Biol*, **146**, 113-124.

Bao-Lei, T., Zhu-Zhong, M., Yi, S., Jun-Jie, Q., Yan, D., Hua, L., Bin, L., Guo-Wei, Z. and Zhi-Xian, S. (2006) Knocking down PML impairs p53 signaling transduction pathway and suppresses irradiation induced apoptosis in breast carcinoma cell MCF-7. *J Cell Biochem*, **97**, 561-571.

Barron, M.R., Belaguli, N.S., Zhang, S.X., Trinh, M., Iyer, D., Merlo, X., Lough, J.W., Parmacek, M.S., Bruneau, B.G. and Schwartz, R.J. (2005) Serum response factor, an enriched cardiac mesoderm obligatory factor, is a downstream gene target for Tbx genes. *J Biol Chem*, **280**, 11816-11828.

Bernardi, R., Scaglioni, P.P., Bergmann, S., Horn, H.F., Vousden, K.H. and Pandolfi, P.P. (2004) PML regulates p53 stability by sequestering Mdm2 to the nucleolus. *Nat Cell Biol*, **6**, 665-672.

Berns, K., Hijmans, E.M., Mullenders, J., Brummelkamp, T.R., Velds, A., Heimerikx, M., Kerkhoven, R.M., Madiredjo, M., Nijkamp, W., Weigelt, B., Agami, R., Ge, W., Cavet, G., Linsley, P.S., Beijersbergen, R.L. and Bernards, R. (2004) A large-scale RNAi screen in human cells identifies new components of the p53 pathway. *Nature*, **428**, 431-437.

Bianchi, E., Denti, S., Catena, R., Rossetti, G., Polo, S., Gasparian, S., Putignano, S., Rogge, L. and Pardi, R. (2003) Characterization of human constitutive photomorphogenesis protein 1, a RING finger ubiquitin ligase that interacts with Jun transcription factors and modulates their transcriptional activity. *J Biol Chem*, **278**, 19682-19690.

Bode, A.M. and Dong, Z. (2003) Mitogen-activated protein kinase activation in UV-induced signal transduction. *Sci STKE*, **2003**, RE2.

Brignone, C., Bradley, K.E., Kisselev, A.F. and Grossman, S.R. (2004) A post-ubiquitination role for MDM2 and hHR23A in the p53 degradation pathway. *Oncogene*, **23**, 4121-4129.

Brooks, C.L. and Gu, W. (2006) p53 ubiquitination: Mdm2 and beyond. *Mol Cell*, **21**, 307-315.

Brummelkamp, T.R., Fabius, A.W., Mullenders, J., Madiredjo, M., Velds, A., Kerkhoven, R.M., Bernards, R. and Beijersbergen, R.L. (2006) An shRNA barcode screen provides insight into cancer cell vulnerability to MDM2 inhibitors. *Nat Chem Biol*, **2**, 202-206.

Burma, S., Chen, B.P., Murphy, M., Kurimasa, A. and Chen, D.J. (2001) ATM phosphorylates histone H2AX in response to DNA double-strand breaks. *J Biol Chem*, **276**, 42462-42467.

Cahilly-Snyder, L., Yang-Feng, T., Francke, U. and George, D.L. (1987) Molecular analysis and chromosomal mapping of amplified genes isolated from a transformed mouse 3T3 cell line. *Somat Cell Mol Genet*, **13**, 235-244.

Chan, W.M., Mak, M.C., Fung, T.K., Lau, A., Siu, W.Y. and Poon, R.Y. (2006) Ubiquitination of p53 at multiple sites in the DNA-binding domain. *Mol Cancer Res*, **4**, 15-25.

Chen, J., Marechal, V. and Levine, A.J. (1993) Mapping of the p53 and mdm-2 interaction domains. *Mol Cell Biol*, **13**, 4107-4114.

Chen, Y., Liu, W., Naumovski, L. and Neve, R.L. (2003) ASPP2 inhibits APP-BP1-mediated NEDD8 conjugation to cullin-1 and decreases APP-BP1-induced cell proliferation and neuronal apoptosis. *J Neurochem*, **85**, 801-809.

Ciechanover, A. (2005) Intracellular protein degradation: from a vague idea thru the lysosome and the ubiquitin-proteasome system and onto human diseases and drug targeting. *Cell Death Differ*, **12**, 1178-1190.

Col, E., Caron, C., Chable-Bessia, C., Legube, G., Gazzeri, S., Komatsu, Y., Yoshida, M., Benkirane, M., Trouche, D. and Khochbin, S. (2005) HIV-1 Tat targets Tip60 to impair the apoptotic cell response to genotoxic stresses. *Embo J*, **24**, 2634-2645.

D'Orazi, G., Cecchinelli, B., Bruno, T., Manni, I., Higashimoto, Y., Saito, S., Gostissa, M., Coen, S., Marchetti, A., Del Sal, G., Piaggio, G., Fanciulli, M., Appella, E. and Soddu, S. (2002) Homeodomain-interacting protein kinase-2 phosphorylates p53 at Ser 46 and mediates apoptosis. *Nat Cell Biol*, **4**, 11-19.

Dai, M.S. and Lu, H. (2004) Inhibition of MDM2-mediated p53 ubiquitination and degradation by ribosomal protein L5. *J Biol Chem*, **279**, 44475-44482.

Dai, M.S., Shi, D., Jin, Y., Sun, X.X., Zhang, Y., Grossman, S.R. and Lu, H. (2006) Regulation of the MDM2-p53 pathway by ribosomal protein L11 involves a post-ubiquitination mechanism. *J Biol Chem*, **281**, 24304-24313.

de Laat, W.L., Jaspers, N.G. Hoeijmakers, J.H. (1999) Molecular mechanism of nucleotide excision repair. *Genes Dev,* **13**, 768-785

de Stanchina, E., Querido, E., Narita, M., Davuluri, R.V., Pandolfi, P.P., Ferbeyre, G. and Lowe, S.W. (2004) PML is a direct p53 target that modulates p53 effector functions. *Mol Cell*, **13**, 523-535.

Dellaire, G. and Bazett-Jones, D.P. (2004) PML nuclear bodies: dynamic sensors of DNA damage and cellular stress. *Bioessays*, **26**, 963-977.

Deng, X.W., Caspar, T. and Quail, P.H. (1991) cop1: a regulatory locus involved in light-controlled development and gene expression in Arabidopsis. *Genes Dev*, **5**, 1172-1182.

Derijard, B., Hibi, M., Wu, I.H., Barrett, T., Su, B., Deng, T., Karin, M. and Davis, R.J. (1994) JNK1: a protein kinase stimulated by UV light and Ha-Ras that binds and phosphorylates the c-Jun activation domain. *Cell*, **76**, 1025-1037.

Dornan, D., Shimizu, H., Mah, A., Dudhela, T., Eby, M., O'Rourke, K., Seshagiri, S. and Dixit, V.M. (2006) ATM engages autodegradation of the E3 ubiquitin ligase COP1 after DNA damage. *Science*, **313**, 1122-1126.

Dornan, D., Wertz, I., Shimizu, H., Arnott, D., Frantz, G.D., Dowd, P., O'Rourke, K., Koeppen, H. and Dixit, V.M. (2004) The ubiquitin ligase COP1 is a critical negative regulator of p53. *Nature*, **429**, 86-92.

Doyon, Y., Selleck, W., Lane, W.S., Tan, S. and Cote, J. (2004) Structural and functional conservation of the NuA4 histone acetyltransferase complex from yeast to humans. *Mol Cell Biol*, **24**, 1884-1896.

el-Deiry, W.S., Harper, J.W., O'Connor, P.M., Velculescu, V.E., Canman, C.E., Jackman, J., Pietenpol, J.A., Burrell, M., Hill, D.E., Wang, Y. and et al. (1994) WAF1/CIP1 is induced in p53-mediated G1 arrest and apoptosis. *Cancer Res*, **54**, 1169-1174.

el-Deiry, W.S., Tokino, T., Velculescu, V.E., Levy, D.B., Parsons, R., Trent, J.M., Lin, D., Mercer, W.E., Kinzler, K.W. and Vogelstein, B. (1993) WAF1, a potential mediator of p53 tumor suppression. *Cell*, **75**, 817-825.

Elbashir, S.M., Harborth, J., Lendeckel, W., Yalcin, A., Weber, K. and Tuschl, T. (2001) Duplexes of 21-nucleotide RNAs mediate RNA interference in cultured mammalian cells. *Nature*, **411**, 494-498.

Eymin, B., Claverie, P., Salon, C., Leduc, C., Col, E., Brambilla, E., Khochbin, S. and Gazzeri, S. (2006) p14ARF Activates a Tip60-Dependent and p53-Independent ATM/ATR/CHK Pathway in Response to Genotoxic Stress. *Mol Cell Biol*, **26**, 4339-4350.

Frank, S.R., Parisi, T., Taubert, S., Fernandez, P., Fuchs, M., Chan, H.M., Livingston, D.M. and Amati, B. (2003) MYC recruits the TIP60 histone acetyltransferase complex to chromatin. *EMBO Rep*, **4**, 575-580.

Freedman, D.A., Epstein, C.B., Roth, J.C. and Levine, A.J. (1997) A genetic approach to mapping the p53 binding site in the MDM2 protein. *Mol Med*, **3**, 248-259.

Glockzin, S., Ogi, F.X., Hengstermann, A., Scheffner, M. and Blattner, C. (2003) Involvement of the DNA repair protein hHR23 in p53 degradation. *Mol Cell Biol*, **23**, 8960-8969.

Gottlieb, T.M., Leal, J.F., Seger, R., Taya, Y. and Oren, M. (2002) Cross-talk between Akt, p53 and Mdm2: possible implications for the regulation of apoptosis. *Oncogene*, **21**, 1299-1303.

Gray, W.M., Hellmann, H., Dharmasiri, S. and Estelle, M. (2002) Role of the Arabidopsis RING-H2 protein RBX1 in RUB modification and SCF function. *Plant Cell*, **14**, 2137-2144.

Green, D.R. and Evan, G.I. (2002) A matter of life and death. *Cancer Cell*, **1**, 19-30.

Grossman, S.R., Deato, M.E., Brignone, C., Chan, H.M., Kung, A.L., Tagami, H., Nakatani, Y. and Livingston, D.M. (2003) Polyubiquitination of p53 by a ubiquitin ligase activity of p300. *Science*, **300**, 342-344.

Hay, R.T. (2005) SUMO: a history of modification. *Mol Cell*, **18**, 1-12.

Hermeking, H., Lengauer, C., Polyak, K., He, T.C., Zhang, L., Thiagalingam, S., Kinzler, K.W. and Vogelstein, B. (1997) 14-3-3 sigma is a p53-regulated inhibitor of G2/M progression. *Mol Cell*, **1**, 3-11.

Hibi, M., Lin, A., Smeal, T., Minden, A. and Karin, M. (1993) Identification of an oncoprotein- and UV-responsive protein kinase that binds and potentiates the c-Jun activation domain. *Genes Dev*, **7**, 2135-2148.

Higa, L.A., Yang, X., Zheng, J., Banks, D., Wu, M., Ghosh, P., Sun, H. and Zhang, H. (2006) Involvement of CUL4 ubiquitin E3 ligases in regulating CDK inhibitors Dacapo/p27Kip1 and cyclin E degradation. *Cell Cycle*, **5**, 71-77.

Hlubek, F., Lohberg, C., Meiler, J., Jung, A., Kirchner, T. and Brabletz, T. (2001) Tip60 is a cell-type-specific transcriptional regulator. *J Biochem (Tokyo)*, **129**, 635-641.

Hoeller, D., Hecker, C.M. and Dikic, I. (2006) Ubiquitin and ubiquitin-like proteins in cancer pathogenesis. *Nat Rev Cancer*, **6**, 776-788.

Hofmann, T.G., Moller, A., Sirma, H., Zentgraf, H., Taya, Y., Droge, W., Will, H. and Schmitz, M.L. (2002) Regulation of p53 activity by its interaction with homeodomain-interacting protein kinase-2. *Nat Cell Biol*, **4**, 1-10.

Hollstein, M., Rice, K., Greenblatt, M.S., Soussi, T., Fuchs, R., Sorlie, T., Hovig, E., Smith-Sorensen, B., Montesano, R. and Harris, C.C. (1994) Database of p53 gene somatic mutations in human tumors and cell lines. *Nucleic Acids Res*, **22**, 3551-3555.

Honda, R. and Yasuda, H. (1999) Association of p19(ARF) with Mdm2 inhibits ubiquitin ligase activity of Mdm2 for tumor suppressor p53. *Embo J*, **18**, 22-27.

Ikura, T., Ogryzko, V.V., Grigoriev, M., Groisman, R., Wang, J., Horikoshi, M., Scully, R., Qin, J. and Nakatani, Y. (2000) Involvement of the TIP60 histone acetylase complex in DNA repair and apoptosis. *Cell*, **102**, 463-473.

Jackson, M.W. and Berberich, S.J. (2000) MdmX protects p53 from Mdm2-mediated degradation. *Mol Cell Biol*, **20**, 1001-1007.

Jassim, O.W., Fink, J.L. and Cagan, R.L. (2003) Dmp53 protects the Drosophila retina during a developmentally regulated DNA damage response. *Embo J*, **22**, 5622-5632.

Jin, A., Itahana, K., O'Keefe, K. and Zhang, Y. (2004) Inhibition of HDM2 and activation of p53 by ribosomal protein L23. *Mol Cell Biol*, **24**, 7669-7680.

Kaeser, M.D. and Iggo, R.D. (2004) Promoter-specific p53-dependent histone acetylation following DNA damage. *Oncogene*, **23**, 4007-4013.

Kamine, J., Elangovan, B., Subramanian, T., Coleman, D. and Chinnadurai, G. (1996) Identification of a cellular protein that specifically interacts with the essential cysteine region of the HIV-1 Tat transactivator. *Virology*, **216**, 357-366.

Kamitani, T., Kito, K., Nguyen, H.P. and Yeh, E.T. (1997) Characterization of NEDD8, a developmentally down-regulated ubiquitin-like protein. *J Biol Chem*, **272**, 28557-28562.

Kamura, T., Conrad, M.N., Yan, Q., Conaway, R.C. and Conaway, J.W. (1999) The Rbx1 subunit of SCF and VHL E3 ubiquitin ligase activates Rub1 modification of cullins Cdc53 and Cul2. *Genes Dev*, **13**, 2928-2933.

Kapetanaki, M.G., Guerrero-Santoro, J., Bisi, D.C., Hsieh, C.L., Rapic-Otrin, V. and Levine, A.S. (2006) The DDB1-CUL4ADDB2 ubiquitin ligase is deficient in xeroderma pigmentosum group E and targets histone H2A at UV-damaged DNA sites. *Proc Natl Acad Sci U S A*, **103**, 2588-2593.

Kashuba, E., Mattsson, K., Klein, G. and Szekely, L. (2003) p14ARF induces the relocation of HDM2 and p53 to extranucleolar sites that are targeted by PML bodies and proteasomes. *Mol Cancer*, **2**, 18.

Khelifi, A.F., D'Alcontres, M.S. and Salomoni, P. (2005) Daxx is required for stress-induced cell death and JNK activation. *Cell Death Differ*, **12**, 724-733.

Kim, K.I., Giannakopoulos, N.V., Virgin, H.W. and Zhang, D.E. (2004) Interferon-inducible ubiquitin E2, Ubc8, is a conjugating enzyme for protein ISGylation. *Mol Cell Biol*, **24**, 9592-9600.

Kitagawa, D., Kajiho, H., Negishi, T., Ura, S., Watanabe, T., Wada, T., Ichijo, H., Katada, T. and Nishina, H. (2006) Release of RASSF1C from the nucleus by Daxx degradation links DNA damage and SAPK/JNK activation. *Embo J*, **25**, 3286-3297.

Kulikov, R., Boehme, K.A. and Blattner, C. (2005) Glycogen synthase kinase 3-dependent phosphorylation of Mdm2 regulates p53 abundance. *Mol Cell Biol*, **25**, 7170-7180.

Kurki, S., Latonen, L. and Laiho, M. (2003) Cellular stress and DNA damage invoke temporally distinct Mdm2, p53 and PML complexes and damage-specific nuclear relocalization. *J Cell Sci*, **116**, 3917-3925.

Kusch, T., Florens, L., Macdonald, W.H., Swanson, S.K., Glaser, R.L., Yates, J.R., 3rd, Abmayr, S.M., Washburn, M.P. and Workman, J.L. (2004) Acetylation by Tip60 is required for selective histone variant exchange at DNA lesions. *Science*, **306**, 2084-2087.

Latonen, L. and Laiho, M. (2005) Cellular UV damage responses--functions of tumor suppressor p53. *Biochim Biophys Acta*, **1755**, 71-89.

Leduc, C., Claverie, P., Eymin, B., Col, E., Khochbin, S., Brambilla, E. and Gazzeri, S. (2006) p14(ARF) promotes RB accumulation through inhibition of its Tip60-dependent acetylation. *Oncogene*.

Legube, G., Linares, L.K., Lemercier, C., Scheffner, M., Khochbin, S. and Trouche, D. (2002) Tip60 is targeted to proteasome-mediated degradation by Mdm2 and accumulates after UV irradiation. *Embo J*, **21**, 1704-1712.

Legube, G., Linares, L.K., Tyteca, S., Caron, C., Scheffner, M., Chevillard-Briet, M. and Trouche, D. (2004) Role of the histone acetyl transferase Tip60 in the p53 pathway. *J Biol Chem*, **279**, 44825-44833.

Lemercier, C., Legube, G., Caron, C., Louwagie, M., Garin, J., Trouche, D. and Khochbin, S. (2003) Tip60 acetyltransferase activity is controlled by phosphorylation. *J Biol Chem*, **278**, 4713-4718.

Lin, J., Chen, J., Elenbaas, B. and Levine, A.J. (1994) Several hydrophobic amino acids in the p53 amino-terminal domain are required for transcriptional activation, binding to mdm-2 and the adenovirus 5 E1B 55-kD protein. *Genes Dev*, **8**, 1235-1246.

Llanos, S., Clark, P.A., Rowe, J. and Peters, G. (2001) Stabilization of p53 by p14ARF without relocation of MDM2 to the nucleolus. *Nat Cell Biol*, **3**, 445-452.

Lloyd, S.A. (1993) Stratospheric ozone depletion. *Lancet*, **342**, 1156-1158.

Logan, I.R., Sapountzi, V., Gaughan, L, Neal, D.E., Robson, CN. (2004) Control of human PIRH2 protein stability: involvement of TIP60 and the proteosome. *J Biol Chem.* 2004 Mar 19; **279,** 11696-704

Lohrum, M.A., Ludwig, R.L., Kubbutat, M.H., Hanlon, M. and Vousden, K.H. (2003) Regulation of HDM2 activity by the ribosomal protein L11. *Cancer Cell*, **3**, 577-587.

Louria-Hayon, I., Grossman, T., Sionov, R.V., Alsheich, O., Pandolfi, P.P. and Haupt, Y. (2003) The promyelocytic leukemia protein protects p53 from Mdm2-mediated inhibition and degradation. *J Biol Chem*, **278**, 33134-33141.

Lu, C., Zhu, F., Cho, Y.Y., Tang, F., Zykova, T., Ma, W.Y., Bode, A.M. and Dong, Z. (2006) Cell apoptosis: requirement of H2AX in DNA ladder formation, but not for the activation of caspase-3. *Mol Cell*, **23**, 121-132.

Lu, H. and Levine, A.J. (1995) Human TAFII31 protein is a transcriptional coactivator of the p53 protein. *Proc Natl Acad Sci U S A*, **92**, 5154-5158.

Maya, R., Balass, M., Kim, S.T., Shkedy, D., Leal, J.F., Shifman, O., Moas, M., Buschmann, T., Ronai, Z., Shiloh, Y., Kastan, M.B., Katzir, E. and Oren, M. (2001) ATM-dependent phosphorylation of Mdm2 on serine 395: role in p53 activation by DNA damage. *Genes Dev*, **15**, 1067-1077.

Meek, D.W. and Knippschild, U. (2003) Posttranslational modification of MDM2. *Mol Cancer Res*, **1**, 1017-1026.

Megumi, Y., Miyauchi, Y., Sakurai, H., Nobeyama, H., Lorick, K., Nakamura, E., Chiba, T., Tanaka, K., Weissman, A.M., Kirisako, T., Ogawa, O. and Iwai, K. (2005) Multiple roles of Rbx1 in the VBC-Cul2 ubiquitin ligase complex. *Genes Cells*, **10**, 679-691.

Mendoza, H.M., Shen, L.N., Botting, C., Lewis, A., Chen, J., Ink, B. and Hay, R.T. (2003) NEDP1, a highly conserved cysteine protease that deNEDDylates Cullins. *J Biol Chem*, **278**, 25637-25643.

Michael, D. and Oren, M. (2003) The p53-Mdm2 module and the ubiquitin system. *Semin Cancer Biol*, **13**, 49-58.

Mihara, M., Erster, S., Zaika, A., Petrenko, O., Chittenden, T., Pancoska, P. and Moll, U.M. (2003) p53 has a direct apoptogenic role at the mitochondria. *Mol Cell*, **11**, 577-590.

Min, K.W., Kwon, M.J., Park, H.S., Park, Y., Yoon, S.K. and Yoon, J.B. (2005) CAND1 enhances deneddylation of CUL1 by COP9 signalosome. *Biochem Biophys Res Commun*, **334**, 867-874.

Mittal, V. (2004) Improving the efficiency of RNA interference in mammals. *Nat Rev Genet*, **5**, 355-365.

Moller, A., Sirma, H., Hofmann, T.G., Rueffer, S., Klimczak, E., Droge, W., Will, H. and Schmitz, M.L. (2003) PML is required for homeodomain-interacting protein kinase 2 (HIPK2)-mediated p53 phosphorylation and cell cycle arrest but is dispensable for the formation of HIPK domains. *Cancer Res*, **63**, 4310-4314.

Momand, J., Zambetti, G.P., Olson, D.C., George, D. and Levine, A.J. (1992) The mdm-2 oncogene product forms a complex with the p53 protein and inhibits p53-mediated transactivation. *Cell*, **69**, 1237-1245.

Morimoto, M., Nishida, T., Nagayama, Y. and Yasuda, H. (2003) Nedd8-modification of Cul1 is promoted by Roc1 as a Nedd8-E3 ligase and regulates its stability. *Biochem Biophys Res Commun*, **301**, 392-398.

Nag, A., Bagchi, S. and Raychaudhuri, P. (2004) Cul4A physically associates with MDM2 and participates in the proteolysis of p53. *Cancer Res*, **64**, 8152-8155.

Nalepa, G., Rolfe, M. and Harper, J.W. (2006) Drug discovery in the ubiquitin-proteasome system. *Nat Rev Drug Discov*, **5**, 596-613.

Napoli, C., Lemieux, C. and Jorgensen, R. (1990) Introduction of a Chimeric Chalcone Synthase Gene into Petunia Results in Reversible Co-Suppression of Homologous Genes in trans. *Plant Cell*, **2**, 279-289.

Niida, H. and Nakanishi, M. (2006) DNA damage checkpoints in mammals. *Mutagenesis*, **21**, 3-9.

Nordentoft, I. and Jorgensen, P. (2003) The acetyltransferase 60 kDa trans-acting regulatory protein of HIV type 1-interacting protein (Tip60) interacts with the translocation E26 transforming-specific leukaemia gene (TEL) and functions as a transcriptional co-repressor. *Biochem J*, **374**, 165-173.

Obaya, A.J. and Sedivy, J.M. (2002) Regulation of cyclin-Cdk activity in mammalian cells. *Cell Mol Life Sci*, **59**, 126-142.

Oliner, J.D. (1993) Discerning the function of p53 by examining its molecular interactions. *Bioessays*, **15**, 703-707.

Oliner, J.D., Kinzler, K.W., Meltzer, P.S., George, D.L. and Vogelstein, B. (1992) Amplification of a gene encoding a p53-associated protein in human sarcomas. *Nature*, **358**, 80-83.

Pan, Z.Q., Kentsis, A., Dias, D.C., Yamoah, K. and Wu, K. (2004) Nedd8 on cullin: building an expressway to protein destruction. *Oncogene*, **23**, 1985-1997.

Park, Y.B., Park, M.J., Kimura, K., Shimizu, K., Lee, S.H. and Yokota, J. (2002) Alterations in the INK4a/ARF locus and their effects on the growth of human osteosarcoma cell lines. *Cancer Genet Cytogenet*, **133**, 105-111.

Pomerantz, J., Schreiber-Agus, N., Liegeois, N.J., Silverman, A., Alland, L., Chin, L., Potes, J., Chen, K., Orlow, I., Lee, H.W., Cordon-Cardo, C. and DePinho, R.A. (1998) The Ink4a tumor suppressor gene product, p19Arf, interacts with MDM2 and neutralizes MDM2's inhibition of p53. *Cell*, **92**, 713-723.

Ravant, J.L., Douki, T., Cadet, J. (2001) Direct and indirect effects of UV radiation on DNA and its components, *J Photochem Photobiol,* **63**, 88-102

Reyes, J.C. (2001) PML and COP1--two proteins with much in common. *Trends Biochem Sci*, **26**, 18-20.

Rodriguez, M.S., Desterro, J.M., Lain, S., Midgley, C.A., Lane, D.P. and Hay, R.T. (1999) SUMO-1 modification activates the transcriptional response of p53. *Embo J*, **18**, 6455-6461.

Rodway, H., Llanos, S., Rowe, J. and Peters, G. (2004) Stability of nucleolar versus non-nucleolar forms of human p14(ARF). *Oncogene*, **23**, 6186-6192.

Sanger, F. Nicklen, S. and Coulson, A.R. (1977) DNA sequencing with chain-terminating inhibitors. *Proc Natl Acad USA*, **74,** 5463-67

Salomoni, P. and Khelifi, A.F. (2006) Daxx: death or survival protein? *Trends Cell Biol*, **16**, 97-104.

Sapountzi, V., Logan, I.R. and Robson, C.N. (2006) Cellular functions of TIP60. *Int J Biochem Cell Biol*.

Scheinfeld, M.H., Matsuda, S. and D'Adamio, L. (2003) JNK-interacting protein-1 promotes transcription of A beta protein precursor but not A beta precursor-like proteins, mechanistically different than Fe65. *Proc Natl Acad Sci U S A*, **100**, 1729-1734.

Sdek, P., Ying, H., Chang, D.L., Qiu, W., Zheng, H., Touitou, R., Allday, M.J. and Xiao, Z.X. (2005) MDM2 promotes proteasome-dependent ubiquitin-independent degradation of retinoblastoma protein. *Mol Cell*, **20**, 699-708.

Sheridan, A.M., Force, T., Yoon, H.J., O'Leary, E., Choukroun, G., Taheri, M.R. and Bonventre, J.V. (2001) PLIP, a novel splice variant of Tip60, interacts with group IV cytosolic phospholipase A(2), induces apoptosis, and potentiates prostaglandin production. *Mol Cell Biol*, **21**, 4470-4481.

Sun, Y., Jiang, X., Chen, S., Fernandes, N. and Price, B.D. (2005) A role for the Tip60 histone acetyltransferase in the acetylation and activation of ATM. *Proc Natl Acad Sci U S A*, **102**, 13182-13187.

Tang, J., Qu, L.K., Zhang, J., Wang, W., Michaelson, J.S., Degenhardt, Y.Y., El-Deiry, W.S. and Yang, X. (2006) Critical role for Daxx in regulating Mdm2. *Nat Cell Biol*, **8**, 855-862.

Tao, W. and Levine, A.J. (1999) P19(ARF) stabilizes p53 by blocking nucleo-cytoplasmic shuttling of Mdm2. *Proc Natl Acad Sci U S A*, **96**, 6937-6941.

Taubert, S., Gorrini, C., Frank, S.R., Parisi, T., Fuchs, M., Chan, H.M., Livingston, D.M. and Amati, B. (2004) E2F-dependent histone acetylation and recruitment of the Tip60 acetyltransferase complex to chromatin in late G1. *Mol Cell Biol*, **24**, 4546-4556.

Tiscornia, G., Tergaonkar, V., Galimi, F. and Verma, I.M. (2004) CRE recombinase-inducible RNA interference mediated by lentiviral vectors. *Proc Natl Acad Sci U S A*, **101**, 7347-7351.

Treier, M., Staszewski, L.M. and Bohmann, D. (1994) Ubiquitin-dependent c-Jun degradation in vivo is mediated by the delta domain. *Cell*, **78**, 787-798.

Tyteca, S., Vandromme, M., Legube, G., Chevillard-Briet, M. and Trouche, D. (2006) Tip60 and p400 are both required for UV-induced apoptosis but play antagonistic roles in cell cycle progression. *Embo J*, **25**, 1680-1689.

Vousden, K.H. and Lu, X. (2002) Live or let die: the cell's response to p53. *Nat Rev Cancer*, **2**, 594-604.

Wang, H., Zhai, L., Xu, J., Joo, H.Y., Jackson, S., Erdjument-Bromage, H., Tempst, P., Xiong, Y. and Zhang, Y. (2006) Histone H3 and H4 ubiquitylation by the CUL4-DDB-ROC1 ubiquitin ligase facilitates cellular response to DNA damage. *Mol Cell*, **22**, 383-394.

Wang, X., Taplick, J., Geva, N. and Oren, M. (2004) Inhibition of p53 degradation by Mdm2 acetylation. *FEBS Lett*, **561**, 195-201.

Ward, I.M., Minn, K. and Chen, J. (2004) UV-induced ataxia-telangiectasia-mutated and Rad3-related (ATR) activation requires replication stress. *J Biol Chem*, **279**, 9677-9680.

Watson, I.R., Blanch, A., Lin, D.C., Ohh, M. and Irwin, M.S. (2006) Mdm2-mediated NEDD8 modification of TAp73 regulates its transactivation function. *J Biol Chem*.

Watson, I.R. and Irwin, M.S. (2006) Ubiquitin and ubiquitin-like modifications of the p53 family. *Neoplasia*, **8**, 655-666.

Weber, J.D., Kuo, M.L., Bothner, B., DiGiammarino, E.L., Kriwacki, R.W., Roussel, M.F. and Sherr, C.J. (2000) Cooperative signals governing ARF-mdm2 interaction and nucleolar localization of the complex. *Mol Cell Biol*, **20**, 2517-2528.

Weber, J.D., Taylor, L.J., Roussel, M.F., Sherr, C.J. and Bar-Sagi, D. (1999) Nucleolar Arf sequesters Mdm2 and activates p53. *Nat Cell Biol*, **1**, 20-26.

Welchman, R.L., Gordon, C. and Mayer, R.J. (2005) Ubiquitin and ubiquitin-like proteins as multifunctional signals. *Nat Rev Mol Cell Biol*, **6**, 599-609.

Wu, S., Loke, H.N. and Rehemtulla, A. (2002) Ultraviolet radiation-induced apoptosis is mediated by Daxx. *Neoplasia*, **4**, 486-492.

Wu, X., Bayle, J.H., Olson, D. and Levine, A.J. (1993) The p53-mdm-2 autoregulatory feedback loop. *Genes Dev*, **7**, 1126-1132.

Wurtele, H. and Verreault, A. (2006) Histone post-translational modifications and the response to DNA double-strand breaks. *Curr Opin Cell Biol*, **18**, 137-144.

Xiao, H., Chung, J., Kao, H.Y. and Yang, Y.C. (2003) Tip60 is a co-repressor for STAT3. *J Biol Chem*, **278**, 11197-11204.

Xirodimas, D.P., Saville, M.K., Bourdon, J.C., Hay, R.T. and Lane, D.P. (2004) Mdm2-mediated NEDD8 conjugation of p53 inhibits its transcriptional activity. *Cell*, **118**, 83-97.

Xu, Z.X., Timanova-Atanasova, A., Zhao, R.X. and Chang, K.S. (2003) PML colocalizes with and stabilizes the DNA damage response protein TopBP1. *Mol Cell Biol*, **23**, 4247-4256.

Yi, C., Wang, H., Wei, N. and Deng, X.W. (2002) An initial biochemical and cell biological characterization of the mammalian homologue of a central plant developmental switch, COP1. *BMC Cell Biol*, **3**, 30.

Zhang, Y., Xiong, Y. and Yarbrough, W.G. (1998) ARF promotes MDM2 degradation and stabilizes p53: ARF-INK4a locus deletion impairs both the Rb and p53 tumor suppression pathways. *Cell*, **92**, 725-734.

Zipper, H., Brunner, H., Bernhagen, J. and Vitzthum, F. (2004) Investigations on DNA intercalation and surface binding by SYBR Green I, its structure determination and methodological implications. *Nucleic Acids Res*, **32**, e103.

8   APPENDIX

8.1   Modification of Tip60 by Ubiquitin-like proteins

The regulation of protein activity is mainly accomplished on the level of posttranslational modifications. In this work, the impact of Tip60 on p53 and Mdm2 posttranslational modifications was investigated. We were now interested, whether Tip60 itself is modified by Ubiquitin-like proteins like Nedd8 or SUMO-1.

So far, the only described posttranslational modifications of Tip60 represent its phosphorylation by the Cyclin b/cdc2 kinase (Lemercier et al., 2003), its ubiquitination by Mdm2 (Legube et al., 2002) and its acetylation by the histone acetyl transferase p300 (Col et al., 2005).

8.1.1   Tip60 is modified by Nedd8

Since Mdm2 is capable of acting as an E3 ligase for Nedd8 and we further observed an inhibition of Mdm2-mediated neddylation of p53 by Tip60 (chapter 5.2.2), we asked whether Tip60 might be modified by Nedd8. To test, whether Tip60 is neddylated, Tip60 was coexpressed with His-tagged Nedd8 and hUbc12 followed by a Nickel-His-tag Pulldown. As shown in Figure 8.1, the coexpression of His-12-Nedd8 resulted in the appearance of bands with lower electrophorectic mobility, corresponding to neddylated Tip60 forms (lane 2). Upon additional coexpression of hUbc12, a further accumulation of slower migrating Tip60 bands was observed, which confirms the identity of neddylated Tip60 (lane 4). These findings suggest that Tip60 is modified by Nedd8. As Nedd8 is not able to form chains like ubiquitin (reviewed in Hoeller et al., 2006), the appearance of several slower migrating bands points to the modification of multiple lysines in Tip60.

8.1.2   Impact of Mdm2 on Tip60 neddylation

Next, we wanted to investigate whether Mdm2 had an impact on the neddylation of Tip60. To this end, Mdm2 was overexpressed together with Tip60 and the Nedd-CS. As shown in Figure 8.2, Mdm2 coexpression did not stimulate neddylation of Tip60 but rather led to a decrease in neddylated Tip60 and unmodified Tip60 (compare lanes 3+4). Since Mdm2-mediated ubiquitination of Tip60 targets it for degradation, it is likely that the decrease of neddylated Tip60 is due to a decrease of total Tip60

levels. This finding suggests that not every substrate of Mdm2 ubiquitination is at the same time subject to neddylation by Mdm2. It remains to be determined if Mdm2 catalyzes the neddylation of further substrates apart from p53 and itself.

8.1.3 Mapping of neddylation sites on Tip60

Next, we were interested, which domains on Tip60 were targeted by neddylation. So far, no general consensus motif for neddylation, apart from one for cullins, has been described (Pan et al., 2004). Therefore, we overexpressed different Tip60 deletion mutants together with the Nedd8-conjugating system and performed a His-tag-Pulldown. However, no change of the neddylation pattern was observed upon deletion of Exon 5 , the MYST domain or the complete C-terminus from amino acid 390 onwards (Figure 8.3). This suggests that Tip60 is most probably modified in its N-terminal region.
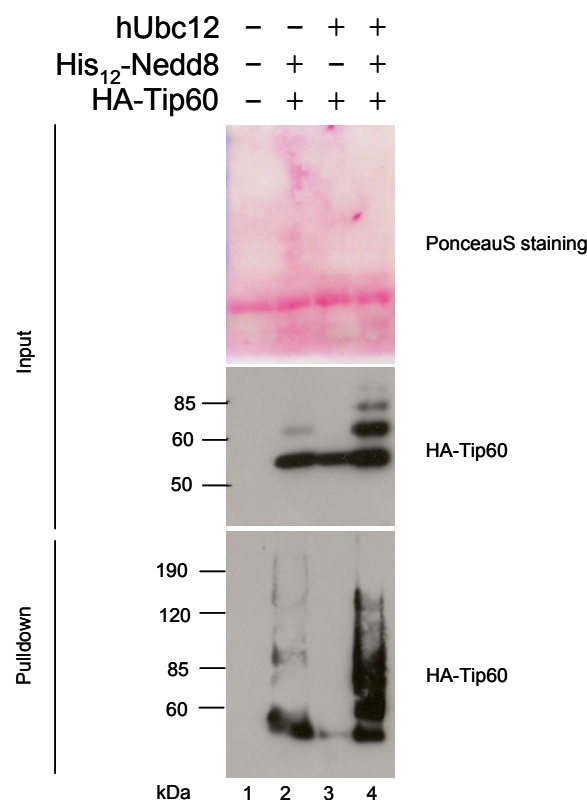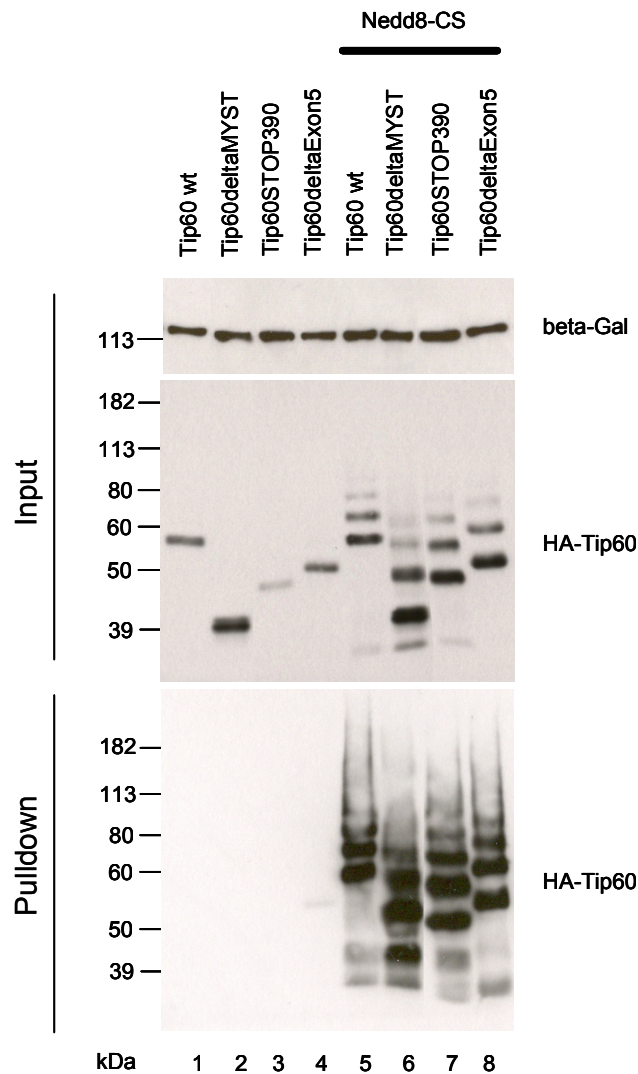

Figure 8.1: Neddylation of Tip60.
U2OS cells were transfected with the indicated combinations of the expression plasmids for His-tagged Nedd8, hUbc12, Tip60 and Mdm2. The cells were harvested 36 h post transfection and were lysed in His-tag-Pulldown lysis buffer folllowed by the His-tag Pulldown procedure. The proteins were separated by SDS-PAGE and detected by immunoblotting.
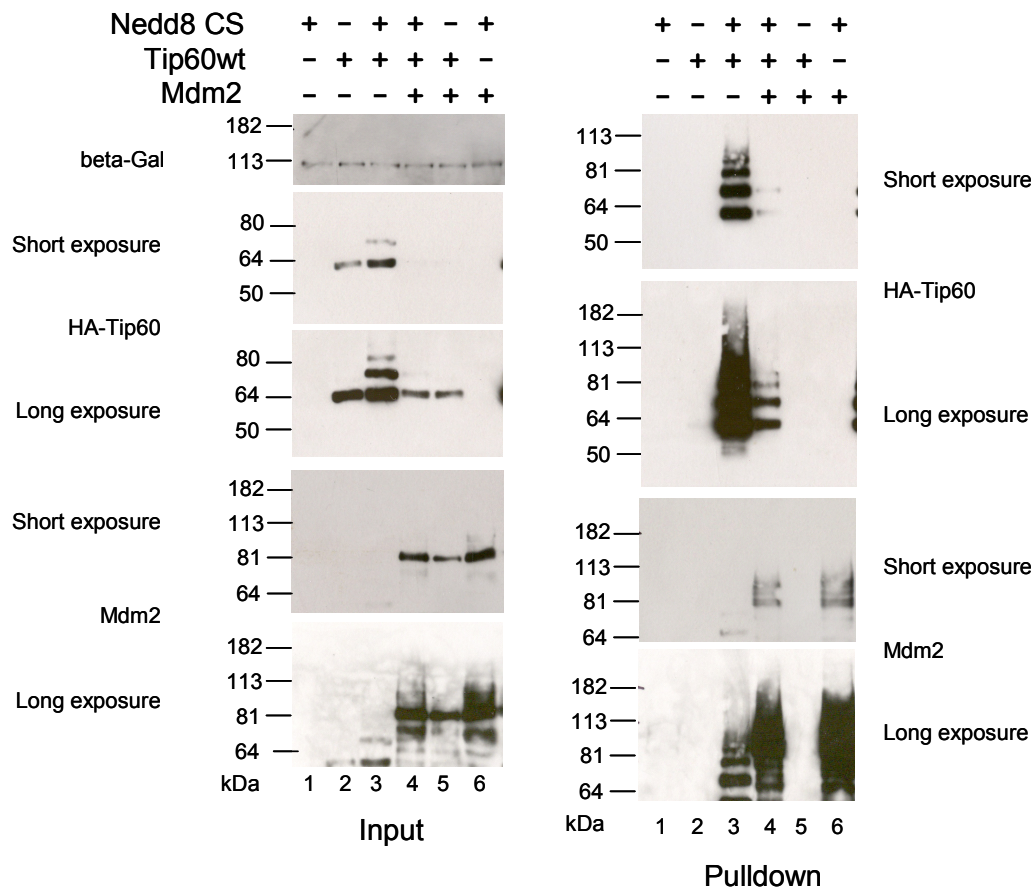
Figure 8.2: Impact of Mdm2 on Tip60 neddylation
U2OS cells were transfected with the indicated combinations of the expression plasmids for His-tagged Nedd8, hUbc12, Tip60 and Mdm2. The cells were harvested 36 h post transfection, lysed in His-tag-Pulldown lysis buffer folllowed by the His-tag pulldown procedure. The proteins were separated by SDS-PAGE and detected by immunoblotting.

The potential function of Tip60 neddylation remains to be determined. It is conceivable that the neddylation of Tip60 regulates the association with other proteins as Mdm2 or binding partners in the NuA4-Tip60 complex.

8.1.4 Tip60 is modified by SUMO-1

Given the fact, that Tip60, Mdm2 and p53 colocalise with PML nuclear bodies that have been described to be sites of protein modification with the Ubiquitin-like modifier SUMO-1, we were interested whether Tip60 could be modified with SUMO-1. As Nedd8, SUMO-1 belongs to the family of Ubiquitin-like proteins. It exhibits a sequence identity of 20% to Ubiquitin and has been implicated in several cellular pathways like DNA damage repair and maintenance of genomic intergrity (reviewed in Hay, 2005).

Figure 8.3: Neddylation of Tip60 mutants.
U2OS cells were transfected with the indicated combinations of the expression plasmids for His-tagged Nedd8, hUbc12, Tip60. The cells were harvested 36 h post transfection and were lysed in His-tag-Pulldown lysis buffer folllowed by the His-tag Pulldown procedure.

Its conjugation to proteins requires the E1 activating enzyme SAE1/SAE2 and the E2 conjugating enzyme Ubc9. E3 ligases for SUMO-1 have also been decribed.

Furthermore, a search for SUMOylation consensus sites using the SUMOplot site in the internet (http://www.abgent.com/doc/sumoplot), revealed several potential sumoylation sites in Tip60. A SUMOylation consensus site consists of the following amino acids: ψ-K-x-D/E (where lysine is the modified amino acid, ψ is a hydrophobic residue and x is any amino acid residue) To test this, Tip60 was coexpressed with His-tagged SUMO-1 in U2OS cells followed by a Nickel-His-tag pulldown. As shown in Figure 8.5, the coexpression of Tip60 with SUMO-1 led to the occurrence of slower migrating bands, corresponding to SUMOylated Tip60 forms.

```
Tip60 Isoform 2

   1    MAEVGEIIEG CRLPVLRRNQ DNEDEWPLAE ILSVKDISGR KLFYVHYIDF
  51    NKRLDEWVTH ERLDLKKIQF PKKEAKTPTK NGLPGSRPGS PEREVPASAQ
 101    ASGKTLPIPV QITLRFNLPK EREAIPGGEP DQPLSSSSCL QPNHRSTKRK
 151    VEVVSPATPV PSETAPASVF PQNGAARRAV AAQPGRKRKS NCLGTDEDSQ
 201    DSSDGIPSAP RMTGSLVSDR SHDDIVTRMK NIECIELGRH RLKPWYFSPY
 251    PQELTTLPVL YLCEFCLKYG RSLKCLQRHL TKCDLRHPPG NEIYRKGTIS
 301    FFEIDGRKNK SYSQNLCLLA KCFLDHKTLY YDTDPFLFYV MTEYDCKGFH
 351    IVGYFSKEKE STEDYNVACI LTLPPYQRRG YGKLLIEFSY ELSKVEGKTG
 401    TPEKPLSDLG LLSYRSYWSQ TILEILMGLK SESGERPQIT INEISEITSI
 451    KKEDVISTLQ YLNLINYYKG QYILTLSEDI VDGHERAMLK RLLRIDSKCL
 501    HFTPKDWSKR GKW
```

Figure 8.4: Potential SUMOylation consensus sites in Tip60 as obtained with SUMOplot™ (www.abgent.com)
Amino acid sequence of Tip60. Consensus sites with a low probability are marked in blue, those with a high probability in red.

8.1.5 Mapping of SUMOylation sites on Tip60

Next, we wanted to investigate whether the deletion of certain Tip60 domains would abolish the appearance of SUMOylated Tip60 forms. For this purpose, different Tip60 deletion mutants were coexpressed with His-12-SUMO-1 in U2OS cells followed by a Nickel-His-tag-pulldown.

All Tip60 deletion mutants tested are still modified with SUMO-1 as seen in Figure 8.5. Also the mutation of two SUMOylation consensus sites in Tip60 did not result in decreased SUMOylation of Tip60 (data not shown). Therefore it remains to be determined which lysine residues of Tip60 are modified by Tip60. Furthermore, it is unclear whether the SUMOylation of Tip60 actually occurs under physiological conditions and which role it has. Since PML NBs have been shown to be sites of increased SUMO-1 modification, it would be conceivable that the relocalization of Tip60 to the PML NBs is required for this modification to occur. Again, it could play a role in regulating the activity of the Tip60 protein, or its association of other proteins of the Tip60 complex. Previous reports point to a rather inhibitory role of SUMOylation in transcription (reviewed in Hay, 2005).
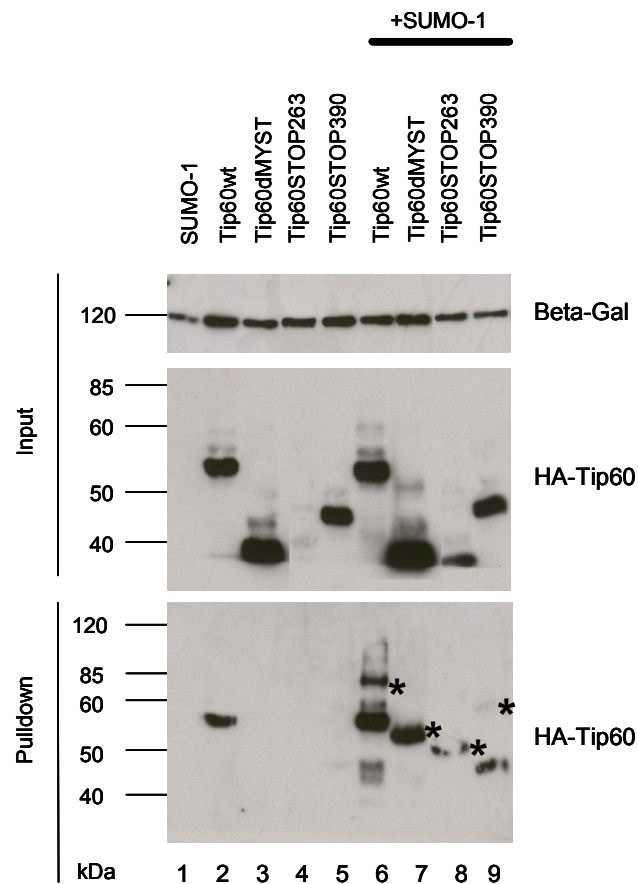
Figure 8.5: SUMOylation of Tip60 mutants in U2OS cells.
U2OS cells were transfected with expression plasmids for His-tagged SUMO-1, and Tip60 as well as different Tip60 deletion mutants. The cells were harvested 36 h post transfection and were lysed in His-tag-Pulldown lysis buffer folllowed by the His-tag Pulldown procedure (Chapter 4.2.5), SDS-PAGE and immunoblot analysis. Asteriks indicate bands that correspond to SUMOylated Tip60 forms.

8.2 The Impact of Tip60 on the localization of Mdm2-analogues

Since we found that expression of Tip60 together with Mdm2 led to a redistribution of both proteins to nuclear dot-like structures (5.4.4) and given the fact that Tip60 had been found to colocalize also with hPirh2 (Logan et al., 2004), a Mdm2-analogue, we asked whether Tip60 could colocalize with another Mdm2 analog, called COP1. COP1 (constitutive photomorphogenetic 1) was only recently identified as an E3-Ubiquitin-Ligase for p53 (Dornan et al., 2004). It is the human homolog of a plant protein that is required for the proper regulation of photomorphogenesis (Deng et al., 1991).

8.2.1 The Mdm2-analogue COP1 colocalizes with Tip60 to PML nuclear bodies

To study the effect of Tip60 on COP1 localization, EGFP-COP1 was expressed either alone or together with HA-Tip60 in U2OS cells and a co-immunofluorescence

was performed. As shown in Figure 8.6, COP1 and Tip60 exhibit a colocalization in nuclear dots and also in clusters in the cytoplasm (panel B) whereas COP1 alone does not localize to nuclear dots (panel A). However, the colocalization is not so clear as in the case of Mdm2 and Tip60. The intracellular localization of COP1 had previously been shown be both cytoplasmic and nuclear (Bianchi et al., 2003; Yi et al., 2002). Nevertheless, this finding hints to a potential physical association of Tip60 and COP1.

Next, we were interested in whether the nuclear dots formed by Tip60 and COP1 would also colocalize with PML nuclear bodies as in the case of Mdm2 and Tip60. To test this, we coexpressed HA-Tip60 and EGFP-COP1 and performed a co-immunofluorescence where the cells were stained with an antibody against PML and EGFP-COP1. Indeed, the dots formed by Tip60 and COP1 colocalized very strongly with the PML nuclear bodies as seen in Figure 8.6 C, thereby establishing a parallel to the situation with Mdm2 and Tip60. In fact, this is the first hint that COP1 localizes to PML nuclear bodies, despite the observation that plant COP1 and mammalian PML exhibit a similar intracellular localization (Reyes, 2001).

In conclusion, these results suggest that Tip60 does not only associate and regulate Mdm2 but that it also potentially acts on its analogue COP1. Taken together, Tip60 might regulate p53 abundance and activity by interfering with the three most important p53 antagonists: Mdm2, hPirh2 and COP1.

It remains to be elucidated whether Tip60 actually directly interacts with COP1 and whether it inhibits its activity towards p53. However, the fact that Tip60 overexpression leads to an increase in p53 levels (Chapter 5.1.1) does not exclude an effect of Tip60 on COP1 activity apart from inhibiting Mdm2. A role of Tip60 in the inhibition of postubiquitination step could also accommodate the inhibition of COP1-dependent p53 degradation. Recently it was reported that COP1 is phosphorylated by ATM, leading to its degradation (Dornan et al., 2006). Since Tip60 acetylation of ATM is required for its activation, it could make sense that Tip60 also directly interferes with COP1. However, this remains to be determined.

Taken together, the data presented in this appendix point to many functions of Tip60 that still await their identification.
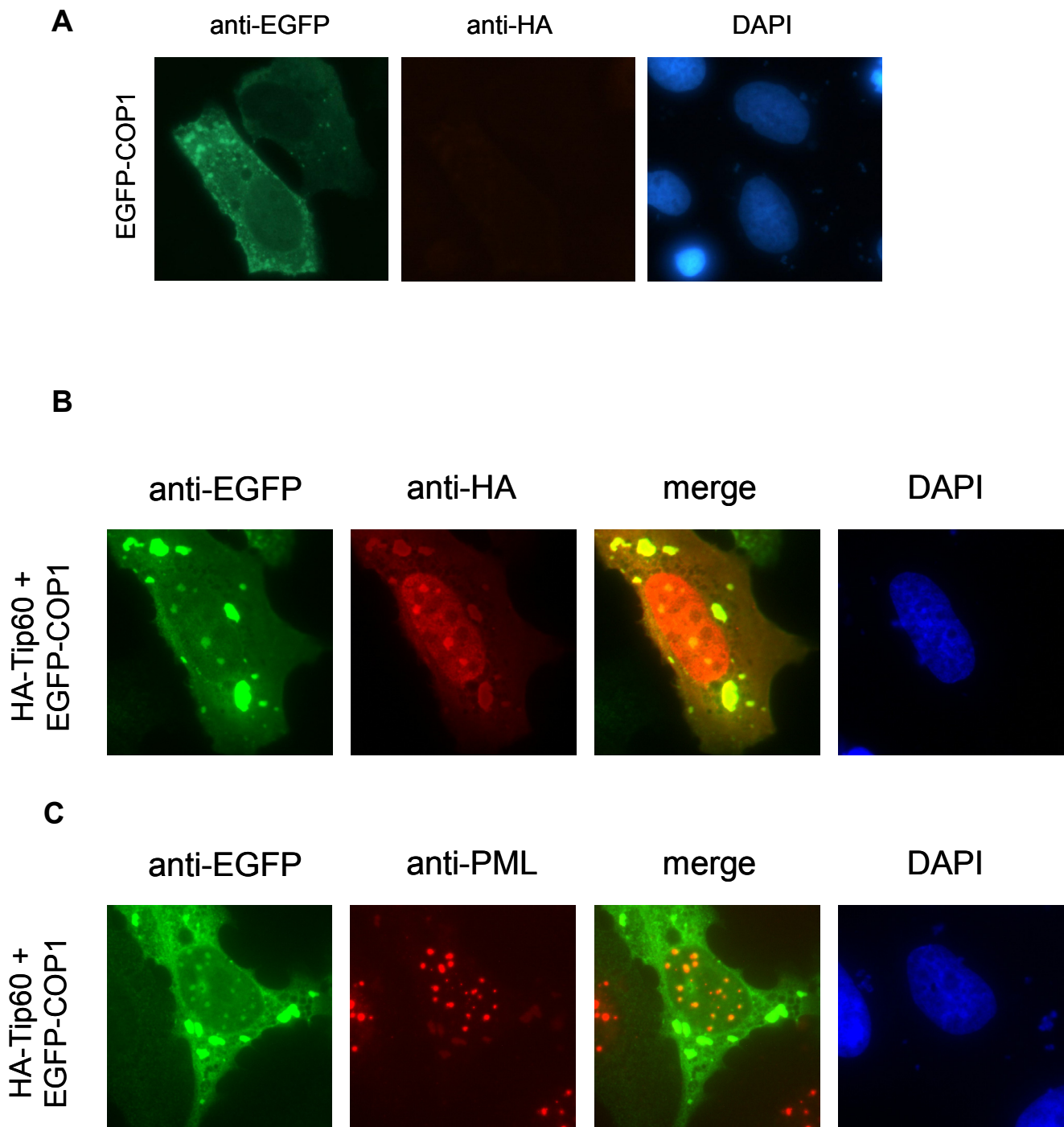
A

B

C

Figure 8.6 Impact of Tip60 on the intracellular localization of COP1.
(A) U2OS cells were transfected with an expression plasmid for EGFP-COP1. After 24 h, the cells were fixed with 4% PFA, permabilized with triton X-100 and stained with the indicated antibodies. Nuclei were visualized by DAPI staining.
(B) U2OS cells were transfected with expression plasmids for and HA-Tip60 and EGFP-COP1, fixed with 4% PFA and further processed as in **(A)**.
(C) U2OS cells were transfected with expression plasmids for and HA-Tip60 and EGFP-COP1, fixed with 4% PFA and further processed as in **(A)**, but stained with antibodies against the EGFP-tag and PML.

Abbreviations

Abs	absorption
APS	ammonium persulfate
APP-BP1	amyloid precursor binding protein 1
ATM	ataxia telangiectasia mutated
ATP	adenosine triphosphate
ATR	ataxia telangiectasia related
Bax	BCL2-associated X protein
bp	base pairs
BSA	bovine serum albumin
c	concentration
C	Desoxycytidine monophosphate
CBP	CREB binding protein
cdc	cell division cycle
CDK	cyclin-dependent kinase
Chk	checkpoint kinase
CIP	calf instestine phosphatase
COP1	constitutive photomorphogenetic 1
cDNA	complementary DNA
C-terminus	carboxy terminus
Daxx	death domain associated protein
Da	Dalton
DABCO	1,4-Diazobicyclo-[2.2.2]-octane
DAPI	4´,6-Diamidino-2-Phenylindole
DSB	double strand break
dATP	Deoxyadenosine triphosphate
dCTP	Deoxycytidine triphosphate
Ddi1	DNA damage molecule 1
ddNTP	dideoxyribonucleic acid
dH$_2$O	destilled water
DMEM	Dulbecco`s Modified Eagle Medium
DMSO	Dimethylsulfoxide
DNA	deoxyribonucleic acid

dNTP	Deoxy ribonucleic triphosphat
ds	double strand
Dsk2	dominant repressor of Kar2
DTT	1,4-Dithiothreitole
dTTP	Deoxythymidine triphosphate
dUTP	Deoxyuridine triphosphate
E.coli	*Escherichia coli*
E2F	E2-binding protein (E2F transcription factor)
EB	elution Buffer
ECL	enhanced chemoluminescence
EDTA	ethylene diamine tetraacetate
EGFP	enhanced green fluorescent protein
EHF	Expand-HIFI polymerase system
F	Farad
F(ab)	antigen-binding fragment
FBS	fetal bovine serum
g	gram
G	Desoxyguanosine monophosphate
GAPDH	glyceraldehyde-3-phosphate dehydrogenase
H2AX	histone 2AX
H3	histone 3
H4	histone 4
HAT	histone acetyl transferase
h	hour
HIPK	homeodomain-interacting protein kinase
hPirh2	human p53-inducible protein with RING-H2 domain
HSP70	heat shock protein 70 kDa
HTATIP	HIV-1 Tat interacting protein
Ig	immunoglobulin
IP	immunoprecipitation
IR	ionising radiation (e.g. gamma radiation)
JNK	jun-N-terminal kinase
kb	kilobases
L	liter

λ	wavelength in nm
m	milli (10^{-3})
M	molar
μ	micro (10^{-6})
MAPK	mitogen activated protein kinase
Mdm2	murine mouse double minute clone 2
MG	molecular weight
MG132	proteasome inhibitor
min	minute
MYST	MOZ, Ybf2/Sas3, Sas2, Tip60
mRNA	messenger RNA
n	nano (10^{-9})
N	normal
Nedd8	neural precursor cell expressed developmentally downregulated 8
Noxa	NADPH oxidase activator 1
NuA4	nucleosome acetyltransferase of H4
N-Terminus	amino terminus
qRT-PCR	quantitative Realtime PCR
Ω	ohm
p	pico (10^{-12})
ψ	hydrophobic amino acid
p53BP1	p53 binding protein 1
PAGE	poly-acryl-amide-gel electrophoresis
PAS	protein-A-sepharose
PBS	phosphate buffered saline
PCR	polymerase chain reaction
PFA	paraformaldehyde
PIKK	phosphatidylinositol 3-kinase-related kinase
PLIP	cPLA2 interacting protein (Tip60 isoform)
PML	promyelocytic leucemia protein
PML-NB	promyelocytic leucemia protein nucelar bodies
POD	promyelocytic oncogenic domain
Puma	p53-induced modulator of apoptosis

PVDF   polyvinylidene fluoride

pRb   retinoblastoma protein

RING   really interesting new gene

RISC   RNA induced silencing complex

RNA   ribonucleic acid

RNAi   RNA interference

RNase   ribonuclease

RT   reverse transcriptase

rpm   rounds per minute

s   second

SAE1/SAE2   SUMO-1 activating enzyme subunit 1/2

SCF   Skp1/Cul1/F-box

SDS   sodium-dodecyl-sulfate

siRNA   small-interfering RNA

ss   single strand

SUMO   small ubiquitin like modifier

suppl.   supplemented

SV40-L-TAg   Simian virus 40 large T Antigen

T   Deoxythymidine phosphate

TAE   tris acetic acid

TBA   tris borate

TEMED   N,N,N´,N´-Tetramethyldiamine

Tip49   TATA-binding protein (TBP)-interacting protein

Tip60   HIV-1 tat-interacting protein, 60 kDa

TRRAP   transformation/transcription domain-associated protein

U   units

UBL   Ubiquitin like

UV   ultra violet

V   volt

v/v   volume/volume

w/v   weight/volume

X   any amino acid

Acknowledgements

Curriculum Vitae

Personal details

Surname:	Dohmesen
Name:	Christoph Josef
Nationality:	German
Born:	19/03/1977
Marital status:	Single
Working Address:	Medical Biotechnology Center
	Winsløwparken 25.1, DK-5000 Odense C
Private Address:	Provstegade 10.1.4, DK-5000 Odense C
Work Phone:	0045 6550 3957
Private Phone:	0045 66135013
Work Email-address:	cdohmesen@health.sdu.dk
Private Email-address:	dohmesenchristoph@web.de

Education

University

2003 to date	PhD thesis in the lab of Prof. Matthias Dobbelstein in Marburg; since January 2005 at the Medical Biotechnology Center, Southern University of Denmark, Odense, Denmark
December 2002	Graduation as Biologist (Diploma); grade 1,1 (1,0 = best)
2002	Diploma thesis in the lab of Prof. Matthias Dobbelstein, Institute of Virology, Philipps-University Marburg
1997 – 2002	Study of Biology at the Philipps-University Marburg, Germany
September 2001 – December 2001	Erasmus Exchange Trimester at the University of Oxford in the group of R. Chalmers

Extracurricular courses

01.08.2000 – 30.09.2000	Practical course at the BASF AG, Ludwigshafen, Germany

School

1996	final high school examination („Abitur"), grade 1,9 (1,0 = best)
1983 – 1996	Primary school and Grammar school in Mönchengladbach, Germany

Workshops/ Conferences

- Annual Conference of the German Society of Virology, 26 -29th March 2003, Berlin, Germany, **"Impact of Hypoxia on Adenovirus replication"** <u>Christoph Dohmesen</u>, Germán Horn, Constanze Moeritz, Norbert Weissmann, Werner Seeger and Matthias Dobbelstein

Oral Presentations:

- 7TH NorFa p53/Cell Cycle Workshop,10-12th June 2005, Falsterbo, Sweden **"The role of Tip60 in the p53-pathway"** <u>Christoph Dohmesen</u> and Matthias Dobbelstein

- 3rd International MDM2 Workshop; 9-12th September 2005, Konstanz, Germany **"Regulation of the p53-antagonist and its partners by Tip60"** <u>Christoph Dohmesen</u>, Max Koeppel, Raffaela Santoro and Matthias Dobbelstein

- Fyn Breastcancer Meeting, 20th September 2005, Denmark, Odense, **"Regulation of the p53-antagonist and its partners by Tip60"** <u>Christoph Dohmesen</u>, Max Koeppel, Raffaela Santoro and Matthias Dobbelstein

- 9th DACR ANNUAL MEETING 2006, Copenhagen, Denmark, **"TIP60 relocalizes Mdm2 to the PML oncogenic domains, leading to decreased Nedd8 conjugation and enhanced stability of p53 and Mdm2"** <u>Christoph Dohmesen</u>, and Matthias Dobbelstein

- 8TH NorFa p53/Cell Cycle Workshop,16-18th June 2006, Pühajarve, Estonia, **"TIP60 relocalizes Mdm2 to the PML oncogenic domains, leading to decreased Nedd8 conjugation and enhanced stability of p53 and Mdm2"** <u>Christoph Dohmesen</u>, Max Koeppel and Matthias Dobbelstein

Prices:

- 3rd Poster price at the Annual Conference of the German Society of Virology, 2003, Berlin, **"Impact of Hypoxia on Adenovirus replication"** <u>Christoph Dohmesen</u>, Germán Horn, Constanze Moeritz, Norbert Weissmann, Werner Seeger and Matthias Dobbelstein

Publications

- **Specific Inhibition of MDM2-mediated Neddylation by TIP60,** <u>Christoph Dohmesen</u>, Max Koeppel and Matthias Dobbelstein, submitted

Languages skills

Excellent written and verbal skills in English
Good written and verbal skills in Spanish
Basic knowledge of French and Danish

Odense, 26th of October 2006, Christoph Dohmesen

Erklärung

ich versichere, daß ich meine Dissertation

„The histone acetyl transferase Tip60 as a regulator of tumor suppression"

selbständig, ohne unerlaubte Hilfe angefertigt und mich dabei keiner anderen als der von mir
ausdrücklich bezeichneten Quellen und Hilfen bedient habe.
Die Dissertation wurde in der jetzigen oder einer ähnlichen Form noch bei keiner anderen
Hochschule eingereicht und hat noch keinen sonstigen Prüfungszwecken gedient.

Odense, den 26.Oktober 2006   Christoph Dohmesen
(Ort/Datum)   (Unterschrift mit Vor- und Zuname)